TRABAJO DE FIN DE MASTER

ETS INGENIERÍA DE CAMINOS,
CANALES Y PUERTOS

Prevención de la compactación del suelo por operaciones
agrícolas: una perspectiva geotécnica

Presentado por

López Rodero, Ramón

Para la obtención del

Master Universitario en Ingeniería de Caminos, Canales y Puertos

Curso: 2019/2020
Fecha: 16/07/2020
Tutor: José Bernardo Serón Gáñez
Cotutor: Gemmina di Emidio

FACULTY OF ENGINEERING AND ARCHITECTURE

Prevention of soil compaction by agricultural operations: a geotechnical perspective

Ramón López Rodero
Student number: 01901870

Supervisors: Prof. dr. ir. Gemmina Di Emidio, Prof. dr. ir. Wim Cornelis
Counsellors: Dr. ir. Juan Carlos Rojas Vidovic (USFX), Adriaan Vanderhasselt, Prof. dr. ir. Adam Bezuijen

Master's dissertation submitted in order to obtain the academic degree of
Master of Science in Civil Engineering

Academic year 2019-2020

GHENT UNIVERSITY

FACULTY OF ENGINEERING
AND ARCHITECTURE

Prevention of soil compaction by agricultural operations: a geotechnical perspective

Ramón López Rodero
Student number: 01901870

Supervisors: Prof. dr. ir. Gemmina Di Emidio, Prof. dr. ir. Wim Cornelis
Counsellors: Dr. ir. Juan Carlos Rojas Vidovic (USFX), Adriaan Vanderhasselt,
Prof. dr. ir. Adam Bezuijen

Master's dissertation submitted in order to obtain the academic degree of
Master of Science in Civil Engineering

Academic year 2019-2020

GHENT
UNIVERSITY

Preface

The initial purpose and idea of this thesis dissertation was to perform a series of one-dimensional consolidation tests (e.g. oedometer tests) on a series of samples taken from Belgian fields to study and prevent the risk to soil compaction. Through the variation and measurement of different physical soil parameters such as bulk density, permeability, soil suction, etc., multiple linear regressions would be defined for the estimation of the precompression stress.

Nevertheless, due to the COVID-19 crisis, it was impossible to accomplish these experiments at the laboratory. Consequently, the content and main objectives of this thesis dissertation were restructured, as shown in the introductory chapter, Chapter 1.

Acknowledgements

To all the people that directly or indirectly made a positive influence on this thesis dissertation.

I am grateful to Prof. Gemmina di Emidio for her guidance, advice, and structured work.

I am grateful to Adriaan Vanderhasselt for his helpful assistance through all the course, his guidance and his knowledge, thank you for your effort.

I am also thankful for the guidance and help by Prof. Wim Cornelis.

I want to give thanks to Per Schjønning from Aarhus University and Thomas Keller from Swedish University of Agricultural Sciences since they helped and provided me useful publications by e-mail communication, they are very efficient, I appreciate it.

I would like to appreciate the effort as well by Maarten Volckaert for helping and teaching me how to use the cell device for the oedometer-tensiometer and the connections, even if we could not do the tests in the end.

Finally, I am grateful to my family for always trusting on me and to all the wonderful people that I met during my stay in Ghent, especially, to my beloved girl Vittoria, for her constant love and support.

June 2020,

Ramón López Rodero.

Prevention of soil compaction by agricultural operations: a geotechnical perspective

Ramón López Rodero

Master's Dissertation. Master of Science in Civil Engineering

1st Promoter: Prof. Dr. Ir. Gemmina Di Emidio

2nd Promoter: Prof. Dr. Ir. Wim Cornelis

Guidance Committee: Adriaan Vanderhasselt

Academic year 2019-2020

Ghent University – Faculty of Engineering and Architecture

Department of Civil Engineering

In the last decades, the use of heavy agricultural machinery on cultivated soils has negatively impacted many important soil functions by soil compaction. This process is a combination of both geotechnical processes of compaction, in the strict sense, and consolidation. However, in geotechnics, this densification can positively affect soil foundational behaviour.

In soil physics, compaction is expected to occur when the applied stress overcomes the soil strength, commonly expressed as the precompression stress (σ'_p). This parameter can be estimated by various methods from compression curves obtained by oedometer tests. The calculation method together with soil conditions and laboratory aspects, should be carefully selected in order to obtain best possible results. Pedotransfer functions are another good alternative for σ'_p prediction from readily available soil properties.

Results of previous laboratory tests used in this master dissertation showed that most common drivers to estimate σ'_p are: soil particle size distribution (mainly clay content), matric potential, bulk density and OM content, in agreement with most of the literature.

The web-based computer model Terranimo® is a great tool for farmers and soil researchers to evaluate the risk of soil compaction under agricultural vehicles. It determines the transmitted stresses through the soil profile which are mainly affected by wheel load, tyre inflation pressure and soil water field conditions.

Keywords: soil compaction, precompression stress, Terranimo®, geotechnics, soil physics.

Prevention of soil compaction by agricultural operations:
a geotechnical perspective

Ramón López Rodero

Supervisors: Gemmina Di Emidio, Wim Cornelis, Adriaan Vanderhasselt

Abstract - **In the last decades, the use of heavy agricultural machinery on cultivated soils has negatively impacted many important soil functions by soil compaction. This process is a combination of both geotechnical processes of compaction, in the strict sense, and consolidation. However, in geotechnics, this densification can positively affect soil foundational behaviour.**

In soil physics, compaction is expected to occur when the applied stress overcomes the soil strength, commonly expressed as the precompression stress (σ'_p). This parameter can be estimated by various methods from compression curves obtained by oedometer tests. The calculation method together with soil conditions and laboratory aspects, should be carefully selected in order to obtain best possible results. Pedotransfer functions are another good alternative for σ'_p prediction from readily available soil properties.

Results of previous laboratory tests used in this master dissertation showed that most common drivers to estimate σ'_p are: soil particle size distribution (mainly clay content), matric potential, bulk density and OM content, in agreement with most of the literature.

The web-based computer model Terranimo® is a great tool for farmers and soil researchers to evaluate the risk of soil compaction under agricultural vehicles. It determines the transmitted stresses through the soil profile which are mainly affected by wheel load, tyre inflation pressure and soil water field conditions.

Keywords - **soil compaction, precompression stress, Terranimo®, geotechnics, soil physics.**

I. INTRODUCTION

Soil is a heterogeneous natural medium that supports life on earth. It provides a range of ecosystem services very useful for our common welfare. Root growth, water movement, aeration, and heat transfer are directly influenced by the physical properties of soils. Therefore, food production, water storage, carbon sequestration, water quality and flood protection depend on the structure of the soil. Nowadays, soils are clearly suffering the devastating effects of global warming, affecting, and putting extra pressure on soil functions. For this reason, preserving and maintaining them in a good quality, as well as efficient soil management and sustainable agriculture become even more important.

The increase in the weight of heavy machinery used for field operations in modern agriculture results in a considerable increase in vertical stresses reaching the subsoil, where conventional ploughing techniques can no longer restore the compacted layer. This poses a considerable risk to the soil through the degradation of physical, chemical, and biological soil functioning by compaction. Thus, soil compaction has turned into one of the most important threats to soil quality in the last decades.

II. LITERATURE REVIEW

Firstly, it should be clarified that soil compaction can be studied from various perspectives which result in different professional approaches. In this thesis, two of them are covered: geotechnics or engineering field vs soil physics or agronomy field.

In *geotechnics*, soil compaction refers to the process of densification of an unsaturated soil by expulsion of air from its voids under application of stress or mechanical pressure. Soil compaction is often intended for the purpose of improving soil resistance and bearing capacity. This process is normally quick, due to short-term loading and does not affect the water content. In this way, a differentiation can be made with soil consolidation, despite both processes cause a reduction in the volume of the soil due to its compressibility characteristics. Consolidation is a slow process in which long-term and static loading causes a densification, typically, of the

saturated soil by expulsion of the pore water. It can naturally occur due to the structural loads from foundations. Laboratory tests measure compaction, e.g. dry unit weight tests (Standard and Modified Proctor test), consolidation, e.g. uniaxial compression or oedometer test ($\geq$ 24 h loads) (Figure 1) and penetration, e.g. California Bearing Ratio (CBR) test, Standard Penetration test (SPT) and Cone Penetration test (CPT), which are very popular within in-situ testing.
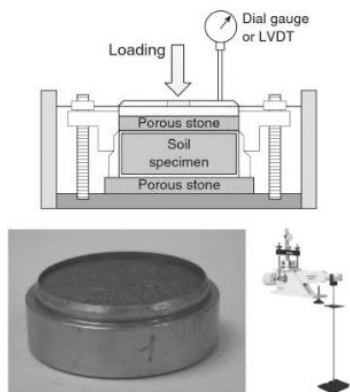

FIGURE 1. CONSOLIDATION PRINCIPLE SKETCH - SAMPLE IN RING - COMPLETE SETUP [2].

In *soil physics*, soil compaction encompasses a combination of both engineering processes, compaction, and consolidation. In contrast to geotechnics, in which soil compaction was intended on purpose, here, the purpose is to prevent this process from happening, since it might provoke several detrimental effects on agricultural soils. The most common laboratory test to measure the risk to soil compaction is the oedometer test (~ 30 min loads or continuous loading), mainly used to obtain stress-strain relationship curves and the subsequent soil strength (= precompression stress). However, soil sampling is often time and work-intensive, marginal destruction of the soil cores is difficult to avoid and friction and/or disturbance at the ring walls can affect the results of the compression tests. Therefore, in-situ testing is a good alternative as well, e.g. plate sinkage test. In addition, other common in-situ tests are sand cone, rubber balloon or density gauge, amongst many others.

The context of this thesis is the study of risk to soil compaction on agricultural fields; therefore, compaction will be viewed from a soil physics perspective. Mechanization in modern agriculture and the continuing trend towards larger vehicles implies an increase in the mechanical stresses reaching topsoil and subsoil layers, and consequently, there is an increase in the risk of soil compaction.

Most risk assessments models for agricultural soils are based on a comparison of the exerted vertical stress with some estimate of soil strength derived from uniaxial, confined compression tests. Based on soil mechanics, a sharp bend of the stress-strain curve from such tests is expected. The stress at this point is typically labelled as the *precompression stress* or *preconsolidation pressure*, σ'_p or PCS. According to the theory, the strain at stress levels lower than σ'_p is supposed to be elastic, while strain above σ'_p is plastic. It should therefore be safe to expose the soil to stresses lower than σ'_p, and to avoid higher stresses. Nevertheless, this analysis is questionable since it was proved that little residual strain appeared before reaching the σ'_p value [5].

Casagandre (1936) first graphically derived σ'_p from a lab-generated soil compression curve by testing intact unsaturated soils subjected to one-dimensional confined compression. σ'_p was found at the intersect between the bisecting line at the point of maximum curvature and the virgin compression line. Besides Casagrande's, other direct estimation methods from compressive curves have been developed, e.g. Schmertmann, (1955), Junior and Pierce (1995), Arvidsson et al. (2003), Gregory et al. (2006). Based on a practical comparison, some are more robust than others, e.g. Gregory et al. (2006) [4] [14]. However, for a good evaluation, several performances and comparison should be done, considering that these methods are not interchangeable. Other relevant aspects that affect σ'_p and compression curves are: loading time in the oedometer test (continuous increase in loading and 30 min loads are widely used; with increasing loading time, compaction increases and PCS is lower [1] [4] [5]), initial matric potential (higher stress and deformation for wetter soils [1] [7] [12]), dimension of sample cores [15], type of compaction test (use of plate sinkage test in field for obtaining compression curves avoid the disturbance and errors from laboratory tests [5]).

Indirect empirical estimation of the PCS by pedotransfer functions (PTFs) has become very popular, since direct methods are often time-consuming and laborious, require expensive-sophisticated devices, skilled technicians and could be a source of certain testing errors. PTFs are equations which are able to predict a dependent variable (PCS) by multiple linear regression on independent variables. These predictor variables (or drivers) include soil properties associated with soil compaction, such as particle size distribution, initial matric potential, bulk density, organic matter content, etc. PTFs from most of the literature showed that PCS was positively correlated with soil bulk density and negatively correlated with initial soil water content [Lebert and Horn (1991); Alexandrou and Earl (1998); Imhoff et al. (2004); Mosaddeghi et al. (2006); Saffih-Hdadi et al. (2009); Rücknagel et al. (2012)].

The models that are normally used to predict and evaluate the risk to soil compaction by agricultural operations contain three main components. The first component consists of the upper boundary conditions: contact area and vertical stress distribution exerted by the machinery at the soil/tyre interface. The second one is the stress propagation from the surface through the entire soil profile. Finally, the last step is the estimation of the soil strength (= PCS) which is compared to the transmitted soil stress. Non-recoverable soil deformation occurs if the soil (yield) strength (PCS) is exceeded. Based on this idea, the computer model Terranimo® is an interesting and useful decision support tool that estimates the risk of soil compaction by agricultural machinery.

Terranimo® is a user-friendly tool, with an interface allowing the user to easily enter the type of machinery, tyre characteristics, inflation pressure, soil texture and soil water status, as input data. Then, results are shown as output data: contact stress at the tyre/soil interface and transmitted vertical stresses through the soil profile vs. soil strength load capacity (yield strength). This tool is useful for farmers, advisors, consultants, and soil researchers interested in reducing the risk of harmful compaction by modifying the machinery operating conditions with the prevailing soil characteristics.

Tyre inflation pressure is the most easily adaptable factor. It directly affects the tyre-soil contact area, which in turn affects soil stress and its distribution. Within a certain range, soil stress increases with tyre pressure and it could explain most variation in soil stress in both top and sub soil layers under different wheel loads [9]. According to the elasticity theory, for a given load applied to a given soil, an increase in soil water content yields a higher concentration of stresses under the centre of the load and a deeper propagation of stresses [7].

The principles and models behind Terranimo® are analysed as follows. Soil precompression stress is calculated by a pedotransfer function developed on a dataset of results from uniaxial, confined compression tests [Schjønning et al., manuscript in preparation]. The variation in PCS could be described by a combination of the soil organic matter content, soil bulk density, and soil suction stress (calculated as the matric potential times soil saturation). The function used in the current version of Terranimo® only uses clay content and matric potential as predictors. The trend in soil strength predicted by this and other pedotransfer function shows a decrease with increasing clay content [12]. This is in agreement with general experience, with clay-holding soils being mechanically very weak when wet but strong when dry [12]. Finally, precompression stress increases with an increase in soil organic matter content and soil bulk density [12].

In Terranimo®, the vertical stress distribution exerted from the wheels at the tyre-soil contact area is estimated by the *FRIDA model* [13]. This model describes the shape of the tyre-soil contact area with a super ellipse. FRIDA is able to describe the actual conditions very well, in particular the predominant influence of tyre inflation pressure (Figure 2).
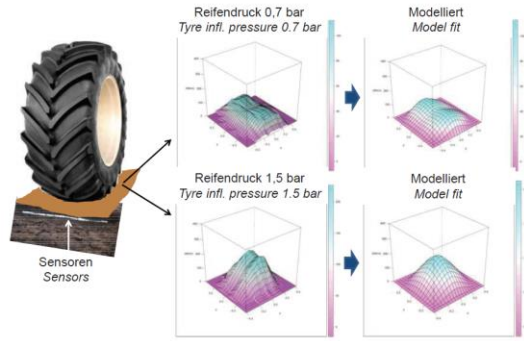
FIGURE 2. MEASURED (LEFT DIAGRAMS) AND FRIDA MODELLED STRESS STATES BETWEEN TYRE AND SOIL AT DIFFERENT TYRE INFLATION PRESSURES [12]

The FRIDA parameters α and β reflect the tyre's ability to distribute the stress in the driving direction and in the transversal direction, respectively. Both parameters increased with increases in the relevant contact area dimension. A power-law function and a decay function are described by these parameters α and β, respectively [Keller, 2005]. The parameters of the FRIDA model are estimated by multiple regression from tyre and loading characteristics [11]. It was found that the tyre volume (Vtc) and a ratio of actual to recommended inflation pressure (Fw) accounts for nearly all the variation in measured contact areas. The α parameter was further affected by Fw, while tyre inflation pressure (Kr) and tyre deflection (L) were added to model performance for the β parameter [11].

Finally, the vertical stresses transmitted through the soil profile are calculated semi-analytically by the Söhne (1953) approach with the FRIDA-estimated contact area point stresses as input. The stress propagation is also based on the formulas of Boussinesq (1885) and Fröhlich (1934), precursors of the Söhne model. The concentration factor ν is a key element, which determines the pattern of the stress propagation in the soil. In Terranimo®, the suggested values of concentration factor (ν) are:

- Dry soil (pF 2.7): ν = 4 ('hard')
- Moist soil (pF 2.0): ν = 5 ('firm')
- Wet soil (pF 1.7): ν = 6 ('soft')

III. MATERIALS AND METHODS

The used dataset was provided by the Soil Physics Research Group from UGent. It consists of a total of 126 soil core samples from various agricultural soils in Flanders. We developed new PTFs by stepwise multiple linear regression to estimate the precompression stress. Each dependent PCS value (seven determination methods; see De Pue et al., 2020) was predicted by a selection of independent variables (soil properties) that contributed significantly to the model, called predictors. The initial dataset was divided into two groups, depending on the land use (cropland or grassland). The PCS determination methods that were used from the compression curves are as follows:

- *PCS_Cas*: Casagrande's procedure.
- *PCS_L1*: stress at the intersection of VCL with the x-axis at strain = 0.
- *PCS_L2*: stress at a predefined strain of 2.5%.
- *PCS_L3*: stress at the intercept of the VCL and a regression line with the first two points of the curve.
- *PCS_L4*: stress at the intercept of the VCL and regression line with the first three points of the curve.
- *PCS_G3*: fitting of three-parameter Gompertz type equation to stress-strain curve.
- *PCS_Gomp*: fitting of four-parameter Gompertz type equation.

The PCS_Cas method was used by Davidowski and Koolen (1974) based on Casagandre (1930) graphical procedure. PCS_L1, PCS_L2, PCS_L3, PCS_L4 correspond to the four methods used by Arvidsson and Keller (2004). Curves from these first five methods were fitted by the fourth-order polynomial function. PCS_G3 and PCS_Gomp are the modified (three parameters) and the original (four parameters) Gompertz function used by Gregory et al. (2006), respectively.

The initial soil properties that were entered and would play a significant role in the PCS model were: Sn (%), Si (%), Cl (%), OM (%), pF (log of initial matric potential in hPa), BD (Mg/m^3), CSR (Clay/Sand ratio), StI (structural stability index, function of OC, Cl and Si). One new variable, suggested by Per Schjønning (2020, personal communication) was also introduced: preload suction stress, PSS (hPa). The PSS is an expression of the effective stress prior to loading the samples. It is calculated as the product of soil pore saturation and the numerical value of the matric potential [10].

The statistical software used for the regression process was SPSS. We first ran the multiple regression with the stepwise method. However, the results were not very reliable (only pF and BD were withdrawn as significant predictors) and the R^2 coefficients were very low. Afterwards, we tried running the same data with the backward method with a slightly higher significant probability and the results improved significantly (p=0.10). To measure the accuracy of the newly developed PTFs, two of the most common statistical metrics were computed: mean absolute error (MAE) and root mean square error (RMSE). Moreover, for a better prediction assessment, the coefficient of determination (R^2 and adjusted R^2) were calculated. These values examine how strong the linear relationship is between the measured PCS from oedometer testing and the predicted PCS from the pedotransfer functions.

Lastly, an analysis in *Terranimo® expert* was performed to assess the risk to soil compaction on a vineyard in Valdepeñas, south-centre of Spain. Realistic input data of the machinery equipment that is normally used by the vine farmer (my father) was provided and soil characteristics from a nearby cropland was used. Thus, output stresses transmitted to the soil will be obtained and any possible risk of compaction will be determined.

For vineyards, the machinery required are tractors that can pass through crop lines without any problem. Therefore, a small machine is used: 90 HP tractor of 5800 kg weight. The equipped implement is a plough of 2000 kg weight (Figure 3). The tyre characteristics are:

- Front tyres: Mitas traction AC 70 T tyres. Dimension: 320/70R20. Wheel load: 600 kg. Inflation pressure: 0.60 bar (recommended).

- Back tyres: Mitas traction HC 70 tyres. Dimension: 420/70R28. Wheel load: 2300 kg. Inflation pressure: 1.50 bar (recommended).

Regarding type of soil, the texture class is clay loam, with an average clay content of ~ 40 g 100 g^{-1} (or 40%). Moisture field conditions during field traffic are quite dry since rains over this zone are scarce (highly negative matric potential).
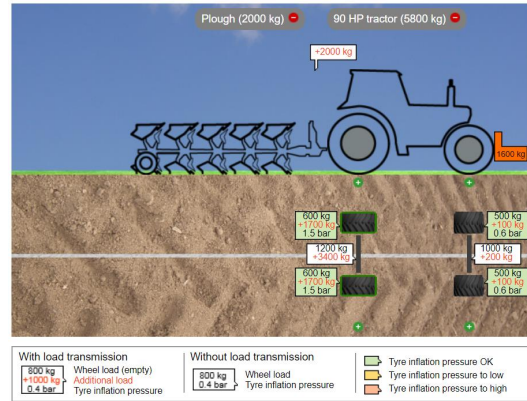

FIGURE 3. MACHINE AND TYRE CHARACTERISTICS IN TERRANIMO® INPUT TAB

IV. RESULTS AND DISCUSSION

A. PTFs development

Method	LU	PTF Equations - *SPSS*	MAE	RMSE	R²	R² (adj)
PCS_Cas	CL	1,463 - 0,017 Cl + 0,148 OC + 0,187 pF + 0,584 BD - 0,027 StI	-4,5	161,5	0,313	0,267
	GL	2,252 - 0,004 Si + 0,032 Cl	-34,1	147,4	0,200	0,159
PCS_L1	CL	2,133 - 0,019 Cl + 0,001 PSS + 0,065 CSR - 0,029 StI	5,1	39,6	0,193	0,151
	GL	0,918 - 0,005 Si + 0,023 Cl + 0,430 pF - 0,001 PSS + 0,205 CSR	-4,2	31,8	0,318	0,224
PCS_L2	CL	1,732 - 0,029 Cl + 0,337 BD + 0,195 CSR - 0,019 StI	-11,8	55,1	0,193	0,151
	GL	-0,487 - 0,003 Si + 0,515 pF + 0,964 BD - 0,002 PSS + 0,304 CSR - 0,036 StI	-9,0	37,7	0,279	0,152
PCS_L3	CL	1,125 - 0,014 Cl + 0,141 OC + 0,169 pF + 0,644 BD - 0,047 StI	-14,9	94,8	0,364	0,322
	GL	2,352 - 0,005 Si + 0,427 OC - 0,047 StI	-17,8	79,4	0,141	0,073
PCS_L4	CL	1,372 - 0,002 Si - 0,028 Cl + 0,184 OC + 0,163 pF + 0,656 BD + 0,130 CSR - 0,068 StI	-23,2	87,9	0,417	0,362
	GL	2,429 - 0,005 Si + 0,380 OC - 0,049 StI	-13,5	-73,2	0,185	0,120
PCS_G3	CL	3,219 - 0,101 OC - 0,0533 BD	-28,2	76,8	0,183	0,152
	GL	1,192 + 0,017 Cl + 0,533 pF - 0,002 PSS + 0,091 CSR	-23,6	63,0	0,455	0,396
PCS_Gomp	CL	2,608 - 0,003 Si - 0,080 CSR	-75,8	184,2	0,105	0,071
	GL	-0,440 + 0,052 Cl + 0,248 OC + 0,770 pF + 0,519 BD - 0,003 PSS	-48,8	150,2	0,401	0,318

TABLE 1. PTF EQUATIONS AND PREDICTABILITY COEFFICIENTS BY SPSS FOR EACH PCS CALCULATION METHOD AND LAND USE.

Cropland. Soil properties that significantly contributed to the PCS estimation and appeared in most of these PTFs equations (Table 1) were: Structural quality Index (StI) and Clay content (Cl), which were negatively correlated, and Bulk Density (BD), Organic matter Content (OC) and Clay/Sand ratio (CSR) which were positively correlated. This is in agreement with most of the PTFs found in literature.

The strongest PTF correlation amongst selected predictors was calculated with PCS_L4 (R^2 = 0.417) (Figure 5). However, in terms of accuracy, the lowest error deviation was given by PCS_L1 (MAE = 5.1; RMSE = 31.6). In addition, these PCS values are very well fitted to the predicted values (PCS_L2 as well, (Figure 4)). However, it is shown that a range of PCS values was poorly predicted with both methods compared to other methods results (< 150 kPa).
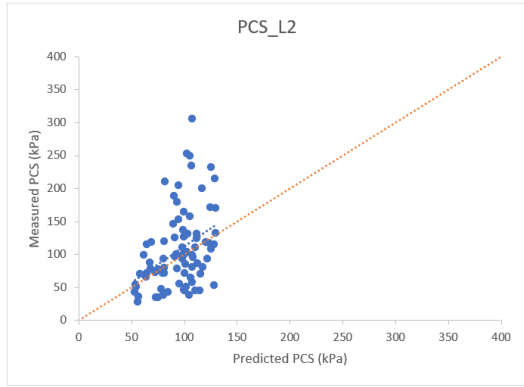
FIGURE 4. PCS PREDICTED (X-AXIS) VS. PCS MEASURED (Y-AXIS) IN CROPLAND WITH PCS_L2 METHOD

FIGURE 5. PCS PREDICTED (X-AXIS) VS. PCS MEASURED (Y-AXIS) IN CROPLAND WITH PCS_L4 METHOD.

FIGURE 6. PCS PREDICTED (X-AXIS) VS. PCS MEASURED (Y-AXIS) IN GRASSLAND WITH PCS_L1 METHOD.
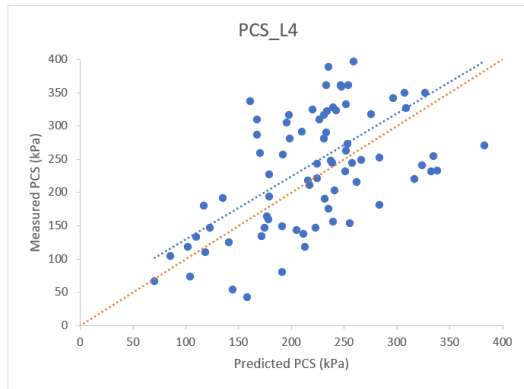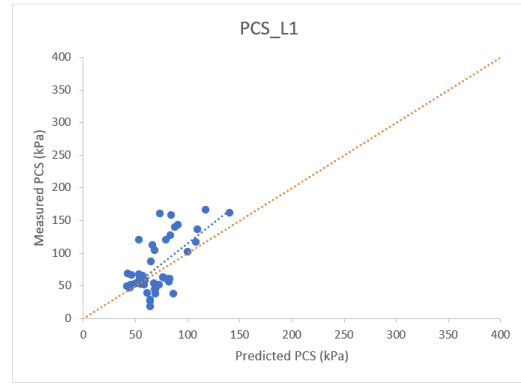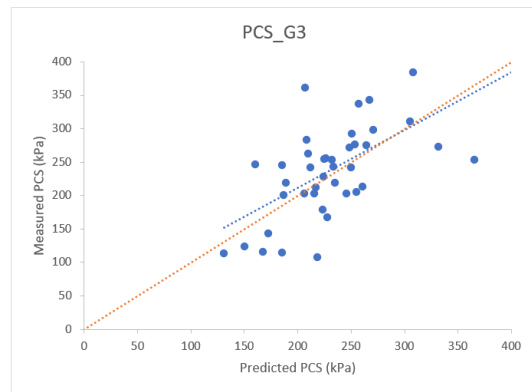

FIGURE 7. PCS PREDICTED (X-AXIS) VS. PCS MEASURED (Y-AXIS) IN GRASSLAND WITH PCS_G3 METHOD.

Grassland. Predictors that significantly contributed to most of the PTFs equations (Table 1) were: Silt content (Si) and Preload Suction Stress (PSS), which were negatively correlated, and Organic matter (OC) and Matric potential (pF), which were positively correlated. These results also agree with most of the literature shown above.

Based on the coefficient of determination, the best correlation was obtained by method PCS_G3 (R^2 = 0.455). Based on the estimation error, the best prediction was done again with PCS_L1 outcomes (MAE = - 4.2; RMSE = 31.8) (Figure 6), but, similarly as above, PCS values were quite underestimated. However, it is shown that PCS_G3 method gave a very good regression performance by fitting to the predicted values line (Figure 7).

By comparing cropland and grassland plots, PCS values for cropland results are more dispersed and its variability is higher, in agreement with [1]. This can be attributed to frequent passes of tractor wheels along this section. The predicted PTFs are in accordance as well with Terranimo® findings [12].

Regarding method of calculation, it should be noted that the inflection point of a fourth-degree polynomial method does not depend on the choice of pre-set stresses, nor does it assume a sigmoid shape or a linear VCL and subjectivity is eliminated [4]. Therefore, PCS_Gomp method is robust, and the resulting PCS showed a significant relation with the soil properties and stress history of the soil.

B. Terranimo® practical case

Soil stress vs. soil (yield) strength up to 1.0 m depth (Figure 8) shows that, for the first 20 cm, rear wheels (brown curve) are inside the transition (yellow) zone, where soil stress is 75-125% of soil strength. Consequently, considerable risk of

compaction could be expected, and special caution should be considered.
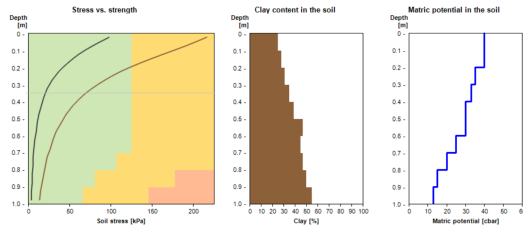

FIGURE 8. STRESS VS. STRENGTH – CLAY CONTENT – MATRIC POTENTIAL.

Next, the following 3D diagram (Figure 9) shows the vertical stresses and contact characteristics and pressures at the soil/tyre interface. We notably observe maximum stresses of 240 kPa and mean ground pressures of 104 kPa for the rear wheels.
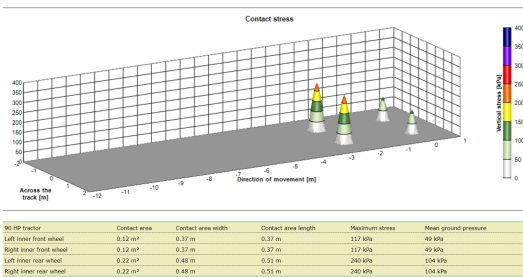

FIGURE 9. 3D DIAGRAM OF THE CONTACT PRESSURE.

Finally, soil stress propagation based on the Söhne model is shown at the rear axle (Figure 10). Again, highest stresses are expected for the rear wheels, which are around 250 kPa at a surface level (0.10 m depth). This behaviour is normal since rear axle has to carry most of the tractor weight plus the extra 2 tones due to the plough. Hence, based on this analysis performed in Terranimo®, we can conclude that no severe risk of compaction will be expected, except for the 10 cm depth at the rear wheels, where special caution should be put.
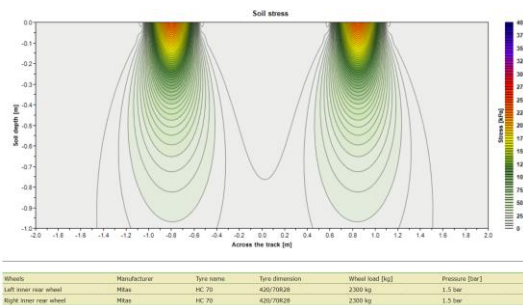

FIGURE 10. SOIL STRESS PROPAGATION AT THE REAR AXLE.

V. CONCLUSIONS

Soil compaction assessment and prediction is extremely important for reaching a well and controlled soil behaviour. From a soil physics perspective, compaction is a risk and the goal is to minimize its effect on field crops. From a geotechnical point of view, soil compaction and consolidation should be managed on purpose for a better foundation resistance.

Which ideal tests should be performed will depend on the situation and, mainly, on the specialist knowledge and experience. We encourage further development on new compaction tests, especially for the agricultural applications, given that most of the actual tests were specifically developed for engineering purposes.

Precompression stress is widely used as a threshold value to assess when the soil will suffer severe risk of compaction and unrecoverable deformation. However, its concept is questionable in this context since it was proved that little residual strain, after loads being released, appeared before reaching the PCS value. Therefore, further investigation should be done.

Different factors affecting PCS estimation of strain-stress relationships from compression tests were studied, such as method used, loading duration, soil properties, moisture content, etc. Regarding which direct estimation method is the optimal, despite there are some methods more robust than others, it can be concluded that for an adequate evaluation, a set of several performances should be carried out to compare and analyse different results, considering that they are not interchangeable.

Pedotransfer functions are in theory a very interesting and strong tool in predicting the precompression stress parameter. There are some PTFs equations in literature that estimate PCS from a wide variety of soil properties as predictors variables. Some of the most and stronger ones are soil particle size distribution, bulk density, matric potential, and OM content, in agreement with our own PTF development. Nevertheless, we highly recommend a more extended research since the obtained equations have, to some extent, low coefficients of determination.

Finally, this study showed that Terranimo® is a formidable user-friendly tool to determine stresses transmitted through the soil profile by agricultural machinery, which are mainly affected by machinery weight, tyre inflation pressure and soil water conditions. It should be noted that it is important to respect the recommended inflation pressure by the tyre manufacturer, since little deviation could cause high detrimental effects on our soil. In addition, one should avoid driving when water content and moisture conditions are significant. Thus, as a conclusion, Terranimo® is a powerful tool to evaluate the risk of soil compaction in cultivated field and should be much more recognised.

REFERENCES

[1] Alosnos, Elmer (2015). Determination and Prediction of Risk to Soil Compaction from Agricultural Operations. Master dissertation. UGent.

[2] Briaud, Jean-Louis (2013). Introduction to geotechnical engineering: unsaturated and saturated soils. 172-190.

[3] Cavalieri, K. M. V., Arvidsson, J., da Silva, A. P. and Keller, T. (2008). Determination of precompression stress from uniaxial compression tests. Soil and Tillage Research, 98(1):17–26.

[4] De Pue, Jan (2019). Advances in modelling vehicle-induced stress transmission in relation to soil compaction. Ghent University – Faculty of bioscience engineering. 63-81.

[5] Keller, Thomas (2004). Soil Compaction and Soil Tillage – Studies in Agricultural Soil Mechanics Department of Soil Sciences. Doctoral thesis. Swedish University of Agricultural Sciences, Uppsala.

[6] Keller, T., J. Arvidsson, J.B. Dawidowski, A.J. Koolen (2014). Soil precompression stress II. A comparison of different compaction tests and stress–displacement behaviour of the soil during wheeling. Soil & Tillage Research. Volume 77, Issue 1, Pages 97-108.

[7] Lamandé, M. and Schjønning, P. (2011). Transmission of vertical stress in a real soil profile. Soil and Tillage Research. Volume 114, Issue 2, Pages 71-77.

[8] Lebert, M. and Horn, R. (1991). A method to predict the mechanical strength of agricultural soils. Soil and Tillage Research, 19(2-3):275–286.

[9] Schjønning, P, Lamandé, M., Keller, T., Pedersen J., Stettler, M. (2012). Rules of thumb for minimizing subsoil compaction. Volume 28, Issue 3. Pages 378-393

[10] Schjonning & Lamande (2018). Models for prediction PCS from readily available soil properties. Volume 320, Pages 115-125

[11] Schjønning, P., Matthias Stettler, Thomas Keller, Poul Lassen, Mathieu Lamandé (2015). Predicted tyre–soil interface area and vertical stress distribution based on loading characteristics. Volume 152, Pages 52-66.

[12] Schjønning, P., Lamandé, M. (2020). An introduction to Terranimo. Aarhus University, Dept. Agroecology.

[13] Schjønning, P., Lamandé, M., Tøgersen, F.A., Arvidsson, J., Keller, T., (2008). Modelling effects of tyre inflation pressure on the stress distribution near the soil-tyre interface. Biosyst. Eng. 99, 119–133.

[14] Jan De Pue, Gemmina Di Emidio, Adam Bezuijen, Wim M. Cornelis (2019). Functional evaluation of the various calculation methods for precompression stress

[15] De Lima, R.P, Keller, T. (2019). Impact of sample dimensions, soil-cylinder wall friction and elastic properties of soil on stress field and bulk density in uniaxial compression tests. Pages 15-24.

Table of content

List of figures and tables

Figures

CONTENT

Tables

List of symbols and abbreviations

Symbols

σ	Total normal stress
σ'	Effective normal stress
σ_v	Vertical stress
u	Pore water pressure
u_s	Static pore water pressure
u_e	Excess pore water pressure
e	Void index
w	Water content
w_{opt}	Optimum water content
ρ	Bulk density
ρ_d	Dry density
γ_d	Dry unit weight
γ_w	Water density
C_c	Compression index
C_e	Expansion index
G_s	Soil specific gravity
σ'_p	Precompression stress / preconsolidation pressure
W_w	Water weight of the sample
W_d	Weight of dry sample
W_t	Total weight of the sample
V_t	Total volume of the sample
S	Degree of Saturation
ε	Strain
d	Diameter of the sample
h	Height of the sample
c	Cohesion
ϕ	Angle of internal friction
K_{sat}	Saturated Hydraulic conductivity
V_{tc}	Tyre carcass volume
F_w	Wheel load
L	Tyre deflection
K_r	Tyre inflation pressure

Abbreviations

PCS	Precompression stress
BD	Bulk density
PTF	Pedotransfer function
PD	Packing density
SPCT	Standard Proctor Compaction Test
MPCT	Modified Proctor Compaction Test
CRS	Constant Rate of Strain
CBR	California Bearing Ratio
CPT	Cone Penetration Test
SPT	Standard Penetration Test
VCL	Virgin Compression Line

1. Introduction

1.1 Background

Soil is a heterogeneous natural medium that supports life on earth. Being integral to the functioning of the environment, healthy soils provide a range of ecosystem services very useful for our common welfare, such as resisting erosion, receiving and storing water, retaining nutrients and forming a hospitable medium for crops. Nowadays, soils are clearly suffering the devastating effects of global warming, affecting, and putting extra pressure on soil functions. Therefore, preserving and maintaining them in a good quality, as well as efficient soil management and sustainable agriculture become even more important.

One of the main factors that affect soil quality is the degradation by compaction. Soil compaction is the process of densification and distortion of soil by which porosity is reduced, causing deterioration or loss of one or more soil functions (van den Akker, 2008). This process occurs naturally in soil evolution; however, in cultivated soils, it is mainly linked to the passage of agricultural machinery, animals on pasture, climate, or biological activity.

Compaction in agricultural soils is mainly caused by the expansion of highly mechanized crop production systems with intensive field traffic, which places high stresses on the soil. Subsoil compaction occurs when we reach certain depths where conventional ploughing techniques can no longer restore the compacted layer and no clear exposures are visible. Consequently, soil compaction is one of the most difficult soil degradation processes to detect and correct. In Europe, it was recognized by the Commission of the European Communities (2006) as one of the most frequent and challenging threats that affect soil quality in agriculture. Globally, around 68 million hectares are affected by human-induced soil compaction where Europe and Africa contribute around 49% and 26%, respectively (Bouma and Batjes, 2000).

Soil compaction has numerous negative effects on soil quality. One main consequence is the reduction in through flow of water and air. The settlement originating from the compaction results in an increase in mechanical strength and decrease in mass transfer capacity due to their densification. (Radford et al., 2000; Hamza and Anderson, 2005). From an agricultural production point of view, soil compaction reduces germination rate and root colonization (Kirkegaard et al., 1992; Passioura, 2002), which can lead to a reduction in crop efficiency or to greater inputs of water and fertilizer, thereby increasing production costs. If plant growth is reduced, there is a decrease in the inflow of fresh organic matter to the soil, therefore, quantities of mineralizable nutrients are reduced. In addition, soil workability is reduced, soils are harder and will require more fossil energy to re-fragment packed soil.

From an environmental point of view, the impacts of soil compaction have been synthesized by Soane and Van Ouwerkerk (1994); e.g. the reduction of water infiltration notably increases the incidence of runoff and water erosion phenomena. Additionally, emissions gases associated with denitrification raise in compacted soils by the reduction of oxygen diffusion and hydraulic conductivity (Renault and Stengel, 1994).

As it is observed, nowadays, soil compaction is an important issue. Preventing this process from happening can be done by evaluating its risk. A proper assessment and well prevention would be very useful for farmers and policymakers in order to avoid this phenomenon.

The intensity of soil compaction under the passage of agricultural machinery depends on two factors: mechanical stresses applied by the machinery and mechanical strength of the soil. The stresses applied to the ground depends on the weight of the machine, its forward speed, tyre characteristics and tyre inflation pressure (Larson et al., 1994; Chamen et al., 2003). The strength of the soil mainly depends on the frequency of gear passing, soil mechanical characteristics and hydraulic properties, such as soil texture, water content, loading-unloading historical processes, porosity and bulk density.

Analysis of the risk to soil compaction is typically a three-step procedure. Firstly, the boundary conditions by the stress distribution at tyre-soil interface are estimated. Secondly, stress transmission and propagation through the soil profile is determined. Lastly, the soil stress is compared to the soil strength. Non-recoverable soil deformation occurs if the soil strength is exceeded (Horn and Lebert, 1994; Schjønning et al., 2015b). Based on this idea, the computer model Terranimo® is an interesting and useful decision support tool that predicts the risk of soil compaction by farm machinery. This model is analysed and discussed in Chapter 4.

Soil strength is mainly described by two mechanical parameters: precompression stress (PCS) and the compression index (C_c). C_c corresponds to the slope of the compression curve and indicates the rate of permanent deformation. Precompression stress is used as a conservative criterion for susceptibility to compaction. In the compression curve, PCS is the stress at which soil deformation shifts from elastic (recoverable) strain to plastic (non-recoverable) strain. The compression curve (stress-strain curve) is estimated by oedometric tests from the e-log σ_v compression curve, linking void ratio (e) to vertical stress (σ_v) exerted on the sample. Basically, the goal is to minimize the risk of undesirable changes in soil structure due to compaction by limiting the mechanically applied effective stress below PCS values (Horn and Lebert, 1994; Alexandrou and Earl, 1998; Dawidowski et al., 2001). The precompression stress concept and the methods on how it can be estimated are described in Chapter 3.

Nevertheless, the applicability of PCS for unsaturated, structured soils is questionable, as non-recoverable strain occurs already at much lower stresses (Dexter, 1975; Arvidsson and Keller, 2004; Keller et al., 2011). One important constraint is that there is no standardized lab procedure or calculation method to determine PCS; instead, there are various alternative methods based on different approaches. Furthermore, it was found in previous studies that these methods are not interchangeable, and their interpretation could be highly subjective (Arvidsson and Keller, 2004; Cavalieri et al., 2008; De Pue et al., 2020). One important limitation to consider is the lack of easily accessible and representative soil mechanical properties to estimate PCS. In addition, conventional oedometer tests to determine PCS from estimated compression curves are often rigorous and time-consuming. Thus, pedotransfer functions (PTFs) are often used as a very useful and rapid alternative to estimate the desired mechanical properties (e.g. precompression stress).

1.2   Main objectives

A Flemish interdisciplinary team at UGent (Laboratory of Geotechnics, Faculty of Engineering and Architecture (FEA), and Soil Physics Research group, Faculty of Bioscience Engineering (FBE)) is currently cooperating on soil compaction issues with MSc and PhD students in a recently finished European project and an ongoing VLIR-TEAM project (the aim is now to apply the acquired knowhow also in the South, particularly in Bolivia). The major objectives of this cooperation are:

1. To raise awareness on the (economic and environmental) impact of soil compaction.

2. To prevent (further) soil degradation as caused by compaction related to land use, soil type and climate.

3. To extend a decision support tool to evaluate risk to soil compaction with innovations in agricultural tractor machinery.

4. To reduce the risk of soil compaction, through both practice (e.g. farmers) and policy (e.g. regional administration), using the decision support tool.

It is important to clarify that this study primarily concerns the risk to soil compaction on agricultural and environmental soils, which is a matter addressed by the field of Soil Physics. However, it must be emphasised that from an engineering point of view, the soil compaction concept might differ. Therefore, a geotechnics approach comparison was also considered.

The main objectives of this thesis dissertation are:

1. To define and study the soil compaction context by making a comparison between two different approaches: Soil physics vs Geotechnics.

2. To assess the risk to soil compaction by agricultural machinery based on the analysis of the precompression stress (PCS) concept and its calculation methods.

3. To develop new PTFs to estimate PCS based on a dataset from Flemish agricultural land and to investigate the effects and correlations of several soil properties on PCS.

4. To gain insights on how Terranimo© risk assessment tool works related to soil compaction and PCS previous analyses.

1.3   Structure of the master dissertation

The structure of this thesis is divided into five chapters. Each of these chapters is subdivided into several sections, depending on their content, as shown in the Table of Content.

The first chapter, Chapter 1, which ends in this section, is the introductory part where the situational context, objectives and structure are presented.

In Chapter 2, soil compaction is discussed and compared from two different approaches: Geotechnics vs Soil physics. We analyse the concept itself, its characteristics, laboratory and in-situ testing.

The following chapter, Chapter 3, refers to relevant matters in relation to the concept of precompression stress. We study the methods of PCS direct estimation from uniaxial compression stress (from geotechnics and soil physics approaches) and the main factors affecting it. We also analyse the PCS indirect estimation by pedotransfer functions, comparing some of the already developed ones and developing new ones, as well as we investigate the effect of different soil properties on the estimated PCS value.

In Chapter 4 we talk about Terranimo®, how this tool can be properly used to investigate and predict the risk of soil compaction by agricultural machinery and we examine its functionality by performing a practical case.

Finally, Chapter 5, we close this thesis dissertation with relevant outcomes, final conclusions, and further recommendations on soil compaction research.

2. Soil Compaction approaches: Geotechnics vs Soil Physics

2.1 Introduction

In *geotechnics* and *soil mechanics*, when it comes to soil **compaction**, it refers to the process of densification of, typically, an unsaturated soil by expulsion of air from its voids under application of stress or mechanical pressure. In soil engineering, compaction is often intended for the purpose of improving soil resistance and bearing capacity. This process is normally quick, and it does not affect the water content. In this way, a differentiation can be made with soil **consolidation**, despite both processes causing a reduction in the volume of the soil due to its compressibility characteristics. Consolidation is a slow process in which long-term and static loading cause a densification, normally, of the saturated soil by expulsion of the pore water. It naturally occurs due to structural loads from foundations.

In *soil physics* and *agronomy*, **soil compaction** encompasses a **combination** of **both** engineering processes, compaction and consolidation. In contrast to geotechnics, in which soil compaction was intended on purpose, here, the purpose is to prevent this process from happening. As will be explained in the next section, compaction might provoke several detrimental effects on agricultural soils.

2.2 Concept

Geotechnics

According to R.F. Craig's book (2004): *"Craig's Soil Mechanics"*:

Soil can be visualized as a skeleton of solid particles enclosing continuous voids which contain water and/or air. For the range of stresses usually encountered in practice the individual solid particles and water can be considered incompressible; air, on the other hand, is highly compressible. The volume of the soil skeleton as a whole can change due to rearrangement of the soil particles into new positions, with a corresponding change in the forces acting between particles. The actual compressibility of the soil skeleton will depend on the structural arrangement of the solid particles. In a fully saturated soil, since water is considered to be incompressible, a reduction in volume is possible only if some of the water can escape from the voids. In a dry or a partially saturated soil, a decrease in volume is possible due to a reduction in air-filled porosity, resulting in particle rearrangement.

Shear stress can be resisted only by the skeleton of solid particles, by means of forces developed at the interparticle contacts. Normal stress may be resisted by the soil skeleton through an increase in the interparticle forces. If the soil is fully saturated, the water filling the voids can also withstand normal stress by an increase in pressure.

The importance of the forces transmitted through the soil skeleton from particle to particle was recognized in 1923 when Terzaghi presented the **principle** of **effective stress**, an intuitive relationship based on experimental data. The principle applies only to *fully saturated* soils and relates the following three stresses:

- Total normal stress (σ) on a plane within the soil mass, being the force per unit area transmitted in a normal direction across the plane, imagining the soil to be a solid (single-phase) material.

- Pore water pressure (u), being the pressure of the water filling the void space between the solid particles.

- Effective normal stress (σ') on the plane, representing the stress transmitted through the soil skeleton only.

The relationship is:

$$\sigma = \sigma' + u$$

As an illustration of how effective stress responds to a change in total stress, consider the case of a fully saturated soil subject to an increase in total vertical stress and in which the lateral strain is zero, volume change being entirely due to deformation of the soil in the vertical direction. This condition may be assumed in practice when there is a change in total vertical stress over an area which is large compared with the thickness of the soil layer in question.

It is assumed that the initial pore water pressure is constant at a value governed by a constant position of the water table. This initial value is called the static pore water pressure (u_s). When the total vertical stress is increased, the solid particles immediately try to take up new positions closer together. However, if water is incompressible and the soil is laterally confined, no such particle rearrangement, and therefore no increase in the interparticle forces, is possible unless some of the pore water can escape. Since the pore water is resisting the particle rearrangement the pore water pressure is increased above the static value and with it the total stress also increases.

The increase in pore water pressure will be equal to the increase in total vertical stress, e.g. the increase in total vertical stress is carried entirely by the pore water.

The increase in pore water pressure causes a pressure gradient, resulting in a transient flow of pore water towards a free-draining boundary of the soil layer. This flow or **drainage** will continue until the pore water pressure again becomes equal to the value governed by the position of the water table. The component of pore water pressure above the static value is known as the excess pore water pressure (u_e).

At any time during drainage the overall pore water pressure (u) is equal to the sum of the static and excess components:

$$u = u_s + u_e$$

The reduction of excess pore water pressure as drainage takes place is described as dissipation and when this has been completed (e.g. when $u_e = 0$) the soil is said to be in the *drained* condition. Prior to dissipation, with the excess pore water pressure at its initial value, the soil is said to be in the *undrained* condition.

As drainage of pore water takes place the solid particles become free to take up new positions with a resulting increase in the interparticle forces. In other words, as the excess pore water pressure dissipates, the effective vertical stress increases, accompanied by a corresponding reduction in volume. When dissipation of excess pore water pressure is complete the increment of total vertical stress will be carried entirely by the soil skeleton. The time taken for drainage to be completed depends on the permeability of the soil. In soils of low permeability, drainage will be slow, whereas in soils of high permeability, drainage will be rapid. The whole process is referred to as **consolidation**.

When a soil is subject to a *reduction* in total normal stress the scope for volume increase is limited because particle rearrangement due to total stress increase is largely irreversible. As a result of increase in the interparticle forces there will be small elastic strains (normally ignored) in the solid

particles, especially around the contact areas, and if clay mineral particles are present in the soil, they may experience bending. In addition, the adsorbed water surrounding clay mineral particles will experience recoverable compression due to increases in interparticle forces, especially if there is face-to-face orientation of the particles. When a decrease in total normal stress takes place in a soil there will thus be a tendency for the soil skeleton to expand to a limited extent, especially in soils containing an appreciable proportion of clay mineral particles. As a result, the pore water pressure will be reduced, and the excess pore water pressure will be negative. The pore water pressure will gradually increase to the static value. Therefore, flow is taking place into the soil, accompanied by a corresponding reduction in effective normal stress and increase in volume. This process, the reverse of consolidation, is known as **swelling**.

Consolidation *settlement* is the vertical displacement of the surface corresponding to the volume change at any stage of the consolidation process. To study, predict and prevent consolidation settlements is one of the main goals and probably the hardest for a geotechnical engineer.

On the other hand, **compaction** is the process of increasing the density of a soil by packing the particles closer together with a reduction in the volume of air; there is no significant change in the volume of water in the soil. The degree of compaction of a soil is measured in terms of *dry density*, ρ_d , e.g. the mass of solids only per unit volume of soil. The dry density of a given soil after compaction depends on the water content and the energy supplied by the compaction equipment (referred to as the compactive effort).

Soil Physics

Soil compaction has been studied for many years due to its implications for crop yield. Due to decades of increasing mechanization in agriculture, this process has become a worldwide threat to sustainable agriculture owing to its various adverse impacts on soil quality, crop growth and the environment (Huber et al., 2008; Keller et al., 2013; Unger and Kaspar, 1994).

Natural processes such as weight of overlying soil, rain impact, drying and shrinking of clay, and penetration of plant roots induce compaction on soil. However, the process as a result of advanced farm mechanization is more alarming. Considering the important role played by several interacting factors related to machinery, soil, crop and weather, soil compaction is now regarded as a *multi-disciplinary problem* with great importance (Soane and Ouwerkerk, 2013). As world agriculture is challenged to achieve a viable production to feed the ever-growing populations, the need for highly efficient field operations often associated with use of heavy machinery becomes inevitable.

Soil compaction may decrease soil porosity and change pore shape and pore size distribution (Pagliai et al., 2003), decrease aeration (Czyz et al., 2001), decrease water infiltration and increase preferential flow (Kulli et al., 2003), and increase surface runoff with consequent topsoil erosion (Horn et al., 1995). Other indirect effects of soil compaction are increased tillage work (Arvidsson, 1998), increase in greenhouse gas emissions (Ball et al., 1999) and increase in the C:N ratio of the soil (De Neve and Hofman, 2000).

The environmental deterioration of the soil structure resulting from subsoil compaction has a *negative effect* on crop yield due to restricted root growth, reduced biological activity and decreased water accessibility for plants (Schjonning and Rasmussen, 1994; Arvidsson and Hakansson, 1996; Hansen, 1996). Detrimental effects of subsoil compaction may persist for several decades and is thus a threat to the long-term productivity of the soil and its ecological functions (Etana and Hakansson, 1994; Hakansson and Reeder, 1994; Soane and van Ouwerkerk, 1994).

Compaction may occur on the land surface, within the tilled layer. However, it is beneath the primary tillage depth where compaction is more noticeable. The influence of compaction on pore

geometry is complex. It depends on several factors, such as the soil structure, soil composition, water content and the intensity or duration of the process.

Mechanization in modern agriculture and the continuing trend towards larger vehicles implies an increase in the mechanical stresses reaching subsoil layers (Schjønning et al., 2015a) and therefore, an increase in the risk of subsoil compaction (Chamen et al., 2003). Hence, it is important to develop tools to identify the risk of soil compaction and there is a need for technical solutions that reduce the compaction risk at high total loads.

In order to predict soil compaction due to the stress applied by farm vehicles in motion, different models have been proposed. These models contain three main components. The first component consists of the upper boundary conditions: contact area and vertical stress distribution at the *soil/tyre interface*. The second one is the *stress propagation* through the soil profile. The third component is the resulting soil deformation, which can be estimated based on the stress–strain relationship of the specific soil of interest.

Soil compaction models can be divided into two categories, depending on whether the propagation of the stresses is treated independently or not to the computation of the strains. These two categories are pseudo-analytical models and numerical finite element models (FEM) (Défossez and Richard, 2002). The *pseudo-analytical models* first calculate the distribution of stresses in the soil and then, in a second step, the increase in density. On the contrary, models based on the *finite element method* (FEM) calculate simultaneously stresses and deformations of the soil.

Pseudo-analytical models have proved to be satisfactory to homogeneous structures and they are simpler to use than FEM models. However, cultivated soils are inhomogeneous media, so soil mechanical properties are very variable, and this could lead to misinterpretation.

The pseudo-analytical models are the most currently used to predict the risk of agricultural soil compaction (Van den Akker, 2004 ; Arvidsson et al., 2001; Défossez et al., 2003). Finite element models present the advantage of being able to consider the spatial heterogeneities of the mechanical properties of agricultural soils.

One very common approach used in risk assessment involves a quantitative comparison of stress transmitted to the soil profile with soil strength (van den Akker and Hoogland, 2011). This includes modelling of stresses from machinery in combination with estimates of soil mechanical strength from *pedotransfer functions* (PTFs) using readily available soil properties. The stress distribution in a tire-soil contact area may be predicted from tire characteristics (Schjønning et al., 2015a). Transmission of stress from the through the soil profile can be reasonably estimated using the analytical solution obtained by Boussinesq (1885) for the problem of normal loading of the surface of a homogeneous, isotropic, elastic half-space by a concentrated normal force (Keller and Lamandé, 2010). Soil strength, in turn, may be estimated from only three soil parameters: clay content, dry bulk density, and matric potential (Schjønning and Lamandé, 2018). This approach is primarily based on the concept of precompression stress, which is covered in Chapter 3.

The use of *decision support systems* (DSS) in agriculture paved a way for the establishment of useful recommendations for appropriate soil management practices and site-specific solutions to soil compaction problems (Canillas and Salokhe, 2001). Through effective DSS, farmers can predict the potential impact of several factors such as tire specifications, wheel load, inflation pressure, and soil properties on soil structure. For instance, web-based decision support tools such as Terranimo (http://www.terranimo.dk) enables to simulate the complex dynamics when arable soil is loaded with machinery. The *Terranimo® model* (Lassen et al., 2013; Stettler et al., 2014) assesses the risk of soil compaction by comparing the externally applied soil stress and the soil precompression stress. It was already tested on many sites in Nordic countries with most studies

focusing on measuring and simulating soil stress distribution and propagation (Arvidsson and Keller, 2007; Keller, 2005; Schjønning et al., 2008). The tool is useful for farmers and their advisors interested in reducing compaction of their soils by modifying the machinery operating conditions with the prevailing soil characteristics. Terranimo is analysed and discussed in detail in Chapter 4.

However, whether the predicted risks are effectively reflected in a change of soil physical quality has been hardly tested. Moreover, studies that evaluate the effects of soil compaction on a range of soil physical quality indicators are few, especially field studies and short-time experiments or experiments with a lower (but realistic) amount of passes. In these cases, differences in soil physical quality are more difficult to detect and the compaction effects are often not clear (Arvidsson and Håkansson, 2014).

Agricultural engineers should work on the development of better wheel or track systems for use with higher total machine mass (Kutzback, 2000). According to van den Akker et al. (2003), future work in subsoil compaction in Europe should include the development of technical methods to reduce subsoil compaction, such as reducing tyre inflation pressure, ploughing on-land, different wheel arrangements, tracks instead of wheels or automated low-weight machinery.

Soil stress is determined by tyre dimensions, tyre inflation pressure, wheel load and soil properties, including soil wetness. Tyre inflation pressure is the factor most easily adaptable. It directly affects the tyre-soil contact area, which in turn affects soil stress and its distribution. Within a certain range, soil stress increases with tyre pressure and it could explain most variation in soil stress in both top and sub soil layers under different wheel loads (Schjønning et al., 2012). According to the elasticity theory, for a given load applied to a given soil, an increase in soil water content yields a higher concentration of stresses under the centre of the load and a deeper propagation of stresses (Lamandé and Schjønning, 2011).

With soil stress being highly determined by tyre pressure, manufacturers of tyres recommend tyre pressures for field operations depending on axle load, tyre model and size and tractor speed. These pressures are substantially lower than those recommended for road traffic. In practice, however, most farmers or contractors do not deploy a tyre pressure-control system and thus traffic their fields with inappropriate pressures

The weight of machines and their effect on soil properties is often described by axle load (e.g. Alakukku, 1996; Lal and Ahmadi, 2000;). However, Keller (2004) showed that not axle load or total vehicle load but wheel load, is more important to be considered and limited as a strategy to avoid subsoil compaction.

2.3 Characteristics

Geotechnics

Differences

Compaction	Consolidation
Expulsion of air	Expulsion of water
Short term loading	Long term loading
Dynamic loading	Static and constant loading
Quick process	Slow process

Any type of soil	Cohesive and low permeable soil
Unsaturated soils	Saturated soils
Purposely done (by compaction equipment) before construction	Naturally done (by structural loads) during or after construction
Improved soil properties: safer foundations, roads, dams, embankments	Associated to assessment of foundation settlements

Similarities

They cause a reduction in the volume (densification) of the soil which is due to its compressibility characteristics.

Shear strength increases.

Void ratio, compressibility and permeability decreases.

Bearing capacity and settlement characteristics improve.

Dry density increasement results in higher soil mechanical strength in the soil.

Purposes

To increase soil shear strength and therefore its bearing capacity and avoid swelling.

To increase stiffness and reduce subsequent settlement under working loads.

To reduce soil permeability making it more difficult for water to flow through.

Soil Physics

Compaction

Detrimental and unfavourable process.

Dry density increasement results in lower air permeability and hydraulic conductivity in the soil.

Soil physical properties will deteriorate. Soils become less able to absorb and conduct water and nutrients: increasing erosion and runoff and decreasing nutrients in the soil, efficiency of crops, etc.

Purpose

Assessing and preventing the risk of agricultural soils to soil compaction.

2.4 Laboratory tests

According to J.L. Briaud's book (2013): "*Introduction to geotechnical engineering: unsaturated and saturated soils*":

Laboratory testing, in situ testing and geophysical testing are the options a geotechnical engineer has to obtain the necessary soil information.

There are advantages and drawbacks to each one of those options (*Figure 1*). Among the advantages of laboratory tests are that they lend themselves to theoretical analysis, that the boundary conditions

can be controlled. Some of the drawbacks are the small scale of such testing and the influence of disturbance on the results.

Laboratory Testing		In Situ Testing	
Advantages	Drawbacks	Advantages	Drawbacks
Easier to analyze theoretically	Small-scale testing Time-consuming	Large-scale testing Relatively fast to perform	Difficult to analyze theoretically
Drainage can be controlled Elementary parameters easier to obtain Soil identification possible	Stresses must be simulated Some disturbance	Testing done under *in situ* stresses Less disturbance for some tests	Drainage difficult to control Elementary paramaters harder to obtain Soil identification rarely possible

Figure 1. Advantages and drawbacks of laboratory and in situ tests. Source: Geotechnical engineering: unsaturated and saturated soils, J.L. Briaud.

There are plenty of available laboratory tests in geotechnical engineering, as shown in *Figure 2*.
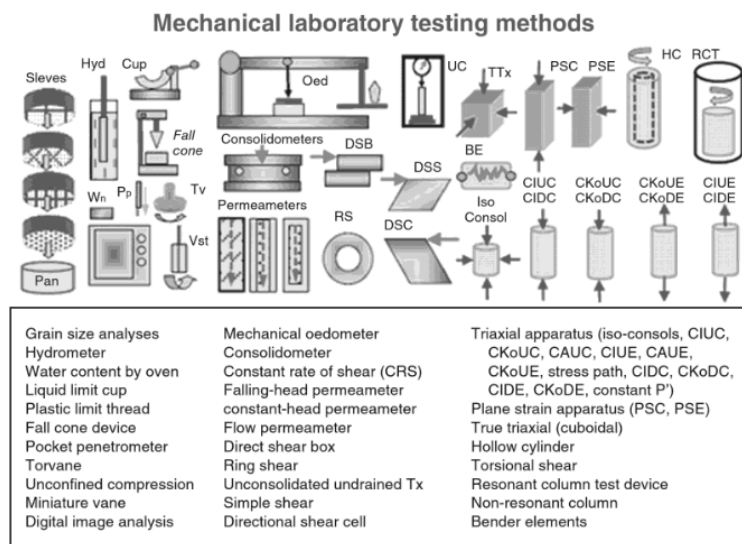
Figure 2. Laboratory tests. Source: Mayne et al. 2009. Courtesy of Professor Paul Mayne, Georgia Institute of Technology, USA

They are typically classified in the following main categories:

1. Tests for index properties (e.g. water content, unit weight, particle size, Atterberg limits).
2. Tests for deformation properties (e.g. consolidation, triaxial, simple shear, resonant column).
3. Tests for strength properties (e.g. direct shear, unconfined compression, triaxial, lab vane)
4. Tests for flow properties (e.g. constant head permeameter, falling head permeameter, erosion tests).

We have focused on the ones primarily related to the thesis topic, **compaction** and **consolidation tests**. One penetration resistance test was also added. For a better understanding, these tests have been divided into *saturated* or *unsaturated* conditions.

It should be noted that all these types of tests are primarily characteristic of the geotechnical field. However, it must be noted that some of them are also very commonly used in the soil physics approach, e.g. oedometer test.

2.4.1 Compaction tests

Unsaturated soils

Dry Unit Weight test

The compaction test dates back to the work of Ralph Proctor, an American civil engineer, in the early 1930s. Today, the test is actually two tests: **Standard Proctor Compaction Test** (SPCT; ASTM D698) and **Modified Proctor Compaction Test**, (MPCT; ASTM D1557). Proctor developed the SPCT, but in the late 1950s, as compaction machines became much bigger than in the 1030s, the MPCT was developed to better correspond to the higher energy generated by the larger roller compactors. In both cases, the result of the test is the dry unit wright or dry density (γ_d) vs. water content (w) curve (*Figure 3*).
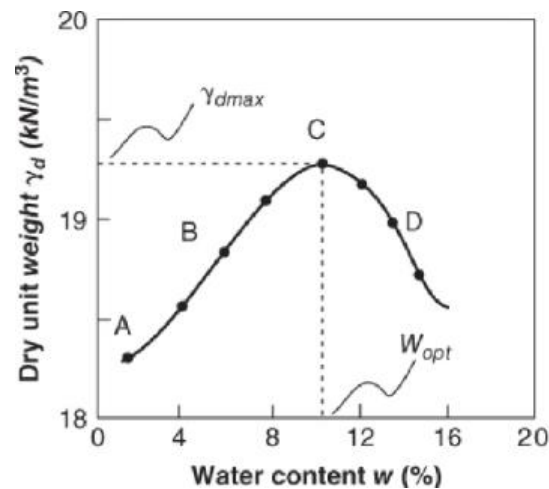
Figure 3. Compaction curve. Source: Geotechnical engineering, J.L. Briaud.

The first step in the **Standard Proctor Compaction Test (SPCT)** is to take a soil sample, dry it, break the clumps of soil down to individual particles (e.g. with a mortar and rubber-tip pestle) and measure its weight W_d. Then, calculate the weight of water W_w that must be added to the dry soil sample to reach a chosen water content w:

$$W_w = w \cdot W_d$$

Add the water to the soil and mix thoroughly. Weigh the empty compaction mould to be used for the test. Using the prepared soil mixture, place a first layer in the compaction mould (*Figure 4a*) and compact that layer of loose soil by dropping a standard compaction hammer a standard number of times. The blows should be distributed evenly across the soil layer to reach uniform compaction. Repeat this process for all layers and aim for the last layer to coincide with the top of the mould. Two mould sizes are used; *Table 1* gives the detailed requirements. At the end, weigh the mould plus soil and calculate the soil weight W_t. The dry unit weight is obtained by:

$$\gamma_d = \frac{W_t}{V_t(1 - w)}$$

where γ_d is the dry unit weight, W_t is the total weight of the soil sample in the mould, V_t is the total volume of the sample and w its water content. The combination of γ_d and w is the water content of the sample. By repeating the SPCT for different water contents, the compaction curve is described point by point (*Figure 3*). Note that this curve has a well-defined bell shape because the vertical scale is concentrated around the range of values within which the dry unit weight varies.
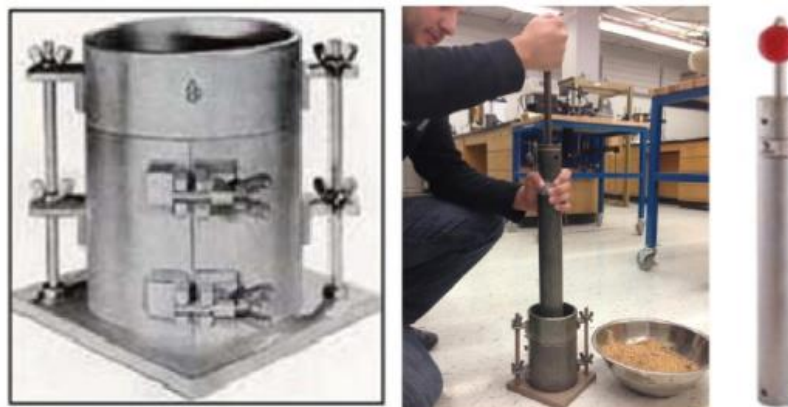
Figure 4. Compaction equipment: (a) Mould. (c) Hammer. (b) Compaction test. Source: courtesy of Forney LP, Hermitage, PA

102 mm diameter, 116 mm high mould	152 mm diameter, 116 mm high mould
3 soil layers	3 soil layers
25 blows per soil layer	56 blows per soil layer
Hammer weight 24.5 N	Hammer weight 24.5 N
Hammer drop height 305 mm	Hammer drop height 305 mm
Volume $9.43 \cdot 10^{-4}$ m^3	Volume $21.2 \cdot 10^{-4}$ m^3
Total energy 600 kN·m / m^3	Total energy 600 kN·m / m^3

Table 1. Standard Proctor Compaction test requirements. Source: Geotechnical engineering: J.L. Briaud.

The reason for this bell curve is that at point A (*Figure 3*), the soil is relatively dry, and it is difficult for a given compaction energy to bring the particles closer together. At point B, the water content is such that water tension exists between the particles and hinders the effectiveness of the compaction process. At point C, the water tension loses its effect and the primary role of the water is to lubricate the contacts between particles, thereby allowing the given compaction effort to reach a low void ratio and a high dry density. At point D, the soil is nearing saturation and the added water simply increases the volume of the voids, which negates the benefit of the compaction.

The compaction curve is bounded on the right side by the saturation line for a degree of saturation equal to 1. Indeed, the relationship between the dry unit weigh γ_d and the water content w is a function of the degree of saturation S:

$$\gamma_d = \frac{S \cdot G_s \gamma_w}{S + G_s w}$$

In 1958, a second compaction test, the **Modified Proctor Compaction Test (MPCT),** was developed as an ASTM standard. A higher compaction standard was necessary to better correspond to the larger and heavier compaction equipment, such as large vibratory compactors and heavier steam rollers. The MPCT is very similar to the SPCT except for the different requirements listed in next table. The data reduction is the same and the result is also the γ_d – w curve. The difference is that, due to the higher compaction effort (2700 kN·m/m^3) compared to 600 kN·m/m^3), the curve for the MPCT is located higher than the curve for the SPCT.

102 mm diameter, 116 mm high mould	152 mm diameter, 116 mm high mould
5 soil layers	5 soil layers
25 blows per soil layer	56 blows per soil layer
Hammer weight 44.5 N	Hammer weight 44.5 N

Hammer drop height 457 mm	Hammer drop height 457 mm
Volume $9.43 \cdot 10^{-4}$ m^3	Volume $21.2 \cdot 10^{-4}$ m^3
Total energy 2700 kN·m / m^3	Total energy 2700 kN·m / m^3

Table 2. Modified Proctor Compaction test requirements. Source: Geotechnical engineering, J.L. Briaud.

The peak of the curve has the coordinates maximum dry density, γ_{dmax} and optimum water content, w_{opt}. The specifications for field applications usually require that the water content be within $\pm$ x% of the optimum water content and that the dry density be at least y% of the maximum dry density. Then these requirements are checked by field testing at the compaction site (in situ testing).

Note that the dry unit weight is used on the vertical axis of the compaction curve and not the total unit weight. The reason is best explained through the example of *Figure 5*. Both soil A and B have a total unit weight of 20 kN/m^3, yet soil A has a dry unit weight of 17.5 kN/m^3 whereas soil B has a dry unit weight of 19 kN/m^3. Soil B has more solid constituents per unit volume and is therefore more compact. The selection of soil B over soil A can be made based on the dry unit weight (19 vs. 17.5) but not on the total unit weight (20 vs. 20).
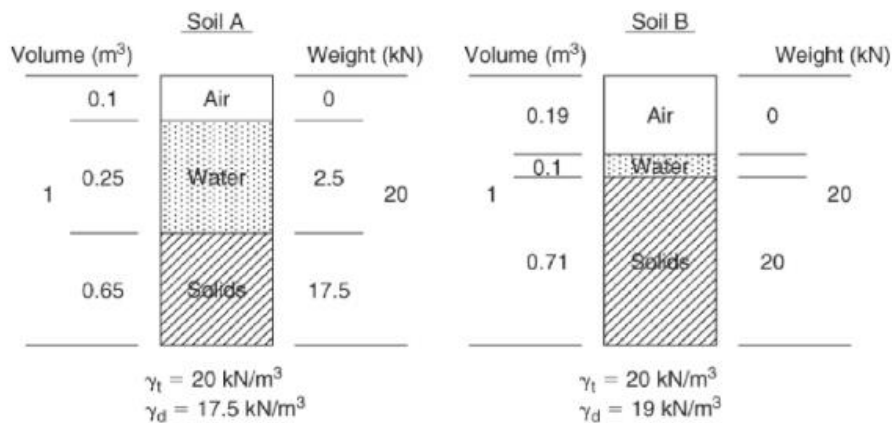
Figure 5. Three-phase diagram showing the usefulness of dry unit weight. Source: Geotechnical engineering, J.L. Briaud.

Soil Modulus test

The test described above yields γ_d – w curve. The soil modulus test, also called the **BCD test** (Briaud et al. 2006), plays a very important role in the field of compaction. One of the major goals of compaction in geotechnics is to minimize soil deformation, so a sufficiently high modulus should be reached for compaction to be adequate. A modulus E vs. water content w can be generated in parallel with the γ_d – w curve by using a device called the BCD (Briaud Compaction Device), shown in *Figure 6* .

This test consists of a 150 mm diameter thin and flexible steel plate at the bottom of a rod with handles – a kind of scientific cane. Strain gages are mounted on the back of the plate to record the bending that takes place during the loading test. When the operator leans on the handle, the load on the plate increases and the plate bends. If the soil is soft (low modulus), the plate bends a lot. If the soil is hard (high modulus), the plate does not bend much. The amount of bending is recorded by the strain gages and is correlated to the modulus of the soil below.
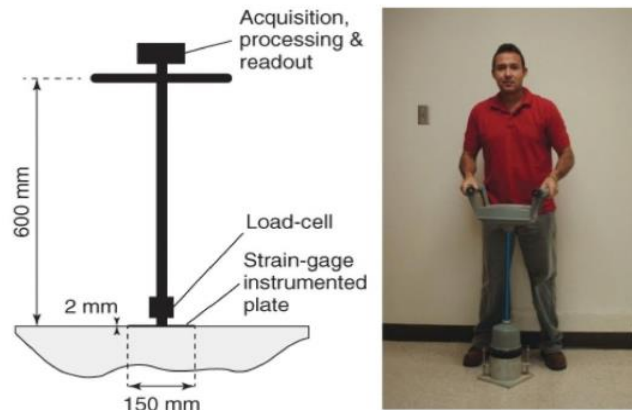
Figure 6. BCD apparatus to get soil modulus during a Proctor Compaction test: (a) BCD principle. (b) BCD on Proctor mould. Source: Geotechnical engineering, J.L. Briaud.

Its procedure goes as follows. First, the BCD plate is placed on top of the sample in the 152 mm diameter compaction mould (*Figure 6b*). The operator then leans on the handles of the BCD and the vertical load increases. When the load goes through 223 N, a load sensor triggers the reading of the strain gages. The device averages the strain gage values, uses the internal calibration equation linking the strains to the modulus, and displays the modulus E. This gives one point on the modulus vs. water content curve. By repeating this test for different water contents, a complete E vs. w curve can be obtained (*Figure 7*).
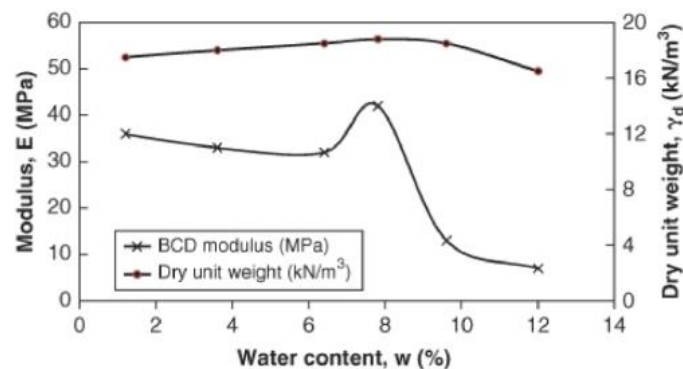
Figure 7. BCD modulus and Dry unit weight curves in compaction test. Source: Geotechnical engineering, J.L. Briaud.

The modulus obtained with the BCD corresponds to a reload modulus, to a mean stress level averaging about 50 kPa within the zone of influence, to a strain level averaging 10^{-3} within the zone of influence, and to a time of loading averaging about 2 s.

2.4.2 Consolidation tests

Saturated soils

The compressive behaviour of soil is usually measured in a *tri-axial* or *uniaxial* compression apparatus. The latter is also referred to as an oedometer (*Figure 8*). When using tri-axial compression tests, the applied compressive stress is usually expressed in terms of the mean normal stress p, whereas when using uniaxial compression tests, the applied stress is expressed in terms of the first principal stress σ_1. Uniaxial compression tests are widely used, as they are easier to conduct compared with tri-axial tests (Keller 2004). A uniaxial strain state appearing during uniaxial testing on soil cores is assumed to be a sufficiently good approximation of the strain state in the subsoil under a running wheel (Koolen & Kuipers, 1983). The most well-known and widely used of uniaxial test is the oedometer test.

The **consolidation/oedometer test** dates back to the early 1900s, and it may be appropriate to attribute its early development to Terzaghi, around 1925, with Casagrande and Taylor making significant contributions as well. This one-dimensional consolidation test (ASTM D2435) is used mostly for determining the compressibility of saturated fine-grained soils.

It consists of placing a disk of soil approximately 25 mm high and 75 mm in diameter in a steel ring of the same dimensions and applying a vertical load on the sample while recording the decrease in thickness of the sample (*Figure 8*). The whole assembly sits in an open cell of water to which the pore water in the specimen has free access. Filter stones are placed at the top and bottom of the sample to allow the water squeezed out of the sample to drain at both ends. The ring confining the specimen may be either fixed (clamped to the body of the cell) or floating (being free to move vertically): the inside of the ring should have a smooth polished surface to reduce side friction. The confining ring imposes a condition of zero lateral strain on the specimen. The compression of the specimen under pressure could be measured by means of a dial gauge operating on the loading cap.
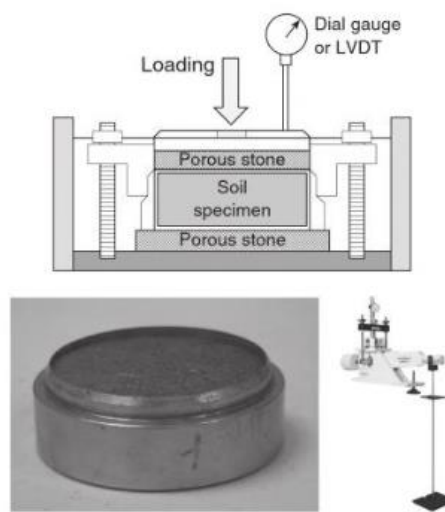
Figure 8. (a) Consolidation principle sketch. (b) Sample in ring. (c) Complete setup. Source: Geotechnical engineering, J.L. Briaud.

There are several loading procedures: incremental loading, constant rate of strain and constant gradient.

The *incremental loading* procedure is the most popular and consists of placing a load on the sample for **24 hours** or more -in **Geotechnics field,** for **engineering purposes-** while recording the decrease in sample thickness. The load creates a constant total normal stress σ on the surface of the sample. When σ is applied, the pore water pressure u goes up because the water has difficulty escaping from the small soil pores quickly enough. It takes some time for u to decrease and come back to its original value. This decrease in u is associated with a corresponding increase in effective stress ($\sigma' = \sigma - u$, in this case because the soil is saturated) and a settlement of the soil; this is the process of consolidation (*Figure 9*).
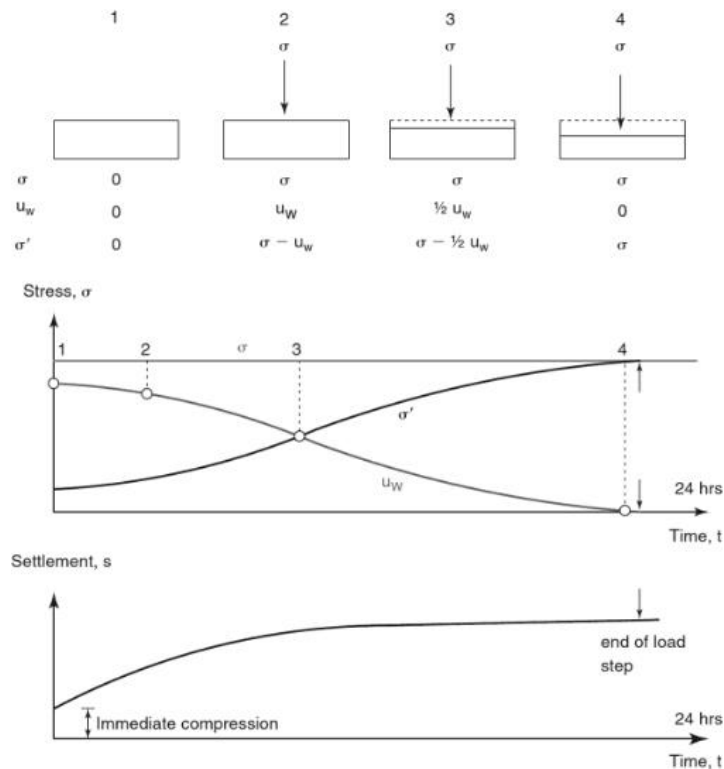
Figure 9. Consolidation process. Source: Geotechnical engineering, J.L. Briaud.

The 24-hour loading step is considered to be sufficient in general for pore wate pressure u to decrease back to zero. Once this is the case, the total vertical applied stress σ_v will be equal to the effective vertical stress σ_v' in the specimen (*Figure 9)*. The loads and associated pressures are applied in a sequence where the load is doubled each time. A typical sequence is 12, 25, 50, 100, 200 kPa for σ. As remarked before, 24-hours loading steps (or longer) are typically used for geotechnical and engineering purposes.

The results are presented by plotting the thickness (or percentage change in thickness) of the specimen or the void ratio at the end of each increment period against the corresponding effective stress (*Figure 10*). The effective stress may be plotted to either a natural or a logarithmic scale. The expansion of the specimen can be measured as well under successive decreases in applied pressure. Moreover, even if the swelling characteristics of the soil are not required, the expansion of the specimen due to the removal of the final pressure should be measured.

The void ratio at the end of each increment period can be calculated from the dial gauge readings and either the water content or the dry weight of the specimen at the end of the test. During each loading step, the decrease in sample height ΔH is recorded as a function of time t to be able to develop the ΔH vs. t curve. The vertical strain ε is obtained by dividing the change in height ΔH by the original height H_0 of the sample.

Before explaining the plotted results from the consolidation test readings, the following definitions regarding soil stress history behaviour should be introduced, according to Smith's book (2014): *Smith's Elements of Soil Mechanics*:

- Overburden: The overburden pressure at a point in a soil mass is simply the weight of the material above it. The effective overburden is the pressure from this material less the pore water pressure due to the height of water extending from the point up to the water table.
- Normally consolidated clay: clay which, at no time in its history, has been subjected to pressures greater than its existing overburden pressure (PCS).

- Overconsolidated clay: clay which, during its history, has been subjected to pressures greater than its existing overburden pressure. One cause of overconsolidation is the erosion of material that once existed above the clay layer. Boulder clays are overconsolidated, as the many tons of pressure exerted by the mass of ice above them has been removed.
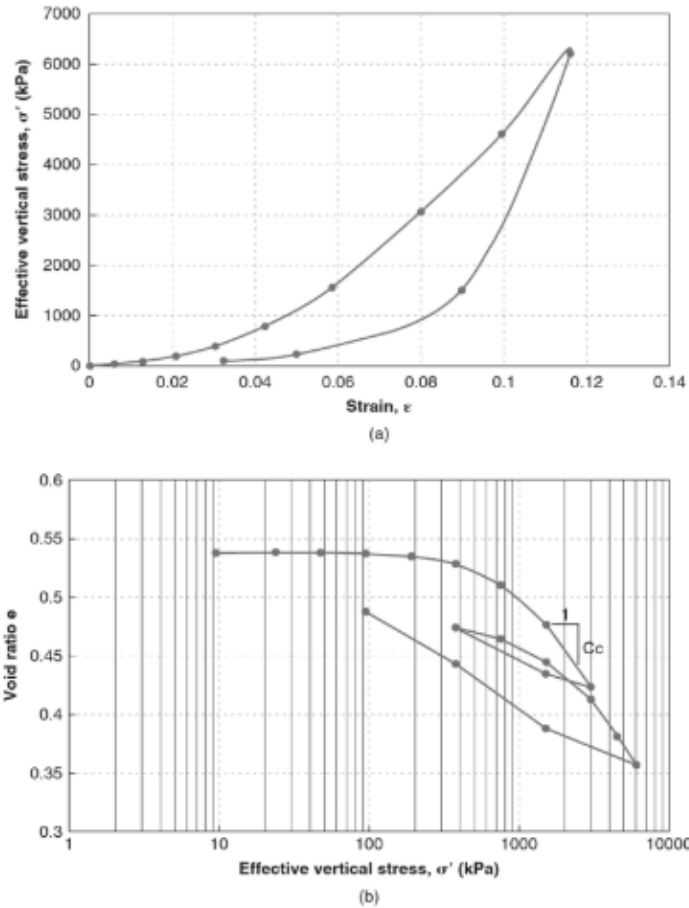
Figure 10. Consolidation curves. (a) ε – σ' curve (b) σ' – e curve. Source: Geotechnical engineering, J.L. Briaud.

The shapes of the curves are related to the stress history of a clay specimen. The e – log σ' relationship for a normally consolidated clay is linear (or nearly so) and is called the virgin compression line. If a clay is overconsolidated, its state will be represented by a point on the expansion or recompression part of the e – log σ' plot (*Figure 10*). The recompression curve ultimately joins the virgin compression line: further compression then occurs along the virgin line. During compression, changes in soil structure continuously take place and the soil does not revert to the original structure during expansion. The plots show that a clay in the overconsolidated state will be much less compressible than that in a normally consolidated state.

The compressibility of the soil can be represented as the compression index C_c, which is defined as the slope of the linear portion of the e – log σ' curve past the initial rounded part of the curve. As such, C_c is:

$$C_c = \frac{\Delta e}{\Delta \log \sigma'}$$

The **preconsolidation pressure, σ'$_p$** (also known as preconsolidation stress, **precompression stress**, **PCS**), is another important soil parameter that can be obtained from the consolidation test. It is the effective vertical stress before which the deformation of the soil, theoretically, is elastic

and reversible and after which this deformation become plastic and irreversible. It can be thought of as a vertical yield stress, although failure does not necessarily happen at σ'_p. This effective stress corresponds to the highest long-term effective stress that the soil has been subjected to. According to the definitions above, σ'_p is the maximum value of pressure exerted on an overconsolidated clay before the pressure was relieved.

The following graphical procedure (Casagrande, 1936) was originally the first method to obtain σ'_p from the consolidation test (*Figure 11*). Choose the point of highest curvature on the ε – log σ' curve (point A). Then draw a horizontal line through that point and a line tangent to the curve at that point. Then draw the bisectrice of the angle formed by these two lines. After this, draw the straight line that best fits the portion of the the ε – log σ' curve past the σ'_p value. The intersection between this best-fit straight line and the bisectrice is a point that defines the preconsolidation pressure σ'_p. .
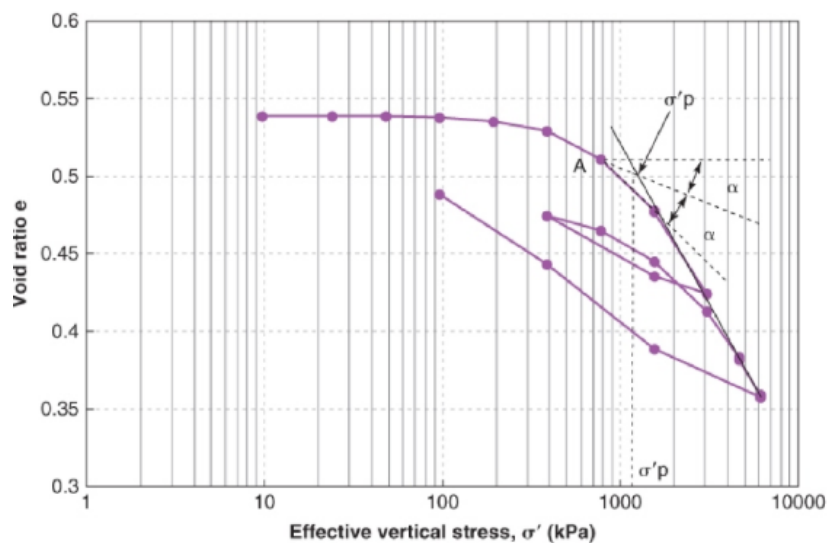
Figure 11. Casagrande method for obtaining σ'_p. Source: Geotechnical engineering, J.L. Briaud.

This procedure is still the most widely used for obtaining σ'_p. However, the visual and graphical determination is very subjective and scale dependent. Analyses and comparisons between different σ'_p determination methods are described in next chapter, Chapter 3.

In **agricultural soil mechanics research**, the load is often applied for **30 minutes** per step only. This might be justified by a much shorter loading time of the soil in the field (Keller 2004). However, the loading time during wheeling in the field is in the order of magnitude of a second, e.g. extremely short. Stafford & De Carvalho Mattos (1981) found that compaction increases with increasing loading time for soils drier than the plastic limit but not for those that are wetter.

The *constant rate of strain (CRS)* procedure consists of the same procedure as the incremental loading but with the following differences. The water is allowed to drain from the top of the sample but not from the bottom, where the pore water pressure is measured. The sample is then deformed at a constant rate of displacement with time. This rate is chosen in such a way that the increase in pore water pressure Δu at the bottom of the sample is kept at 5 to 10% of the vertical stress applied on the sample.

The *constant gradient* procedure consists of the same procedure as the constant rate of strain but with the following differences. When the load is applied, a pore water pressure Δu develops throughout the sample. Soon the excess of pore water pressure at the top decreases to zero, because drainage is allowed, but the bottom pore water pressure remains close to Δu because the sample is

not allowed to drain at the bottom. This creates a gradient between the top and bottom of the sample. This gradient is maintained constant as the load on the sample is slowly increased. However, at the end of each loading step, the pore water pressure is allowed to dissipate to obtain an equilibrium compression of the soil.

Advantages of the consolidation test include its relative simplicity and its good response of the soil sample to one-dimensional confined compression. A drawback is that the confinement provided by the steel ring around the sample prevents lateral deformations and may not represent the true deformation of the soil in the field.

Unsaturated soils

If the soil is unsaturated, the test procedures are unchanged. However, the water is in tension initially when the sample is placed in the oedometer. The increase in vertical stress on the sample as the test proceeds may create enough of an increase in water stress that it goes from tension to compression. If the soil is saturated, it is implicitly assumed that at the end of each 24-hour loading step, the pore water pressure is zero; that way the effective stress on the sample can be calculated for each step. In this case of unsaturated soils, it becomes more difficult to calculate the effective stress on the sample. The following expression can be used if the air stress is zero:

$$\sigma' = \sigma - \alpha\, u$$

Where σ' is the effective stress, σ the total stress, α the water area ratio coefficient and u the pore water pressure. The coefficient α can be estimated as the degree of saturation S, but the error can be ± 40% of the correct value. A better estimate consists of using the air entry value. Either way, obtaining σ' requires that the pore water pressure u be measured during the test (e.g. by adding a tensiometer to control suction during the test). Most of the time, a soil in the saturated state with the water in compression is more compressible than the same soil in the unsaturated state with the water in tension. One exception is collapsible soils, in which an unsaturated soil can experience significant and sudden compression when inundated.

2.4.3 Penetration tests

California Bearing Ratio (CBR) test

CBR test (ASTM D1883) is a measure of resistance of a material to penetration by a standard plunger under controlled density and moisture conditions. It was developed by the California Division of Highways as a method of classifying and evaluating soil subgrade, subbase, and base course materials to the design of pavements from laboratory compacted specimens.

California Bearing Ratio is expressed as the ratio of the unit load of the piston required to penetrate 0.1 in (2.5 mm) and 0.2 in (5 mm) of the test soil to the unit load required to penetrate a standard material of well-graded crusted stone.

CBR test may be conducted in remoulded or undisturbed samples. Test consists of causing a cylindrical plunger of 50 mm diameter to penetrate a pavement component material at 1.25 mm/min. Cylindrical moulds of 150 mm diameter and 175 mm height provided with a collar of about 50 mm length and detachable perforated base.

The procedure is summarized as follows. The mould is filled with the soil specimen. It is compacted into the mould with a rammer. Then the mould is soaked in water for a certain period. Then a loading machine is used to apply load on a plunger. This will penetrate through the soil mould. The machine will penetrate through the soil by increasing the load gradually. There are one proving ring and one dial gauge attached to the machine. The dial gauge indicates the penetration amount. The proving ring indicates the amount of load machine is applying to the surface. For certain amounts

of penetrations, corresponding load values have to be recorded. Later stress vs. penetration curve is drawn by using these values.

From that curve, corresponding stress value is determined. These values are used in the equation mentioned above to calculate the CBR value.

Penetration (mm)	Standard Load (kg)	Unit Standard Load (kg/cm^2)
2.5	1370	70
5	2055	105
7.5	2630	134
10.0	3180	162
12.5	3600	183

Table 3. Standard load values. Source: TheConstructor.org

2.5 In-situ tests

Soil Physics

Soil sampling in the field is time- and work-intensive, and marginal destruction of the soil cores cannot be avoided, even with careful handling (Casagrande, 1936; Dawidowski et al., 2001). There are mainly three (partly counter-effective) sources of error that affect the result of compression tests: non-suit of the soil at the cylinder walls, unevenness and disturbance of the free upper and lower surface, and friction of the soil at the ring walls (Muhs & Kany, 1954; Leussink, 1954; Schmidbauer, 1954).

According to Keller, 2004, a method to avoid these sources of errors is to subject the soil to compression *in situ* by a **plate sinkage apparatus** (*Figure* 12). The soil is thereby subjected to compression at the desired depth with a circular plate. Alexandrou & Earl (1995) showed that the plate sinkage test can be applied for determining the precompression stress. For small deformations, data from confined compression tests are similar to those from plate sinkage tests (Earl, 1997). It is believed that the precompression stress is identified within this range of deformation (Dawidowski *et al.*, 2001). At greater deformations, the further movement of the plate is mainly caused by lateral deformation and not by compaction, whereas in a confined test, the deformation is caused by compaction (Earl, 1997).

Figure 12. In-situ plate sinkage test. Source: Keller, 2004

Precompression stress values derived from the oedometer and the in-situ plate sinkage test generally did not differ from one another, despite the different mechanisms involved.

2.5.1 Compaction tests

Geotechnics

According to "*Craig's Soil Mechanics*", the results of laboratory compaction tests are not directly applicable to field compaction because the compactive efforts in the laboratory tests are different, and are applied in a different way, from those produced by field equipment. However, the maximum dry densities obtained in the laboratory using the 2.5- and 4.5-kg rammers cover the range of dry density normally produced by field compaction equipment.

A minimum number of passes must be made with the chosen compaction equipment to produce the required value of dry density. This number, which depends on the type and mass of the equipment and on the thickness of the soil layer, is usually within the range 3–12. Above a certain number of passes no significant increase in dry density is obtained. In general, the thicker the soil layer the heavier the equipment required to produce an adequate degree of compaction.

There are two approaches to the achievement of a satisfactory standard of compaction in the field, known as method and end-product compaction.

In *method compaction*, the type and mass of equipment, the layer depth and the number of passes is specified. Method compaction is used in most earthworks.

In *end-product compaction* the required dry density is specified: the dry density of the compacted filler material must be equal to or greater than a stated percentage of the maximum dry density obtained in one of the standard laboratory compaction tests. This type of compaction is normally restricted to pulverized fuel ash in general filler and to certain selected fillers.

Gabriel Parada (2018) showed that the control of moisture, stiffness, and density of soils in the field can be evaluated by four different alternatives of compaction measurement devices:

- Volume Replacement Devices
- Density and Moisture Gauges
- Stiffness/Strength Devices
- Intelligent Compaction.

Volume replacement devices

Volume replacement methods are used to determine the in-situ density of compacted soils since they have less calibration requirement. However, they are destructive, significantly sensitive to expertise and skills of its operator and tend to be time-consuming. The Sand Cone (SC), and the Water Balloon (WB) are the most well-known methods, as well as other recent methods used such as the steel shot replacement (SS) developed by the military (Ernest S. Berney IV and James D. Kyzar, 2012). The basic principle of these methods is to calculate the dry density of the compacted soil by dividing the percent of water content by the total volume of the excavated hole.

- **Sand Cone (SC)**

The sand cone (SC) is a volume replacement method which determines the wet density of the soil. It is one of the most recognized and utilized methods for field soil density tests due to its practicality, speed, and reliability. Results obtained using this method tend to depend significantly on the experience and knowledge of technicians, increasing the risk of bias results. This method usually is not recommended for soils that could collapse without significant effort, are not cohesive,

or during situations where water could enter into the excavated hole (Christopher L. Meehan and Jason S. Hertz, 2011).

To perform this test, a small hole (6 in. x 6 in. deep) is excavated by hand using a small shovel or any digging tool (ASTM D 1556). The excavated material is carefully removed and placed in a plastic bag or another container where moisture content will not be lost and is weighed. The sample is dried and weighed again to determine its percent of moisture content. Once the excavated material has been placed in a safe container, calibrated "20-30 Ottawa Sand" is used to fill the hole (Ernest S. Berney et al., 2013).

The volume of the hole is determined by the difference in weight of the calibrated sand. This process gives us the wet density of the compacted material, and its dry density after the sample taken was dried and weighed. Using Proctor density calculated in the laboratory the relative density of the compacted soil is obtained (Soil compaction handbook, 2011).

- **Rubber Balloon (RB)**

The rubber balloon method for field soil density testing (ASTM D 2177) similar to the sand cone, consists of excavating a hole. After which the excavated material is carefully removed and placed in an air-tight plastic bag or another container where moisture content will not be lost and is weighed.

The volume of the hole is measured using a graduated cylinder (1596 ml capacity) contained inside an aluminium cover, and a rubber balloon which is filled with water using a reversible rubber pump. The total volume of water loaded into the balloon, corresponds to the total volume of the dig hole (Christopher L. Meehan and Jason S. Hertz, 2011). The wet density of the soil is determined by dividing the total weight of the removed soil by the volume of the excavated hole. Using the moisture content obtained and the dry density of the soil (after weighing the removed sample, wet and dry), the dry density of the soil can be calculated (Axel Antonio Guzmán Abril, 2013).

As well as the sand cone test, this method can diverge depending on the level of expertise and skills of the operators when preparing and filling the excavated hole. A higher force applied to the apparatus when filling the balloon with water could cause a greater displacement on the evaluated soil (Yong Cho et al., 2011). This method is also considered to be inappropriate for soils with higher organic content or soils with soft clay, sand, and significant amounts of coarse aggregate material, since it could cause deformation of the excavated hole when pressure is applied, or collapsing with no trouble during the creation of the hole (Angella Lekea, 2015).

- **Density Drive-Cylinder (DDC)**

This method consists of obtaining a relatively undisturbed sample of soil by driving a thin walled cylinder open at both ends of the compacted ground (ASTM D2937-17). Once flushed, the material around the cylinder is then excavated. With the empty volume of the cylinder already known, the unit weight of the soil in the cylinder can then be calculated in the lab. While in the lab, a sample of the soil can be dried to provide a dry density of the material. Comparable to the other volume replacement techniques to obtain the wet density of the soil previously mentioned, the outcomes of this method can vary considerably, depending on the level of expertise and experience of the technician who is performing the test. This method is not recommended to be used for soils that deform without effort, excessively soft, not cohesive, or high plasticity (Angella Lekea, 2015)

Density and Moisture Gauges

Currently, most state DOTs and agencies use density and moisture gauges to evaluate the compaction level of unbound materials. The nuclear density gauge (NDG) is the method widely

used by most state DOTs for measuring the field density of compacted soils. However, gauges to measure the density and moisture of compacted soils have been developed as well.

- **Nuclear Density Gauge (NDG)**

The Nuclear Density Gauge (NDG) is a device designed to measure in-situ moisture and density of soils, aggregates, cement, lime-treated materials, and asphalt (Soils and Aggregate Compaction, 2016). They represent a fast and accurate alternative for field technicians and contractors to obtain in-situ soil moisture and density.

The device uses gamma rays from a radioactive source which penetrate the compacted soil, and depending on the number of air voids contained in the ground, gamma rays are reflected and sent back, and registered by the gauge which gives the moisture content, wet density, and dry density of the soil. This density is compared with the maximum dry density of the material previously obtained in the laboratory. Consequently, the relative density of the soil is obtained. Soils with higher density can absorb more radiation than loose soil (Soil compaction handbook, 2011).

The nuclear density gauge (ASTM D2922) is currently the most used method for in-situ density and moisture testing due to its speed of measurement, and alleged accuracy. However, increasing concerns have arisen regarding safety, cost, regulations, certification programs, and licensing process that are bound with these gauges, encouraging the development of alternatives methods to replace these devices.

- **Electrical Density Gauge (EDG)**

The electrical density gauge is a portable device used to measure the moisture content, density, and percent of compaction of soils. The EDG uses high radio frequency waves to measure the dielectric properties, and moisture content of the compacted soil, this includes resistance, capacitance, and real impedance (Munir Nazzal, 2014). Four darts are displayed in a template where the radiofrequency travels. These frequencies are measured between the darts and recorded by the data collection unit (Jeff Brown, 2007). It is necessary for this method to use a soil-specific soil calibration model in order to calculate water content and dry density of the soil (Ellen M. Rathje et al., 2006).

The ASTM D 7698, refers and describes the procedure for this method. In contrast with nuclear devices, this method is not controlled by any government regulation, nor safety provisions, as well any further calibration over time (Christopher L. Meehan and Jason S. Hertz, 2011)

- **Soil Density Gauge (SDG)**

 The soil density gauge is one of the field measurement devices for soil density that are intended to replace the NDG. This device uses electromagnetic wave propagation to measure the moisture content and density of the soil, having non-contacting sensors which consist of a central and an outer ring. The central ring generates a radio frequency into the soil and the response of these frequencies are received by the outer ring, using this information to measure the dielectric properties of the compacted soil (Munir Nazzal 2014).

This a non-intrusive device that permits fast measurements. The SDG has deficiencies as well. Several researchers have struggled with the SDG since algorithms are proprietary and cannot be adequate to different soils, having to input material properties manually (Joshua E. R. Wells, 2014).

- **Moisture-Density Indicator (MDI)**

The Moisture Density Indicator follows the ASTM D 6780. This device uses Time Domain Reflectometry (TDR) to measure the dry density and the moisture content of soils. It consists of

multiple rod probes (compound of four metal probes, one in the centre and three on edge of the head probe) connected to a metal head base, this head is connected by a coaxial cable to a TDR pulse generator.

The TDR is connected to a digital PDA (Personal digital assistant). The PDA emits an electromagnetic pulse through the four metal spikes, and a reflection of this pulse returns in case an anomaly has been found (Munir Nazzal, 2014). The TDR records the travel time through the spikes and the steadiness of the voltage amplitude of the pulse. The centre probe conducts the information to the coaxial cables and the outer spikes as shield conductors. The information is sent throughout the central spike and coaxial cable is evaluated by the PDA, which calculates the electrical properties of the tested material (Amr M. Sallam et al., 2004). The MDI measures the dielectric constant and bulk electrical conductivity of the soil and can be used with two different models, one step and two steps mode.

Stiffness/Strength Devices

- **Clegg Hammer (CH)**

Is an impact soil tester device, that consists of a flat-ended cylindrical mass (hammer) and a guiding tube. The Clegg Hammer, also known as Clegg impact tester, was developed by Dr. Baden Clegg in the University of Western Australia in the 1970s, it has several applications to testing in pavements areas, earthworks construction sites, or turf surfaces.

The hammer is manually released from a setup height. The hammer comes in different weights. Typically, a 10 pounds hammer is used for earthwork and roadwork quality control. The impact of the hammer creates an electrical pulse from which the measurement of deceleration of the hammer is obtained. The produced electrical pulse is converted into units of gravity. The results displayed by the CH are in terms of the CIV (Clegg Impact Value), where one unit is equal to 98.1 m/s^2 . The standard protocol drops the mass at least four consecutive times at the same location. The percent compaction of the material tested can be estimated by determining the CIV.

- **Soil Stiffness Gauge (GeoGauge)**

Originally known as Humboldt Stiffness Gauge, this device consists of an external case housing an electro-mechanical shaker, upper and lower velocity sensors, and a rigid ring-shaped foot is fixed at the base of the case (Ellen M. Rathje et al., 2006). The GeoGauge measures the in-place stiffness of compacted soil by vibrating its rigid ring-shaped foot creating vertical frequencies. This device measures the uniformity of unbound materials through the variability in stiffness throughout a structure. The stiffness is determined at each frequency, and the average is displayed.

- **Light Weight Deflectometer (LWD)**

 The Lightweight Deflectometer (LWD) is a portable falling weight Deflectometer that records the elastic modulus of soils by dropping a mass onto a load plate which rests in the compacted soil and is measured by a sensor located at the centre of the loading plate. Since there are several types of LWD on the market, Munir Nazzal (2014) conducted a comparison between different manufactures finding similarities within the operation process, but variations in the measured results.

- **Dynamic Cone Penetrometer (DCP)**

Developed in South Africa, but currently also used in U.K., Australia, New Zealand, several states in the US, and by the U.S. Army Corps of Engineers (Janine Abyad 2015). This method uses a 15 pounds steel mass, which falls approximately 20 inches striking an anvil. The bottom of the rod has a conic shape with 45 degrees vertex angle and 1.5-inch diameter. The cone penetrates the hand-

augured hole. This test is best performed by two operators, one to conduct the test and the other to record the number of blows and their depth.

The DCP is a portable, easy to use a device that requires no electronics supplements, especially effective to identify the weak layer of soil. This method allows determining a penetration resistance of the evaluated material.

Intelligent Compaction

The Intelligent compaction (IC) is an integrated system that monitors, measures, and controls the quality of the compacted material in real time, recording valuable data during the compaction process which increases efficiency and productivity. This method is based on accelerometer based measurement technology, that is integrated to the compaction machine (typically, soil rollers), and in a mapping-location system (GPS), that records the information from every layer compacted and develops a mapped area where the activity was conducted.

Continuous issues associated with the current quality control practices have derived from poor uniformity in compacted soil layer, non-uniformity with moisture control, and high variability of results when dealing with natural soil. Therefore, over the last decades, significant effort has been made in order to develop new technologies and different approaches when addressing to field quality control of soil compaction. Different innovations and methods thought to revolutionize the industry are in constant development (such as modulus-strength over 19 density measurement), and intelligent compaction planned to be one of them (Antonio Nieves, 2013).

This method can be applied to measure the compaction of soils, aggregate bases, or pavement admixtures.

2.5.2 Penetration tests

Geotechnics

Cone penetration test (CPT)

This test, sometimes referred to as the Dutch cone penetrometer as it was originally developed in The Netherlands, is described fully in EN ISO 22476-1:2012. However, it has gained increasing importance in other parts of the world, especially in connection with soil compaction projects.

 This test involves a cone penetrometer at the end of a series of stiff cylindrical rods being pushed vertically into the ground at a constant rate of penetration. Different types of mechanical and electric cone penetrometers exist, but the electric cone is most widely used.

A record of the resistance to the movement of the cone against depth is taken so that changes in soil strata and other soil strength considerations can be identified. The movement of the cone is resisted by both the ground ahead of the cone and the friction acting on the side of the cone as it is pushed into the ground.

The cone has an apex angle of 60° and diameter of 35.7 mm, giving an end area of 1000 mm^2. The cone is forced downwards at a steady rate (15–25 mm/s) through the soil by means of a load from a vehicle mounted hydraulic jack.

Figure 13. Cone penetration test. Source: Onshore structural design calculations

The penetrometer is a sophisticated device and contains sensors for measuring the force resisting the cone, the side friction placed on the unit (known as sleeve friction) and, where required, the pore pressure acting on the cone penetrometer. Where pore water pressures are recorded, the test is known as piezocone penetration (CPTU) testing. To ensure the instrument is travelling vertically into the ground, an internal inclinometer is also included. This device records the angle of the instrument from the vertical. The CPTU offers the possibility to determine hydraulic soil properties (such as hydraulic conductivity or permeability), but it is most widely used for identification of soil type and soil stratification.

The results obtained from the CPT/CPTU tests are recorded as plots of the measured value (cone resistance, sleeve friction, pore pressure) versus depth. These plots can then be used to assess the strength of the ground profile visually and rapidly. Example plots are shown in *Figure 14*.
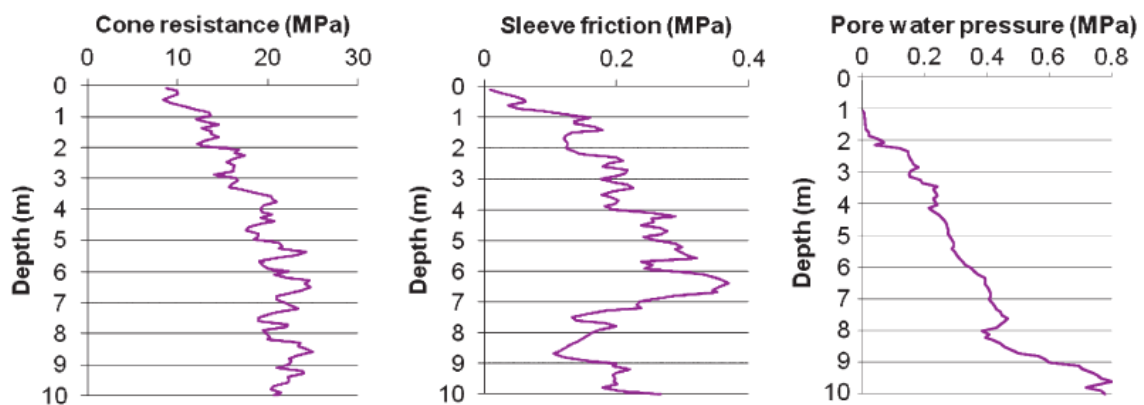
*Figure 14. Plots of cone resistance, sleeve friction and pore pressure with depth from CPT **test.** Source: Smith's Elements of Soil Mechanics.*

The CPT is standardized, and the measurements are less operator dependent than the SPT, explained later, thus giving more reproducible results.

One important objective of the CPT investigations in connection with soil compaction is to obtain information concerning soil stratification and variation in soil properties both in horizontal and vertical directions. The friction ratio is often used as an indicator of soil type (grain size) and can provide valuable information when evaluating alternative compaction methods.

Measurement of the excess pore water pressure with the CPTU can detect layers and seams of fine-grained material (silt and clay). It is also possible to obtain more detailed data concerning soil permeability.

Standard Penetration Test (SPT)

The standard penetration test (SPT) is a well-established and unsophisticated method which was developed in the United States in 1925. It has since undergone refinements with respect to equipment and testing procedure. Standardization of SPT was essential to facilitate the comparison of results from different investigations

This test is generally used to determine the bearing capacity of sands or gravels and is conducted with a split spoon sampler (a sample tube that can be split open longitudinally after sampling) with internal and external diameters of 35 and 50 mm respectively (*Figure 15*).

The equipment is simple, rugged, and relatively inexpensive. Another advantage is that representative soil samples are obtained, even though they are disturbed. Therefore, standardization of SPT was essential in order to facilitate the comparison of results from different investigations. The equipment is simple, rugged, and relatively inexpensive.

The sampler, connected to a sequence of drive rods, is lowered down the borehole until it rests on the layer of cohesionless soil to be tested. It is then driven into the soil until a depth of 450 mm by means of a 63.5 kg hammer free-falling 760 mm for each blow. The number of blows required to drive the last 300 mm is recorded and this figure is designated as the N-value or the penetration resistance of the soil layer. The first 150 mm of driving is ignored because of possible loose soil in the bottom of the borehole from the boring operations. After the tube has been removed from the borehole it can be opened and its contents examined.
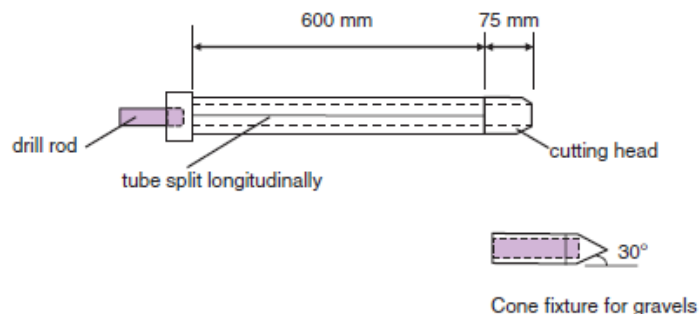
Figure 15. Standard penetration test sampler. Source: Smith's Elements of Soil Mechanics.

The quality of test results depends on several factors, including the actual energy delivered to the head of the drill rod, the dynamic properties (impedance) of the drill rod, the method of drilling, and borehole stabilization. The actual energy delivered can vary between 50% and 80% of the theoretical free-fall energy. Therefore, correction factors for rod energy (60%) are commonly used, according to Seed and De Alba (1986). The SPT can be difficult to perform in loose sands and silts below the groundwater level (typical for land reclamation projects), as the borehole can collapse and disturb the soil to be tested. The following factors can affect the test results: nature of the drilling fluid in the borehole, diameter of the borehole, the configuration of the sampling spoon, and the frequency of delivery of the hammer blows.

It should be noted that drilling and stabilization of the borehole must be carried out with care. In gravelly sand damage can occur to the cutting head of the sampler and a 60° solid cone can be fitted in its place. In such a case the test is recorded as SPT(C). The measured N-value (blows/0.3 m) is the so-called standard penetration resistance of the soil. The penetration resistance is influenced by

the stress conditions at the depth of the test. Peck et al. (1996) proposed, based on settlement observations of footings, the following relationship for correction of confinement pressure: the measured N-value is to be multiplied by a correction factor CN to obtain the reference value N1, corresponding to an effective overburden stress of 1 t/ft^2 (approximately 107 kPa).

$$N_1 = N \cdot CN$$

where CN is a stress correction factor and *p'* is the effective vertical overburden pressure.

$$CN = 0.77 \, log_{10}(\frac{20}{p'}) \; \cdot$$

2.5.3 Compaction equipment

Geotechnics

The following types of compaction equipment are used in the field:

- Smooth-wheeled rollers

- Pneumatic-tyred rollers

- Sheepsfoot rollers

- Grid rollers

- Vibratory rollers

- Vibrating plates

- Power rammers

2.6 Discussion

We should pay particular attention when talking about compaction whether our interest is in regards to agricultural soils or engineering soils.

In *soil physics* approach, when it comes to soil compaction, this process refers to both engineering terms of compaction and consolidation. These two processes cause a densification of the soil because of the application of stress. Due to the increase of the dry density of the soil, this results in a change in macro-porosity, particle connectivity and lower air permeability.

In agronomy, evidently, we want to prevent this from happening, since an increase in dry density results in several detrimental effects on agricultural soils; compaction deteriorate the physical properties of the soil, which become less able to hold and conduct water and nutrients: increasing erosion, runoff and decreasing nutrients transport, efficiency of crops growths, etc.

In the *geotechnics* approach, densification is split up into two distinct processes. On one hand, soil compaction is a quick process, due to a short-term and dynamic loading, which causes an expulsion of air from the voids of any type of unsaturated soil (coarse-grained mainly). On the other hand, soil consolidation is a long process, due to a long-term and static loading which cause an expulsion of water from the voids of any type of saturated soil (fine-grained mainly).

In soil engineering, compaction causes an increase of the dry density, which results in a higher soil mechanical strength, bearing capacity and improvement of the settlement characteristics of the soil. These can be favourable outcomes, which are purposely sought when it comes to a geotechnical approach.

As far as compaction and consolidation research is concerned, it should be noted that almost all of the laboratory and in-situ tests were originally intended for geotechnics, since they basically measure engineering parameters related to soil strength behaviour for foundations matters and settlement analyses (e.g. Proctor test, CBR, CPT…).

However, laboratory testing, such as oedometer and penetrometer, and in-situ testing, such as plate sinkage test, are very commonly used in soil physics and agronomy studies since they allow a great understanding on the soil behaviour. They also provide good determination of relevant soil parameters such as bulk density, void ratio, air permeability, water content or precompression stress, -key parameter on agricultural soil compaction, discussed in next chapter-. Moreover, field density tests can be carried out, if considered necessary, to verify the standard of compaction in engineering earthworks, dry density or air content being calculated from measured laboratory values of bulk density and water content.

3. Precompression Stress

3.1 Concept

Soil compaction has turned into one of the most important threats to soil quality and ecosystem services (Chamen et al., 2015; Schjønning et al., 2015). This is caused by the steady increase in the weight of machinery used in agriculture (e.g., Vermeulen et al., 2013). The size of tyres has increased simultaneously, but the net effect is a significant increase in the stresses reaching the subsoil (Schjønning et al., 2015). Several studies have documented considerable levels of vertical stress reaching deep subsoil layers (e.g., Arvidsson et al., 2002; Keller et al., 2002; Keller and Arvidsson, 2004; Lamandé and Schjønning, 2011a, b, c, 2018). It turned out that considerable residual (plastic) deformation was frequently observed for soil depths from 0.3-0.7 m (Keller et al., 2012).

Modelling approaches have also demonstrated that subsoils are at risk of persistent deformation during typical farming operations at moist to wet conditions (e.g., Arvidsson et al., 2003; Duttmann et al., 2014; Gut et al., 2015). It is thus likely that a range of ecosystem services including crop production and mitigation of environmental impacts from agriculture are threatened by modern farming practices (e.g., Berisso et al., 2012; Etana et al., 2013; Schjønning et al., 2013, 2017a).

Soil may deform plastically at isotropic stress or when subject to shear stress (Keller et al., 2007; Koolen and Kuipers, 1983). This depends on the stress components at any point in the soil profile. The full stress field is extremely difficult to measure, especially for soil in an undisturbed condition (Horn et al., 1992), and hence our knowledge is meagre. Most risk assessments for agricultural soils are based on a comparison of the vertical stress component with some estimate of soil strength deriving from uniaxial, confined compression tests. Based on civil engineering soil mechanics, a sharp bend of the stress-strain curve from such tests is expected (Hartge and Horn, 1984). The stress at this point is typically labelled the **precompression stress**, σ'_p or **PCS**. According to theory, the σ'_p is a theoretical threshold; strain at stress levels lower than σ'_p is supposed to be elastic, while strain above σ'_p is plastic. It should thus be safe to expose soil to stresses less than σ'_p. Higher stresses will cause irreversible deformation and should therefore be avoided in order not to affect soil functions (Lebert and Horn, 1991).

Casagandre (1936) first graphically derived PCS from a lab-generated soil compression curve by testing intact unsaturated soils subjected to one-dimensional confined compression. σ'_p is found at the intersect between the bisecting line at the point of maximum curvature and the virgin compression line (VCL, e.g. the linear plastic part of the log σ - e relation).

In saturated soils, σ'_p is used in settlement theory to estimate the load support capacity of soil (Leonards, 1962; Holtz and Kovacs, 1981). According to Holtz and Kovacs (1981), PCS is an indication of the maximum previously applied stress sustained by a soil and defines the limit of elastic deformation in the soil compression curve.

In agriculture, σ'_p has been commonly used as a metric for soil strength in risk assessment studies for soil compaction in cultivated fields (Hartge and Horn, 1984; Lebert and Horn, 1991; Arvidsson et al., 2003; Imhoff et al., 2004; Schjønning et al., 2015b). The risk of undesirable changes in soil structure due to compaction can be minimized by limiting the mechanically applied effective stress to below the σ'_p values (Horn and Lebert, 1994; Alexandrou and Earl, 1998; Dawidowski et al., 2001).

Besides Casagrande's procedure, which is still regarded as the standard procedure, many other direct (e.g. graphical) and indirect (e.g. empirical) methods to determine σ'_p have been proposed and different alternative approaches have been developed, as shown in the following sections.

The precompression stress is one of the most important input parameters for soil compaction models (Poodt et al., 2003). It is currently the best way to quantify the impacts of traffic on agricultural fields (Schjønning et al., 2015), and mainly depends on soil texture, bulk density, organic content and soil wetness (Hamza and Anderson, 2005). Among these, wetness is regarded as the most important and most dynamic factor influencing soil compaction processes (Soane and Van Ouwerkerk, 1994). In agricultural soils, loads are applied to unsaturated soils and σ'_p has been shown to increase with decreasing soil water content (Lebert et al., 1989; Lebert and Horn, 1991).

3.2   Direct PCS estimation from compression curves

The precompression stress (PCS, σ'_p) is derived from the compressive behaviour of soil, which is expressed graphically in the relationship between the logarithm of applied stress σ and some parameter related to the packing state of the soil, e.g. strain ε, void ratio e, specific volume v or bulk density ρ. It must be noted here that the PCS derived from log σ-e data differs from the PCS derived from log σ-ρ data as shown by Mosaddeghi et al. (2003) (however, the relationships between ε, e and v are linear, meaning that these parameters are interchangeable for the determination of the precompression stress (Keller, 2004)).

When no previous stress has been applied, this relationship is theoretically linear and any applied stress results in an unrecoverable deformation (Larson and Gupta, 1980; Larson et al., 1980; Culley and Larson, 1987; Gupta and Allmaras, 1987; Lebert and Horn, 1991). Nevertheless, when a soil has experienced a previous stress, an applied stress less than the maximum previously applied stress will result in deformation that is relatively small and recoverable (Stone and Larson, 1980; Gupta et al., 1989; Lebert and Horn, 1991).

In order to obtain the compressive curves behaviours of the soil, a uniaxial strain state appearing during uniaxial testing (oedometer test) on undisturbed soil cores is a sufficiently good approximation of the strain state in a soil under a vertical, static load (Lang et al., 1996).

Some studies of soil compressive behaviour have used structurally remoulded and, to a variable degree, homogenised soil in uniaxial, confined compression tests (e.g., An et al., 2015; Saffih-Hdadi et al., 2009). This may decrease the variation among replicate samples tested in the laboratory and hence make it easier to identify the driver soil properties regulating PCS. However, in line with Dexter et al. (1988) we consider the influence of the undisturbed soil matrix as crucial for soil mechanical strength. Quantitative expressions of soil strength for prediction purposes, especially for the subsoil, should thus be based on measurements on minimally disturbed samples.

Soil compaction laboratory methods are often time and work intensive. Moreover, soil is sampled in the field and brought to the laboratory, which may increase margins of error (Dawidowski et al., 2001). Casagrande (1936) concluded that even with the most careful procedure for obtaining undisturbed soil samples, one cannot prevent the sample from being slightly deformed, because the principal stresses in the ground, particularly their ratio, differ from those in the sample after it is removed from its contact with the surrounding mass of soil.

However, the inevitable deformation of the sample during removal from the ground and preparation for the test seems not to affect the magnitude of the estimated pre-consolidation load, because the structure of the major portion of the soil is still intact (Casagrande, 1936). The influence of sources of error during compression tests on PCS was analysed by Muhs and Kany (1954), Leussink (1954) and Schmidbauer (1954). They concluded that there are mainly three (partly counter effective) sources of errors: non-suit of the soil at the cylinder walls, unevenness and disturbance of the free upper and lower surface, and friction of the soil at the ring walls.

To overcome these sources of errors, the soil can be subjected to compression in situ by a *plate sinkage apparatus* (Dawidowski et al., 2001). Alexandrou and Earl (1995) showed that the plate sinkage test can be applied for determining PCS. Earl (1997) showed that for small deformations, the data from confined

compression tests are similar to those obtained from plate sinkage tests. It is believed that the PCS is identified within this range of deformation (Dawidowski et al., 2001). At greater deformations, however, the further movement of the plate is mainly caused by lateral deformation and not by compaction, whereas in a confined test, the deformation is caused by compaction (Earl, 1997). Dawidowski et al. (2001) found that precompression stresses derived from unconfined plate sinkage tests were higher when compared to those determined from confined tests, although not at a significant level. In section 3.2.2, plate sinkage in-situ test is studied and compared to other compaction tests.

Studies have indicated that the laboratory loading characteristics as well as the procedure for calculating σ'_p from the stress-strain curve may influence the estimates (Cavalieri et al., 2008; Keller et al., 2004; Rücknagel et al., 2010). This might explain why plastic strain and effects on soil pore functions have been observed at stress levels less than σ'_p estimated by compression tests in the laboratory (e.g., Keller et al., 2004, 2012; Mosaddeghi et al., 2007). Nevertheless, more knowledge of the loading capacity of agricultural fields is urgently needed. σ'_p has received considerable interest as a predictor of threshold mechanical stress in field traffic (e.g., Arvidsson et al., 2003; Duttmann et al., 2014; Horn and Fleige, 2009; Lebert et al., 2007; Rücknagel et al., 2015).

In the next sections, these relevant concerns and characteristics that could notably affect σ'_p are discussed, e.g. compaction tests (type of procedure, loading time, sample characteristics), method of PCS determination, soil properties and soil conditions (water content, bulk density, matric potential, etc).

3.2.1 Loading time effect

To determine the PCS, load is usually applied stepwise (sequential loading). For construction engineering purposes, the load is typically applied for 24 hours (or longer) per load step. In agricultural soil mechanics research, the load is often applied for 30 minutes per step only. This might be justified by a much shorter loading time of the soil in the field. However, the loading time during wheeling in the field is in the order of magnitude of a second, e.g. extremely short. Stafford & De Carvalho Mattos (1981) found that compaction increases with increasing loading time for soils drier than the plastic limit but not for those that are wetter (Keller, 2004).
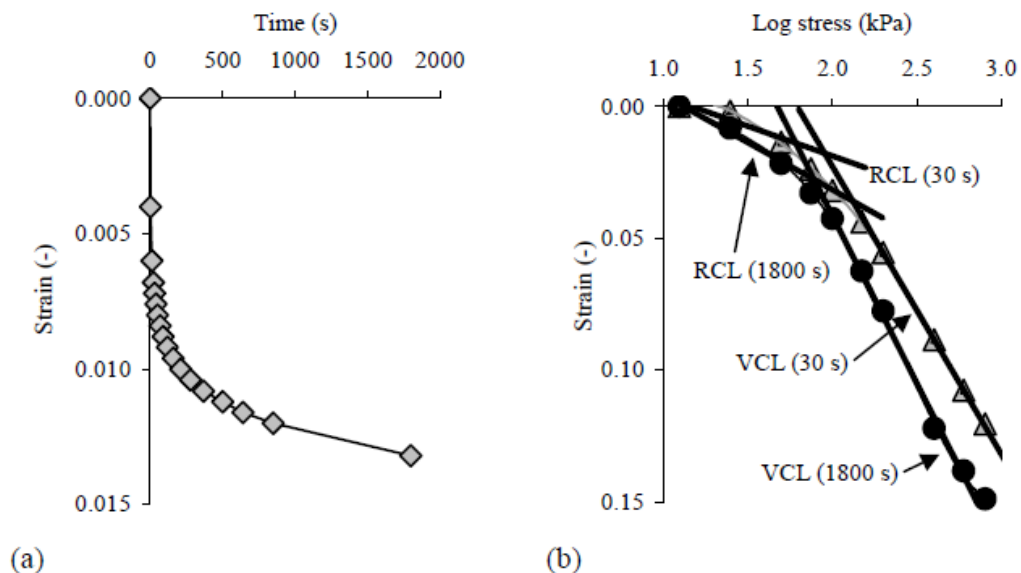
Figure 16. (a) Strain as a function of loading time for a silty clay loam; (b) examples of the compressive behaviour of a sandy loam with a loading time of 1800 s (grey triangles) and 30 s (black circles); σ'p is the intersection of the respective VCL. Source: Keller, 2004

Figure 16a shows the strain as a function of the loading time. Lebert et al. (1989) showed that the PCS increases with decreasing loading time (*Figure 16b*) and that the effect of loading time on PCS is larger the more fine-textured the soil. In general, soil is stronger as the loading rate is higher, but weaker at repeated

loading (Koolen & Kuipers, 1983). Bakker et al. (1995) point out that it is crucial to establish soil mechanical parameters with loading rates similar to those expected in the field.

In another study, Chen et al., 2019 determined that, for short term loading, water potential decreases were consistently found for loading times of 1s or less across all soil materials. For all soil materials, loads applied for 0.1 s accounted for more than 50% of the water potential change that occurred during 1s load application. Increasing soil water content not only reduced the critical stress value, but also reduced the loading time required to reach critical stress water potential.

Chen et al., 2019 also demonstrated that loading time (0–1s), approximating that of implement wheels or planter press wheels, reduces soil water potential sufficiently to affect water movement, potentially important for seed germination associated with planter press wheel operation. Additionally, loads that at least marginally exceed the critical stress static load can be applied for a short time (0–1s) without causing structural degradation.

3.2.2 Sample height effect

The precompression stress is further dependent on sample height (at constant sample diameter) as shown for an Ultuna clay in Keller & Arvidsson (2003). However, there was no clear relationship between the PCS and the sample height.

With increasing sample height, friction of the soil at the cylinder walls increases. As a consequence, strain is under-estimated and therefore the slope of both the RCL and VCL is underestimated, which usually results in an overestimation of the precompression stress. However, the errors, due to non-suit of the soil at the cylinder walls and unevenness and disturbance of the free surface, are usually larger the smaller the sample height. Therefore, high cores should be avoided because of the effect of sidewall friction, while small cores should be avoided because of sample disturbance (Keller, 2004).

Berli (2001) concluded that the influence of sample dimension on the compressive behaviour of a structured soil originates from soil spatial variability and sampling disturbance rather than from sidewall friction. Koolen (1974) measured sidewall friction and concluded that samples for oedometer tests of a ratio of diameter (d) to height (h) of about d/h = 2-3 are reasonable in restricting sidewall friction effects and permitting an acceptable accuracy.

A more recent study by De Lima and Keller (2019) showed that the relative impact of soil-wall friction on sample average behaviour decreased with increasing d/h. These results suggest that the effect of soil-wall friction on sample-average bulk density cannot be neglected unless d/h > 8.

3.2.3 Comparison of different compaction tests and stress-displacement behaviour of the soil during wheeling (Keller et al., 2004)

Although the precompression stress is widely used as a limit for mechanically applied stress to avoid soil compaction, there is no standardisation in how PCS should be measured. Furthermore, the concept of PCS as a threshold between reversible and irreversible deformation has been scarcely tested in combination with wheeling experiments in the field.

In this section, the influence on compaction tests (one field method and two laboratory methods) is presented and how these results relate to the stress-strain behaviour of the soil during wheeling experiments. PCS was determined at 0.3, 0.5 and 0.7m depth for two different soils using different compression test apparatus. The methods used for the determination of the PCS were Casagrande's and a regression method. However, different PCS determination methods are studied and analysed in detail in next section 3.2.6.

Field measurements and soil core sampling were carried out on two soils. Site A is a silty clay loam between 0 and 0.7m depth and a silty loam below 0.7m depth. Site B is a clay in the topsoil, and a silty clay to silty clay loam in the subsoil.

Field method: in situ plate sinkage test

The soil was subjected to compression at 0.3, 0.5 and 0.7m depth with a circular penetrometer plate of 49mm diameter. The penetrometer had a load cell with a maximum loading of 4400 N, corresponding to 2333 kPa. The method is described in detail in Dawidowski et al. 2001. The tests were performed at a compression speed of 7mm s^{-1}.

Laboratory method: uniaxial compression test

For the laboratory tests, cylindrical soil cores (72mm in diameter and 25mm in height) were sampled and subjected to compression in the laboratory at field soil water content.

Sequential loading of the soil cores was carried out in an oedometer described by Eriksson (1982). Vertical normal stresses of 10, 25, 50, 75, 100, 150, 200, 300, 400, 600 and 800 kPa were applied sequentially. Each stress was applied for 30 min.

Testing at constant displacement speed was performed with a universal compression testing machine. Compression speed was 0.5mm s^{-1}. Maximum force was 3260 N, which corresponds to 800 kPa.

Soil displacement and stress during wheeling

At the same two soil sites and at the same time as the soil sampling took place, a wheeling experiment was carried out with a specially constructed trailer. Vertical normal soil stress and vertical soil displacement were measured by installing probes into the soil horizontally from a dug pit. Each probe measured both the vertical normal stress and the vertical displacement simultaneously. Stress was measured by a load cell. The soil displacement was measured using a method based on the physical principle that the pressure of a column of liquid is proportional to its height (Arvidsson and Andersson, 1997).

Compaction tests results

There were quite large differences between the precompression stresses derived with the different tests, and the relationships between the different tests were different for the two soils. Typical examples of compaction curves from both sites are given in *Figure 17*.
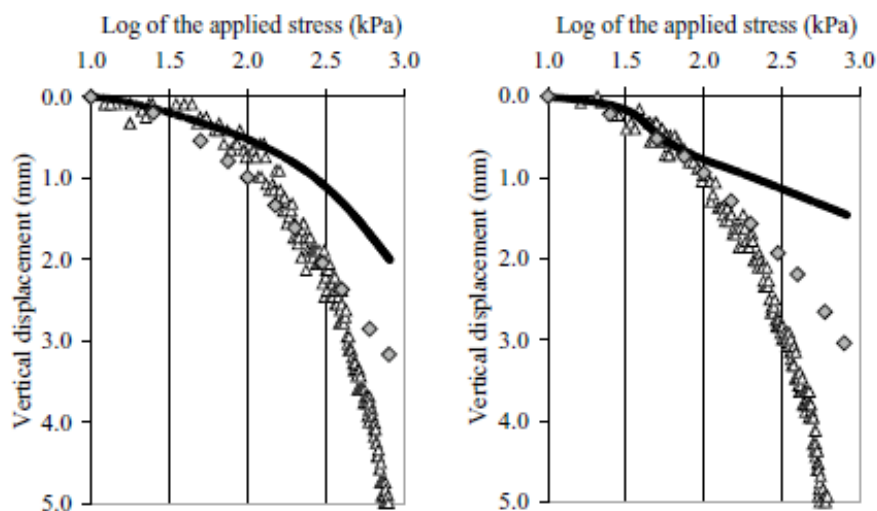
Figure 17. Typical examples of compaction curves from the in situ plate sinkage test (white triangles), the oedometer test (grey rhombi) and the constant speed test (black curve) at 0.3m depth for site A (left-hand side) and site B (right-hand side). Source: Keller et al., 2004

The displacement at a given stress was generally highest for the plate sinkage test, and lowest for the constant speed test, especially at stresses higher than 400 kPa.

The in-situ plate sinkage test and the oedometer test gave similar PCS values, with no significant difference between these two methods on both soils. For the plate sinkage test, the compression speed (7mm s^{-1}) was much higher than the drainage capability of the soil, so that higher PCSs were expected compared to the oedometer test which was a drained test with a long loading time (1800 s). The reason for the PCS obtained from the plate sinkage test being lower than expected might be that the soil under the plate could move laterally and that shearing could take place, which both increased the vertical deformation. Dawidowski et al. (2001) did not find any significant difference between results from confined uniaxial compression tests and in situ plate sinkage tests and suggested that, in spite of different mechanisms involved in the two compression tests, both methods can be applied interchangeably.

At site A, the results obtained from the constant speed test were significantly higher compared to the results from the oedometer and the plate sinkage test. High values from the constant speed test were expected, as it was an undrained test. In contradiction to the results from site A, at site B the PCS derived from the constant speed test was significantly lower than the PCS derived from both the plate sinkage test and the oedometer. This might be explained by a rapid increase in water potential in the sample, e.g. the water potential very quickly became less negative due to the high compression speed, which decreased the sample strength and resulted in a stress–displacement behaviour.

Soil behaviour during wheeling

In *Figure 18*, the measured vertical stress up to the maximum stress is plotted on a logarithmic scale against the measured vertical displacement as is usually done in order to determine PCS. At high stresses, the curve turns into a very steep, almost vertical line, indicating high displacement increments at extremely small stress increments. In contradiction to the laboratory experiments, the curve has not only one bend. Instead, the curve has many bends, which might be due to the collapse of different structures of different scales. In addition, the wheeling in the field is dynamic, with forces acting from different directions. Horn (1990) concluded that during wheeling, dynamic forces would reduce the soil strength more intensely than the forces due to static loading because of the homogenisation of particle arrangement.
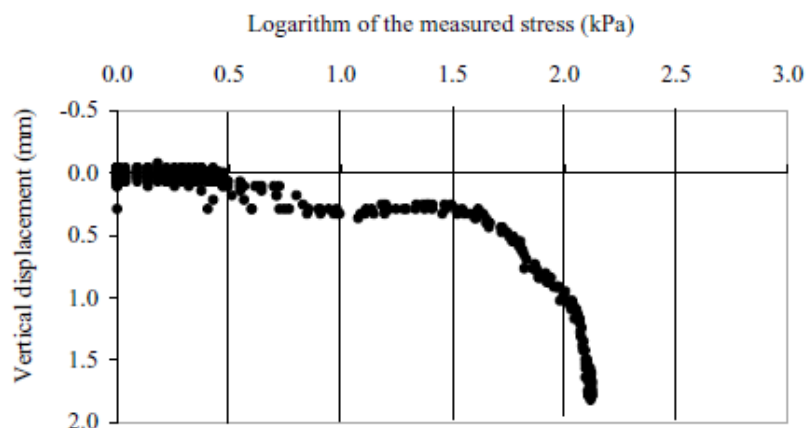
Figure 18. Log stress–displacement diagram up to the maximum measured stress for 0.5m depth during wheeling with 4Mg wheel load at site A.
Source: Keller et al., 2004

Table 4 shows the measured vertical stress and vertical displacement in the soil in comparison with the PCS. At 0.3m depth, measured stresses were equal or higher than the PCS. At 0.5 and 0.7m depth, measured stresses were lower than the PCS for all wheeling occasions. Nevertheless, the 0.5–0.7m layer was residually deformed, e.g. the difference between the residual displacement at 0.5 and 0.7m was greater than zero, except when wheeling with 2Mg wheel load at site A.

Depth (m)	Wheel load and site	Measured vertical stress (kPa)	Mean precompression stress (kPa) derived from			Measured residual vertical displacement (mm)
			Oedometer	Constant speed	In situ plate sinkage	
0.3	2 Mg, site A	148	114	240	200	2.5
	3 Mg, site A	230	114	240	200	5.3
	4 Mg, site A	227	114	240	200	2.3
	3 Mg, site B	237	145	32	136	N/A
	4 Mg, site B	N/A	145	32	136	1.0
0.5	2 Mg, site A	58	201	290	198	0.0
	3 Mg, site A	121	201	290	198	0.4
	4 Mg, site A	133	201	290	198	0.5
	3 Mg, site B	72	98	N/A	126	0.2
	4 Mg, site B	74	98	N/A	126	0.4
0.7	2 Mg, site A	41	147	288	172	0.0
	3 Mg, site A	N/A	147	288	172	0.1
	4 Mg, site A	47	147	288	172	0.2
	3 Mg, site B	65	118	72	146	N/A
	4 Mg, site B	69	118	72	146	0.0

Table 4. Measured vertical stress, precompression stress and measured vertical displacement, respectively, for the different wheeling occasion. Source: Keller et al., 2004

This residual displacement indicated that the PCS did not work as a distinct threshold value between reversible and irreversible deformation. Of course, one may argue that the measured displacements and deformations were rather small. Dawidowski and Koolen (1994) stated that when a soil has been compacted by field traffic or has settled owing to natural causes, a threshold stress (PCS) is believed to exist such that loadings inducing smaller stresses than this threshold cause little additional compaction, and loadings inducing greater stresses cause much additional compaction.

Little compaction might be enough to negatively affect the function of a soil. In addition, with regard to multiple passes of a vehicle, the total deformation will increase with increasing number of passes (Arvidsson et al., 2001; Horn et al., 2003; Trautner, 2003). According to Kirby (1991), compaction damage is to be expected when the normal stress exerted by the tyre or track exceeds a value somewhat less than the precompression stress, since the added shear stresses will cause more compression than the normal stress alone.

Several years after this study, in 2012, Keller et al., examined more closely the soil stress-strain behaviour as measured in-situ during wheeling experiments and related it to stress-strain behaviour and PCS measured in uniaxial compression tests in laboratory (*Figure 19*).
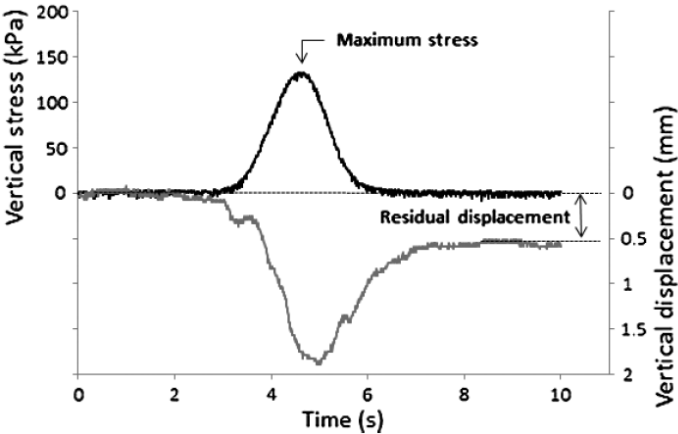
Figure 19. Example of an in-situ measurement of vertical stress (black curve) and vertical displacement (gray curve) as a function of time. The example shows measurements at 0.5-m depth during wheeling with a Twin 700-26.5 tire (wheel load, 40 kN; tire inflation pressure, 140 kPa) on a clay loam soil. Source: Keller et al. 2012.

It was found that residual strain, ε_{res}, could be measured at stresses, σ, lower than the precompression stress, σ'_p. Residual strain was observed in the field when σ exceeded approximately 40 kPa, and when the ratio of σ/σ'_p exceeded roughly 0.1, although ε_{res} was very small at $\sigma/\sigma'_p < 0.5$. These values were similar to those obtained on confined uniaxial compression curves. Based on these results, it could be proposed that the stress in the subsoil should not exceed 40 kPa to avoid compaction, when the soil is at around field capacity.

Casagrande (1936) stated that the most important practical application of σ'_p is in connection with settlement analyses and geological investigations. The approximation that there is no soil compaction if the applied stress is smaller than σ'_p is probably acceptable for civil engineering purposes.

The question is whether this approximation is good enough for the protection of soil physical quality for agricultural purposes. Hence, we must link strain to changes in soil functions. Only residual strain (compaction) that results in negative changes in soil functions may be of significance. However, it will be difficult to assess "soil function" because soils have many functions (e.g., Blum and Santelises, 1994). Nevertheless, it seems that even small residual strain can adversely affect soil functioning. For example, Mosaddeghi et al. (2007) reported that air permeability was significantly reduced on applying stresses smaller than σ'_p. On the basis of these findings, we question the use of σ'_p as a measure of compressive soil strength.

3.2.4 Influence of compression tests (effect of loading duration and initial matric potential) on soil deformation behaviour (stress-strain relationships and PCS) (Elmer Alosnos, 2015)

Total of 126 undisturbed soil samples (mostly silt loams and loamy sands) were brought to the lab for soil analysis at three different initial matric suctions of -6, -10 and -33 kPa (1.8, 2.0 and 2.5 pF, respectively). Results of the confined compression tests (stepwise double incremented loading applied at 1 min, 10 min and 30 min) were used to plot the soil compression curves, which are the graphical representation of the stress-strain relationships with a sigmoidal S-shaped (due to logarithmic scaling of x-axis, log σ_v vs volumetric strain expressed as void ratio, e).
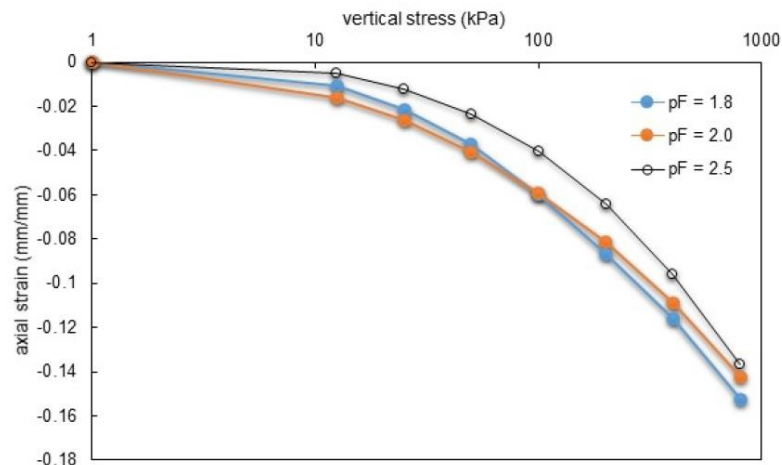
Figure 20. One-dimensional compression curves for soil samples pre-wetted at different water potential (pF=1.8, 2.0, and 2.5). Source: Elmer Alosnos, 2015

As shown in *Figure 20*, initial water potential has significant influence on the stress-strain behaviour. Total volumetric strain tends to be bigger with decreasing water potential (higher pF).

On the other hand, higher deformations were recorded for soils subjected to longer loading durations (*Figure 21*). In general, there was no appreciable steep bend on stress-strain curves observed in all treatments indicating that the soils could be exposed to slight compaction in the past. Substantial strain occurred during the initial 15-20 sec of each loading stage.
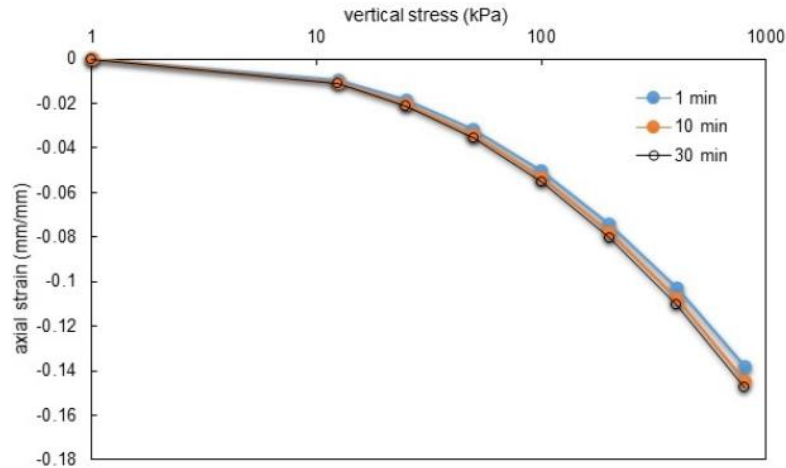
Figure 21. One-dimensional compression curves for soil samples compressed at different loading durations (T=1, 10 and 30 min). Source: Elmer Alosnos, 2015

Regarding PCS, analysis of variance showed that there is no significant interaction effect between loading duration and initial water potential on PCS. However, there is very strong evidence that the different levels of water potential do not all have the same effects on PCS.

As shown in *Figure 22,* PCS increases with decreasing water potential (more negative in kPa, more positive in pF) irrespective of loading duration used and this effect was highly significant . The results obtained in this study confirm the observation by other researchers that PCS increases with increasing soil suction (Alexandrou and Earl, 1998; Defossez et al., 2003; Imhoff et al., 2004; Mosaddeghi et al., 2006). Water influences the structural stability and strength of soil since it acts both as a lubricant and as a binding agent of soil particulates (Carter and Gregorich, 2007). On the other hand, despite of the noticeable change in stress-strain curve pattern when soil is subjected to longer loading duration, it has no significant influence on PCS values. Among all treatments, the lowest and highest PCS obtained were 99.5 kPa (pF=1.8, T=1 min) and 270 kPa (pF=2.5, T=1 min), respectively.
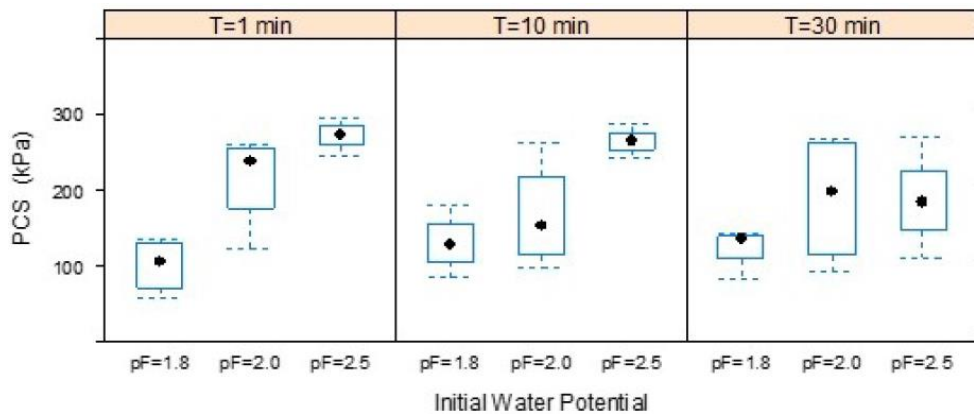
Figure 22. Influence of initial water potential and loading duration. Source: Elmer Alosnos, 2015

3.2.4 Influences by land use and soil depth (Elmer Alosnos, 2015)

Same above 126 undisturbed soil samples from different land use (cropland and grassland) and soil depths (40 and 70 cm) were brought to the lab for soil analysis at three different initial matric suctions of -6, -10 and -33 kPa (1.8, 2.0 and 2.5 pF, respectively). Most of the soil samples were classified as silt loam and loamy sand according to USDA classification.

Figure 23 shows the variations in PCS values at different land use and soil depths. Among the three land uses evaluated, the highest PCS values were recorded in the headland at both depths. This can be attributed

to frequent passes of tractor wheels along this section of the cropland. Headlands serves as field entrances and turning points for field machinery. In cropland centre and grassland, the upper part of the subsoil has higher PCS than deeper in the soil. Apart from differences on exposure of soil to field traffic, differences in pedological processes, soil moisture conditions, and swelling-shrinking intensity (Keller et al., 2004) might be the main reasons of the observed differences in PCS.
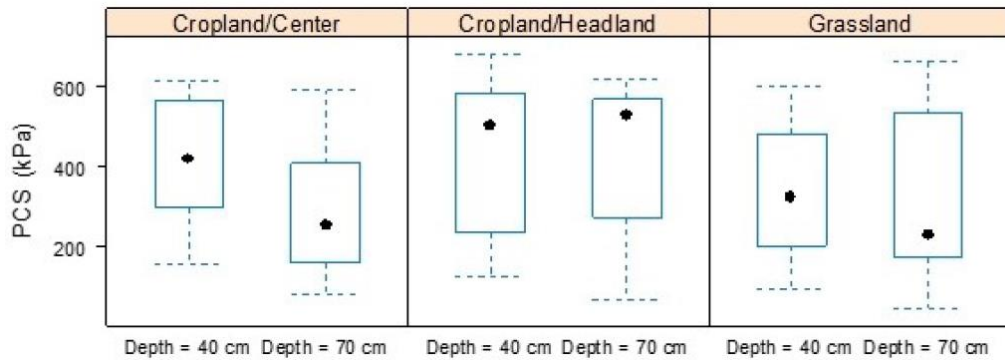
Figure 23. PCS values at different land use and soil depths. Source: Elmer Alosnos, 2015

3.2.6 Evaluation of PCS calculation methods

Soil Physics approach (Jan de Pue, 2019)

There are several methods known for the determination of the σ'_p. The first and still, the standard determination, was originally derived by Casagrande in 1936 from measurements on saturated soils but was shown to be also suitable for unsaturated conditions (Lebert and Horn,1991). It is a graphical procedure to find the intersect between the bisecting line at the point of maximum curvature and the virgin compression line (VCL, e.g. the linear plastic part of the log σ-e relation). In Chapter 2.3, this method is discussed more in detail.

Nevertheless, σ'_p is in many cases not easy to determine according to Casagrande (1936), as log stress-strain curves do not show a clear bend. This was also reported by other researchers, e.g. Berli (2001) who stated that 'the precompression stress is usually not evident as a sharp bend in the compression curve but rather an operationally defined point in an often rather gradual transition between recompression curve and virgin compression line'.

As of Casagrande's procedure, since the visual determination is very subjective and scale-dependent (Keller, 2004), automated methods have been developed (Dawidowski and Koolen, 1994; Baumgartl and Köck, 2004; Rücknagel et al., 2010) and various alternative approaches have been proposed, e.g. based on linear regression (Schmertmann, 1955; McBride and Joosse, 1996; Junior and Pierce, 1995), fitting of a sigmoid or polynomial model (Gregory et al., 2006) or numerical determination of the point of maximum curvature (Lamandé et al., 2017).

There is disagreement between calculation methods for σ'_p. This parameter has a high variability, and as pointed out by Keller et al. (2011), the inflection point of the log σ-e relation is partially a mathematical artefact of the log-transformed stress scale. The intrinsic value of σ'_p for unsaturated, structured soils is contested, and it is unclear which calculation method should be used.

Thus, the following summarized information regarding the functional evaluation of seven existing methods to determine σ'_p for undistorted soil samples was extracted from Jan de Pue's PhD dissertation (2019):

- *PCS$_{Cas}$*: graphical method according to Casagrande (1936) and Dawidowski and Koolen (1994). It is the stress at the intersect between the bisecting line at the point of maximum curvature and the VCL.

- *PCS_{L1}*: intersection of VCL with x-axis at zero strain (Schmertmann, 1955).

- *PCS_{L2}*: stress at a predefined strain, here set to 2,5%, via linear interpolation between the measured points (Arvidsson et al., 2003).

- *PCS_{L3}*: intercept of the VCL and a linear regression with the first two points of the curve (Junior and Pierce, 1995).

- *PCS_{L4}*: intercept of the VCL and a linear regression with the first three points of the curve (Junior and Pierce, 1995).

- *PCS_{G4}*: determined by fitting the Gompertz model to the log σ-e relation (Gregory et al., 2006).

- *PCS_{P4}*: stress at the point of maximum curvature of a 4th degree polynomial regression (Gregory et al., 2006).

These are amongst the most common methods to calculate σ'$_p$ and have been evaluated by several authors before (Arvidsson and Keller, 2004; Cavalieri et al., 2008; da Silva and de Lima, 2016). A visual representation of the determination of σ'$_p$ with the seven methods is shown in *Figure 24*:
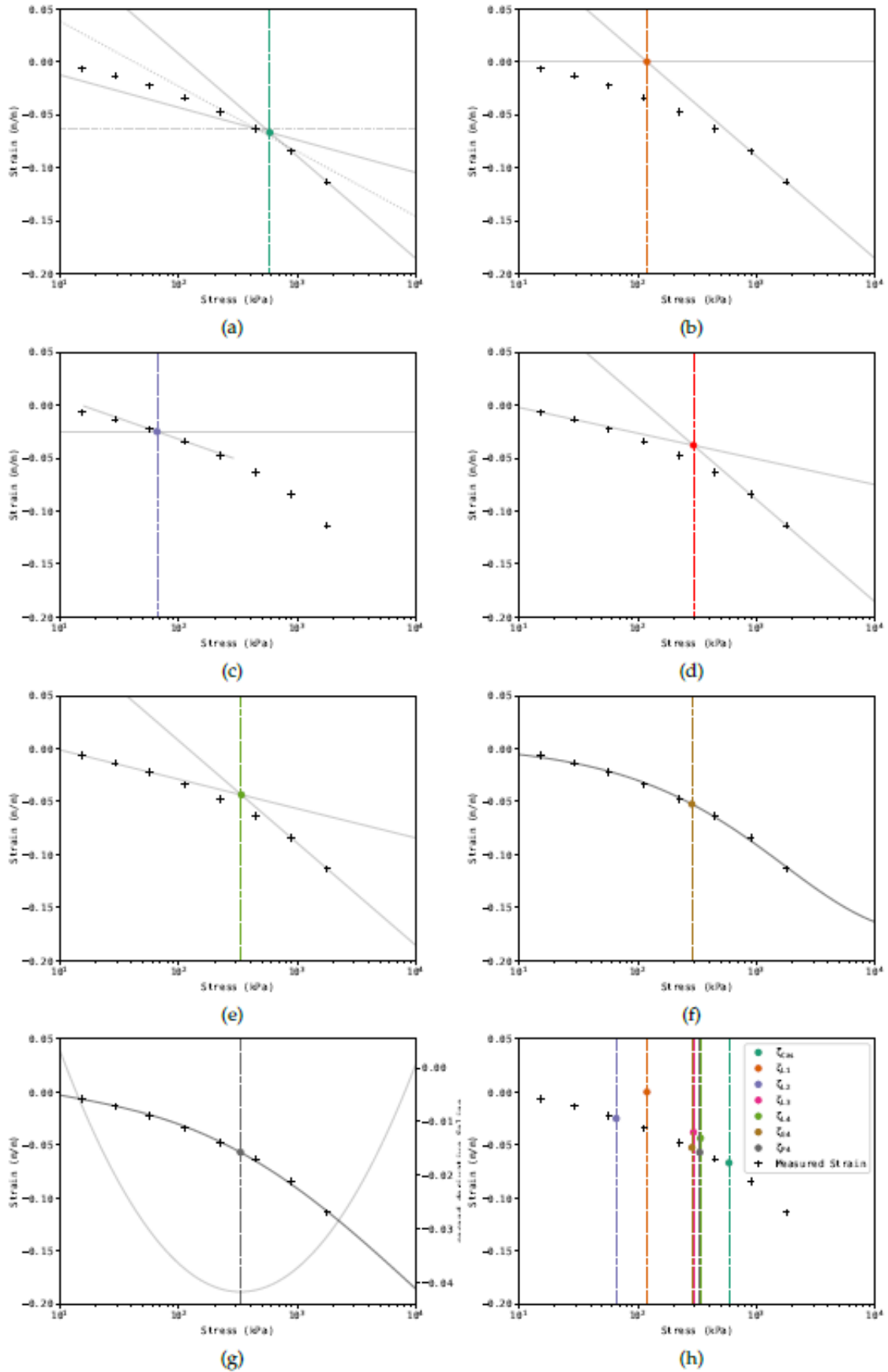
Figure 24. Visualization of the seven calculation methods to determine z in this study: a) PCS_{Cas}, b) PCS_{L1}, c) PCS_{L3}, d) PCS_{L3}, e) PCS_{L4}, f) PCS_{G4}, g) PCS_{P4}; h) shows the PCS values (cfr. vertical lines) computed with the seven methods for a soil sample. The black cross markers indicated the measured stress-strain relation. Source: Jan de Pue, 2019.

Most calculation methods assume a distinct inflection point in the log σ-e measurements. This can be a subjective choice, in particular for undisturbed, unsaturated soils where this point becomes less pronounced (Brumund et al., 1976; Dias Junior, 1994).

Most methods also require a linear VCL, but it can be subjective to select which points belong to this VCL. The sigmoid shape of the log σ-e relation can complicate the selection of VCL points. Conversely, this shape is a requirement for the robust fit of a sigmoid model (Gregory et al., 2006). The fit of a polynomial model does not require a specific shape, only the presence of an inflection point in the data.

In two cases (of 126 samples), the Casagrande algorithm failed because the VCL intersected with the bisecting line before the point of maximum curvature. Due to the unpronounced sigmoid shape of the log σ-e relation the determination of PCS_{G4} and PCS_{P4} failed in five and one instances, respectively. All methods resulted in significantly different values. The median PCS of each method is given in *Table 5*. Highest values were found with PCS_{Cas}, whereas PCS_{L2} showed the lowest values.

Method	PCS (kPa)
PCS_{Cas}	332.60
PCS_{L1}	84.73
PCS_{L2}	81.25
PCS_{L3}	192.28
PCS_{L4}	223.96
PCS_{G4}	253.68
PCS_{P4}	196.23

Table 5. Median PCS for each calculation method. Source: Jan de Pue, 2019.

Most methods showed a significant influence of land use, sampling depth and texture class on PCS. Most methods also found it significantly higher in the headland and at 40 cm (e.g. the plough/tillage layer) than at 70 cm depth. Although a trend of increasing PCS with increasing matric potential can be observed, it was not found to be significant. Only for texture class of sandy silt loam (which contains the largest number of soil samples) a significant influence is found for some methods. The correlations between other soil properties and PCS were found strong with bulk density and gravimetric water content. The significant differences in PCS values is just an indication that the method to be used to determine PCS must be carefully chosen (Cavalieri et al., 2008).

The calculation of PCS after perturbation of the strain data reveals some differences in robustness between the calculation methods. The method of Casagrande seems to be the most sensitive to perturbation. The most robust method is PCS_{L2}.

In agreement with previous studies, it was found that the methods are not interchangeable (Arvidsson and Keller, 2004; Cavalieri et al., 2008). This study extends this with a functional evaluation of these methods based on three criteria: the relation of computed PCS to soil properties and stress history (e.g. land use and sample depth), and robustness of the calculation. *Table 6* gives a summary of these results:

Method	Correlation soil prop.	Influence stress hist.	Robustness	Assumptions
PCS_{Cas}	+	+ −	−	Inflection, Linear VCL
PCS_{L1}, PCS_{L2}	−	+ −	+	Linear VCL
PCS_{L3}, PCS_{L4}	+	+ +	+	Inflection, Linear VCL
PCS_{G4}	−	− −	−	Sigmoid shape

PCS$_{P4}$	+	+ +	+	Inflection

Table 6. Summarizing table indicating Table 3.4: Summarizing table indicating the good (+) and bad (-) performance of each method, and the associated assumptions concerning the shape of the log σ-e relation. Source: Jan de Pue, 2019.

These findings are in accordance with literature for most methods. Several authors (Lebert and Horn, 1991 McBride and Joosse, 1996; Schjønning and Lamandé, 2018) found a significant correlation of PCS with initial water content and bulk density. Soil textural class was found to influence PCS, but similar to previous studies (Salire et al., 1994; Arvidsson and Keller, 2004), it was not significantly correlated to sand, silt or clay content, and no significant correlation was found with OC content.

No distinct interaction between PCS and matric potential was found, but for the samples with sandy silt loam texture class, a significant increase of PCS with decreasing (more negative) matric potential was found with most methods. It should be noted that this class of soil are most abundant in western Europe, where this study was conducted, and matric potential thus significantly affects PCS in this region.

In the development of pedotransfer functions to predict PCS from readily available soil properties, pF is usually considered as a relevant factor (Lebert and Horn, 1991; Schjønning and Lamandé, 2018). The relation to soil properties was found with most calculation methods, except for PCS$_{G4}$ and PCS$_{L2}$.

In this study design, it was hypothesized that undisturbed soil samples from different land use (pasture, headland and centre position of arable land) or sampling depth (compacted layer and subsoil layer) have a significantly different PCS. This was confirmed for the PCS$_{L3}$, PCS$_{L4}$ and PCS$_{P4}$.

Judging from the relation between PCS and the soil properties, the functional value of PCS$_{G4}$ seems to be the most limited. The method strongly depends on the sigmoid shape of the log σ-e relation, which, despite the relatively high stresses used in this study, are not always found. Consequently, the method often fails to determine the inflection point of the curve accurately, and it can be rather sensitive to perturbation of the strain measurement.

The method of Casagrande (PCS$_{Cas}$)is the most commonly applied method to determine PCS but seems to be very sensitive to small variations in the strain data. The low robustness of this method results in a large variation in PCS, suppressing its statistical relevance.

In contrast, the methods proposed by Junior and Pierce (1995) (PCS$_{L3,}$ PCS$_{L4}$) are robust and the obtained PCS is correlated well to the soil properties and load history. A disadvantage of this method is that the selection of points used in the linear regression of the VCL can be arbitrary. Consequently, these methods would be problematic to use as a standard practice.

The inflection point of a fourth-degree polynomial does not depend on the choice of pre-set stresses, nor does it assume a sigmoid shape or a linear VCL The determination of the inflection point and the datapoints belonging to the VCL can be arbitrary (Cavalieri et al., 2008) and more difficult in the case of undisturbed, unsaturated soils (Brumund et al., 1976; Dias Junior, 1994). These sources of subjectivity are eliminated by using the inflection point of a fourth-degree polynomial fit of the log σ-e relation. It was demonstrated that this method (PCS$_{P4}$) is robust and the resulting PCS showed a significant relation with the soil properties and stress history of the soil.

In summary, the calculation methods of PCS$_{L3,}$ PCS$_{L4}$ and PCS$_{P4}$ are most recommended to assess soil strength, according to this functional evaluation. The 4th degree polynomial fit is particularly promising, as it eliminates multiple sources of subjectivity and does not assume a specific shape of the log σ-e relation. Furthermore, it is compatible with data from other uniaxial compression test designs, e.g. a constant strain test (Lamandé et al., 2017).

The dataset, mostly sandy silt loam soils, did not allow to evaluate the performance of the calculation methods for clay soils. Clay soils are found in less than 1.1% of the total area of arable fields in Europe, and this is reflected in the examined dataset (Panagos et al., 2019).

On the other hand, the methods of the calculation methods of Casagrande (1936) (PCS_{Cas}) and Schmertmann (1955) (PCS_{L1}) were originally developed for (saturated) clay soils, as these soils are of major interest in geotechnics. Although less abundant, clay soils are typically more susceptible to soil compaction than soils with a coarser texture (Horn and Fleige, 2009; Van den Akker and Hoogland, 2011), so in the context of soil compaction it is desired to extend this analysis with a larger dataset in future research.

PCS shows a high variability in most studies. This is often attributed to the heterogeneity between samples (Baumgartl and Köck, 2004; Cavalieri et al., 2008), but the robustness of calculation methods for the PCS is also open to question. The proliferation of calculations methods illustrates the lack of consensus concerning the value and interpretation of PCS The lack of standardization undermines the usability of PCS (Keller et al., 2011). Alternatively, methods which rely on a sigmoid-shaped log σ-e relation might also be unreliable as this shape might not be found for all samples, in particular when using undistorbed samples (Tang et al., 2009; Lamandé et al., 2017).

Geotechnics approach (Pilar Soler Arnal, 2009)

In Geotechnics, precompression stress is equally expressed as preconsolidation stress, since the purpose is the analysis in the settlement processes, in contrast to soil physics, in which soil compaction was the main purpose of the study.

The preconsolidation stress (σ'_p) is the maximum effective overburden stress experienced by a soil during its stress history. In terms of elastic media, σ'_p as a yield stress, sets a boundary between two different behaviour zones. Nevertheless, it is noted that soils are not a continuous but particulate media, therefore, the classical definition of yielding is not entirely accurate. At stresses lower than the preconsolidation stress value, the soil is overconsolidated; however, when the current stress exceeds σ'_p, the soil is normally consolidated and the process of compressibility follows the virgin compression line, defined by a steeper

The study of precompression stress is crucial for settlement analysis. since normally consolidated soils experience a much larger settlement than overconsolidated soils undergoing the same overburden. It should be noted that in the geotechnical approach, loading times in the oedometer test for obtaining the consolidation (compression) curves have a 24 hours duration.

This analysis and results were obtained from a Pilar Soler Arnal's thesis dissertation, Georgia Institute of Technology, 2009. This dataset consists of fine-grained soils, which are called Boston Blue Clay from Newbury, Massachusetts, USA.

- *Semi-logarithmic methods*

Casagrande (1936)

The σ'_p per Casagrande approach is 280 kPa. The value is lower than that obtained with other methods due to the curvature of the virgin branch. This is often considered as the reference method and it is graphically simple to perform, however, it implies a subjectivity to define the maximum curvature point.
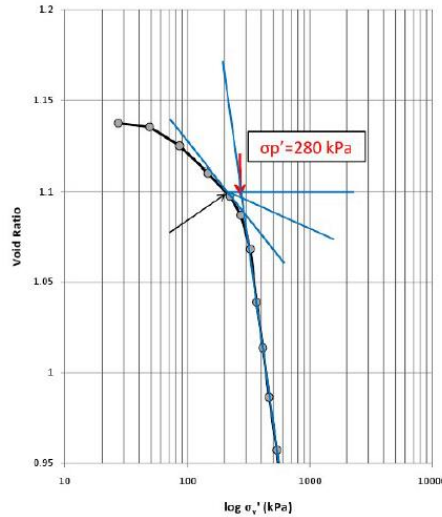
Figure 25. Casagrande's method applied to Newbury data.
Source: Soler Arnal, 2009

Van Zelst (1948)

The rebound method from Van Zelst is simple to apply. A range of σ'_p values is obtained; therefore, the most reliable value seems to be the mean of this range. In the consolidation curve studied, the most probable σ'_p value is the mean of the determined range (210-290 kPa). Thus, the σ'_p using Van Zelst method is 250 kPa, which is lower and more conservative than Casagrande's.
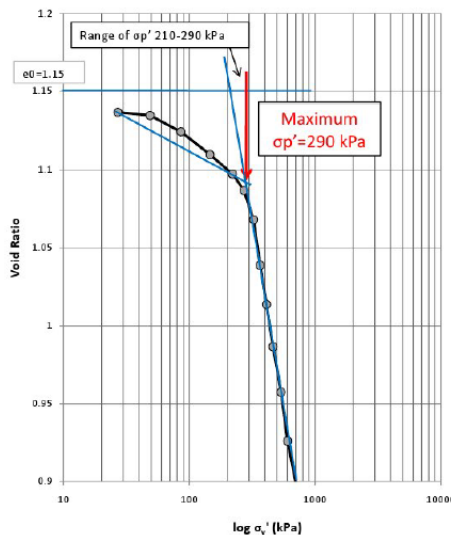
Figure 26. Van Zelst's method applied to Newbury data.
Source: Soler Arnal, 2009

Schmertmann (1955)

The Schmertmann method usually needs a rebound cycle performed during the consolidation test. Due to the lack of this rebound cycle in the analysed curve, the recompression index is assumed to be 10% of the compression index determined form the measured virgin slope ($C_c = 0.44$).

To perform this method, five possible σ'_p values were chosen (250 kPa, 270 kPa, 290 kPa, 320 kPa, 350 kPa). The five reconstructed curves were plotted and then, the void ratio difference (Δe) between the reconstructed curve and the measured curve was determined. The most symmetric of these curves seems to be the one corresponding to 320 kPa (*Figure 28*), thus chosen as σ'_p value. Schmertmann method is very time consuming, requires some subjectivity and need to perform a lot of trials in order to obtain a result for σ'_p.

The

Figure 27. Difference between the reconstructed curve and the measured curve. Source: Soler Arnal, 2009

Figure 28. Schmertmann's method applied to Newbury data. Source: Soler Arnal, 2009

Sällfors (1975)

Sällfors method gives a value of σ'_p too low compared with other methods for Newbury clay data. That may be due to the curvature of the virgin branch. The construction is reasonably easy but requires more time than other methods due to the need to adjust the triangle between the curves. The method is objective.
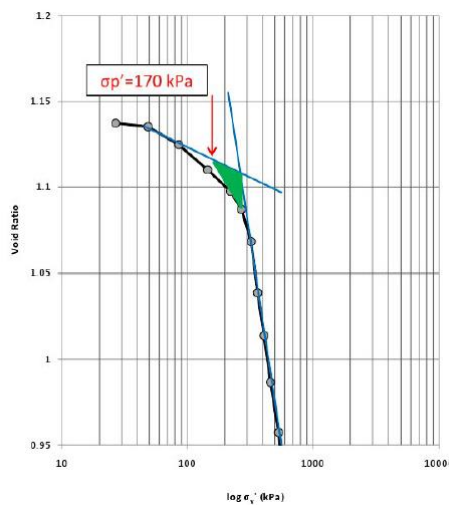
Figure 29. Sällfors' method applied to Newbury data. Source: Soler Arnal, 2009

Pacheco Silva (1970)

The Pacheco Silva method provides a σ'p value lower than other methods. Nevertheless, the graphical construction is easy and does not require subjective interpretation as well as it is scale independent, then it is appropriate to the evaluation the σ'p as a base of comparison.
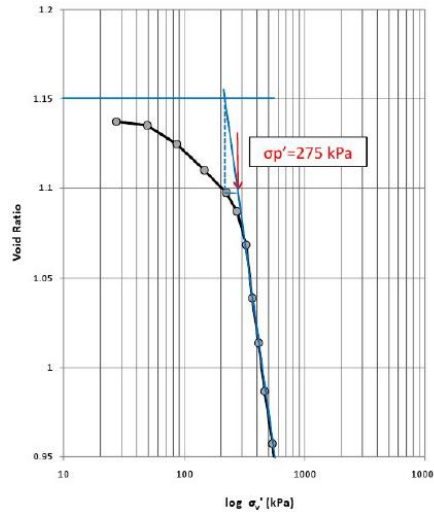
Figure 30.Pacheco Silva's method applied to Newbury data. Source: Soler Arnal, 2009

Hardin (1989)

Although it is not actually a method to especially interpret the $σ'_p$ but an alternative approach to represent the consolidation curve, this method provides a correction for the effective vertical stress by the atmospheric pressure which allows the curve to be depicted straighter than the original log σ-e. Thereby, the interpretation of the yield stress is easy and the result obtained lies close to the set values from other methods.
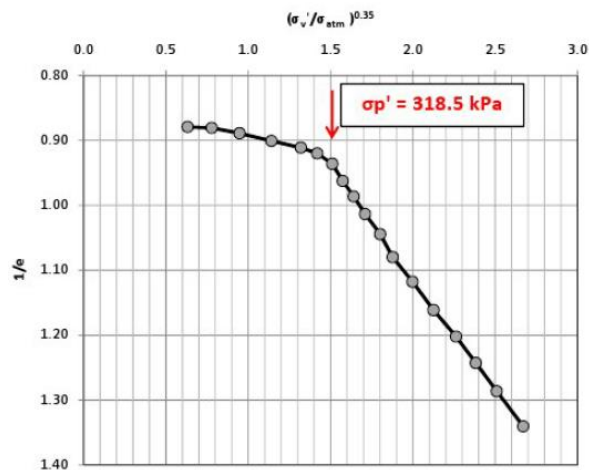
Figure 31. Hardin's representation applied to Newbury data. Source: Soler Arnal, 2009.

- *Bilogarithmic methods*

<u>Oikawa (1987)</u>

This method is similar to the previous from Butterfield but plotted in decimal logarithm scale. The value of preconsolidation stress obtained is 270 kPa, very close to the previous one and the advantages are the same.
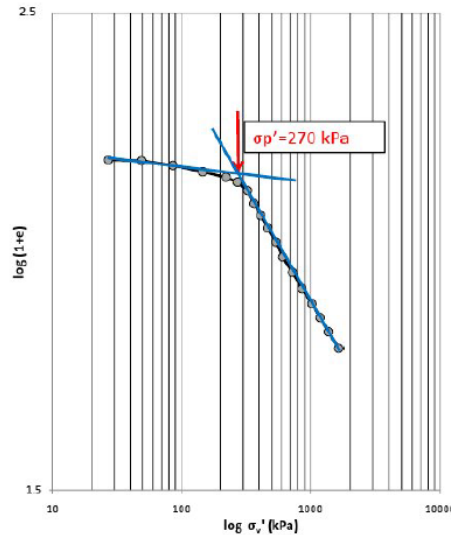
Figure 32. Oikawa's method applied to Newbury data. Source: Soler Arnal, 2009

<u>Butterfield (1979)</u>

The first bilogarithmic method is based in natural logarithm scales and provides a preconsolidation stress value of 270.5 kPa. This method gives a slightly lower value than the Casagrande's one. A bilogarithmic method seems to suit better with the kind of consolidation curve studied since the rounded virgin branch becomes straighter in logarithmic scale, moreover, is fast and easy to apply.
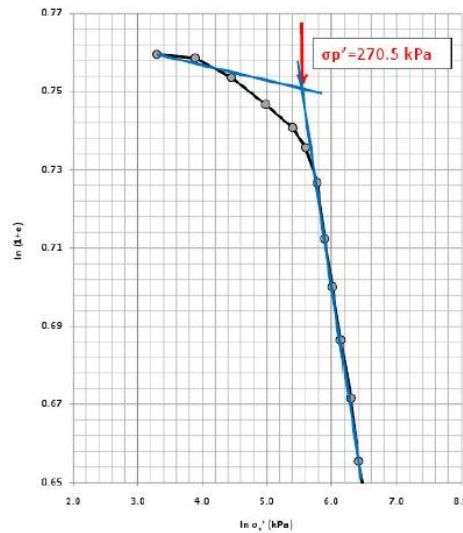
Figure 33. Butterfield's method applied to Newbury data.
Source: Soler Arnal, 2009

<u>Onitsuka (1995)</u>

Onitsuka's method combines natural logarithm scale for the vertical effective stress with decimal logarithm for the void ratio, which does not introduce any advantage comparing with other bilogarithmic methods. The preconsolidation stress appears to be equatl the otucome of the Oikawa method, that is to say 270 kPa.
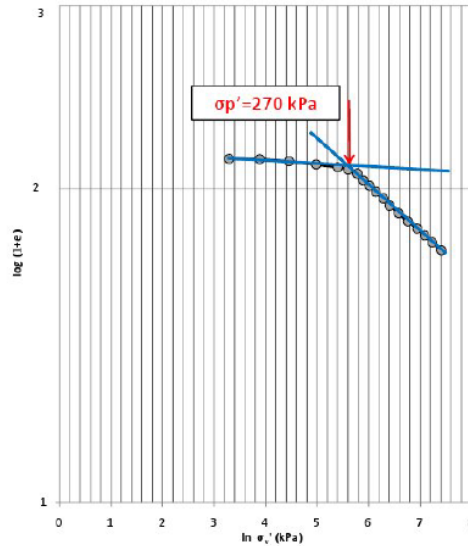
Figure 34. Onitsuka's method applied to Newbury data.
Source: Soler Arnal, 2009

<u>Jose, Sridharan & Abraham (1989)</u>

The last bilogarithmic method is applied with decimal logarithmic scale and provides a preconsolidation stress of 275 kPa. The main difference with the other bilogarithmic methods is that the void ratio is used instead of the specific volume (1+e).
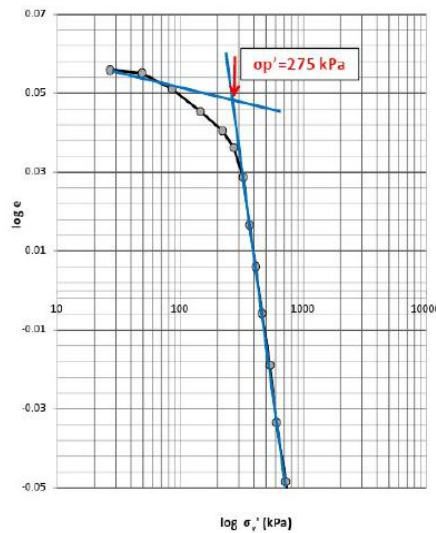
Figure 35. Jose's method applied to Newbury
data. Source: Soler Arnal, 2009

- *Postprocessing methods*

<u>Janbu (1969)</u>

The modulus-stress plot depicts a dispersed point series in the second part whereas it should follow a continuous line marked by the trend line in the graph. In *Figure 37,* the strain-stress plot shows clearer the preconsolidation value of 320 kPa at the inflexion of the curve. This method is fairly accurate in the determination of preconsolidation stress and it is applicable to any type of soil. The transformation of consolidation values (void ratio and vertical effective stress) in tangent modulus requires a post-process and then the method is more time consuming besides interpretation is sometimes difficult. The stress-strain relationship and modulus stress curves are obtained by the following equations:

$$\varepsilon = \frac{e_0 - e}{1 + e_0} \qquad M = \frac{\sigma_{v,i} + \sigma_{v,i+a})/2}{\varepsilon_i - \varepsilon_{i+1}}$$
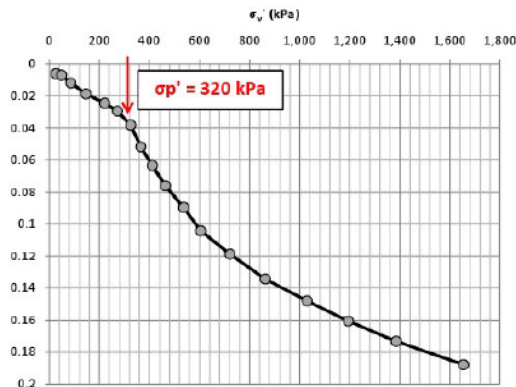
Figure 37. Strain-Stress curve. Janbu's method applied to Newbury data. Source: Soler Arnal, 2009
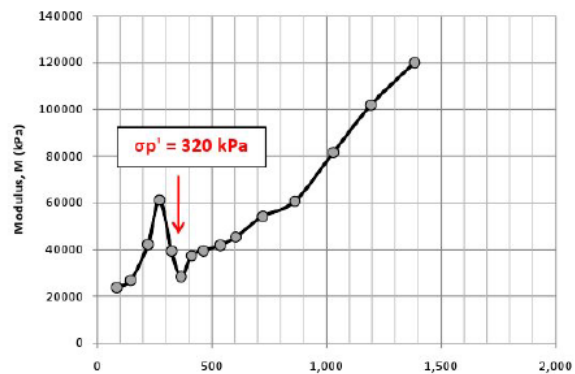
Figure 36. Modulus-Stress curve. Janbu's method applied to Newbury data. Source: Soler Arnal, 2009

<u>Becker et al. (1987)</u>

Work per unit volume method consists of plotting the incremental work against the vertical effective stress in arithmetic scale. The change in strain energy, or work, was obtained based on the average vertical effective stress as described in the expression below:

$$\Delta W = \frac{\sigma'_{v,i} + \sigma'_{v,i+1}}{2} \Delta \frac{e_0 - e}{1 + e_0}$$

The second part of the data seems dispersed due to the quality of the data available. Nevertheless, the preconsolidation stress shown as the intersection of the two data trend lines is in the order of the other methods but provides a lower value. The method is time consuming but objective, although it does not always provide an easy interpretation of the point where preconsolidation stress is provided.
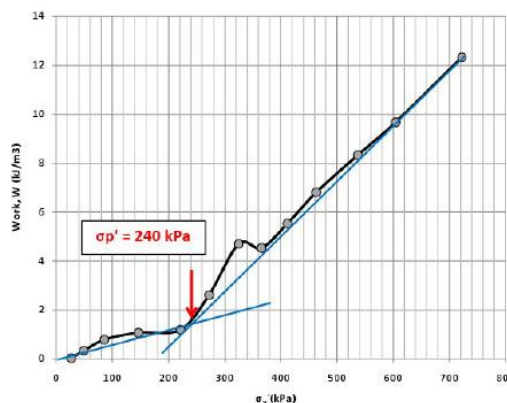
Figure 38. Becker et al. method applied to Newbury data. Source: Soler Arnal, 2009

Burland (1990)

The Intrinsic Compression Line (ICL) dened by Burland was applied to the data. Then the void ratio was transformed into the void index (Iv) and plotted against the vertical effective stress in logarithmic scale. Soil properties show the soil is above the A-line in Casagrande's Plasticity chart as required to apply this method. The void ratio corresponding the liquid limit is figured out from phase relationships and has a value of 1.167.

ICL:

$$I_v = 2.45 - 1.285 \log \sigma'_v + 0.015 \, (log \, \sigma'_v)^3$$

Void Index:

$$I_{vo} = \frac{e - e_{*100}}{C_{*c}}$$

$$e_{*100} = 0.109 + 0.679e_L - 0.089e_L^2 + 0.016e_L^3$$

$$C_{*c} = 0.256e_L - 0.04$$

The intrinsic void ratio at 100 kPa is e*$_{100}$ = 0.806 and the intrinsic compression index C*$_c$ = 0.259.

Burland's method requires a long time for post-processing of the consolidation test data but it gives an accurate value compared with other methods. It is little affected by sample disturbances and subjective judgement.
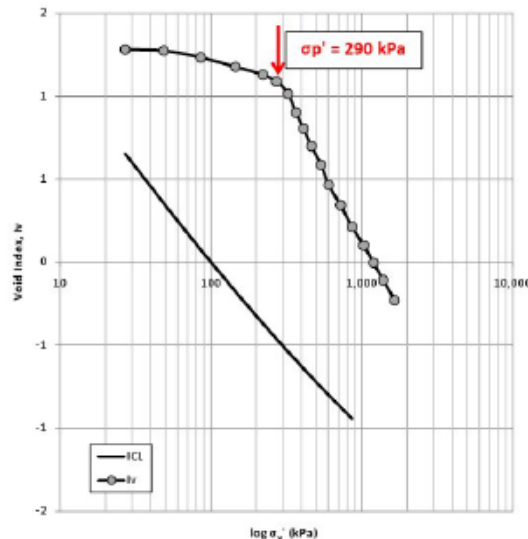
Figure 39. Burland's method applied to Newbury data.
Source: Soler Arnal, 2009

Senol & Saglamer (2002)

The method proposed by Senol and Saglamer is based on the plot of the strain against vertical effective stress, where the strain is obtained from the original values of void ratio by the basic relationship:

$$\varepsilon = \frac{\Delta H}{H_0} = \frac{e_0 - e}{1 + e_0}$$

The preconsolidation stress was determined to be 380 kPa by the intersection of the two extended straight lines. This value is greater than the obtained with other methods.
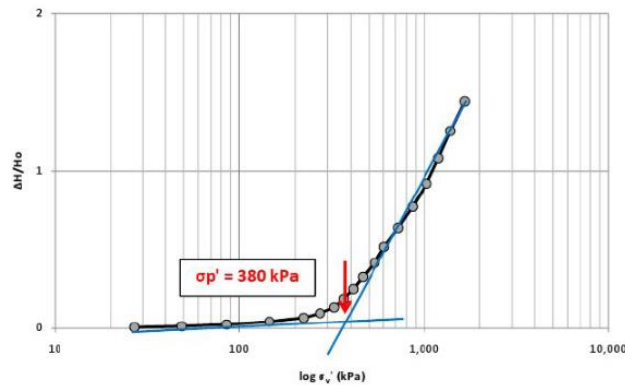
Figure 40. Senol & Saglamer method applied to Newbury data. Source: Soler Arnal, 2009

Jamiolkowski & Marchetti (1969)

The inverse of the coefficient of volume decrease is plotted against the vertical effective stress in logarithmic scale. The plot depicts two parallel lines of about 45o slope with a discontinuity between them, in the middle of which the preconsolidation stress is encountered at 290 kPa stress. The obtained value fits with the other methods. The post-process of the data is based in the calculation of the coefficient of volume decrease following the next equation:

$$m_v = \frac{(e_i + e_{i+1})}{(\sigma_{v,1} + \sigma_{v,i+1})/2} \frac{1}{1 + e_0}$$
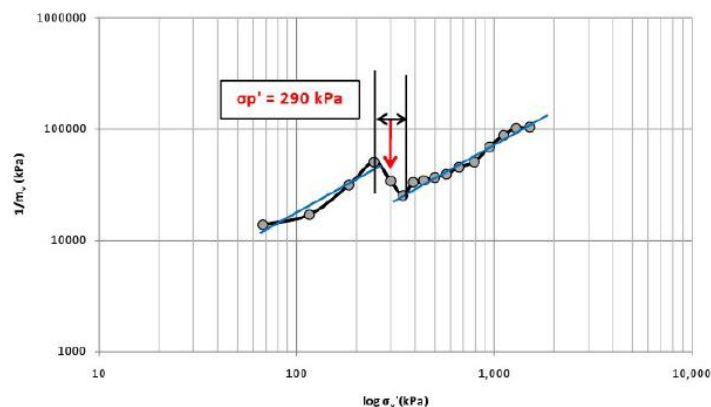
Figure41. Jamiolkowski's method applied to Newbury data. Source: Soler Arnal, 2009

- *Empirical methods*

<u>Andersen et al. (1979)</u>

The backcalculation of preconsolidation stress from shear strength gives the following result:
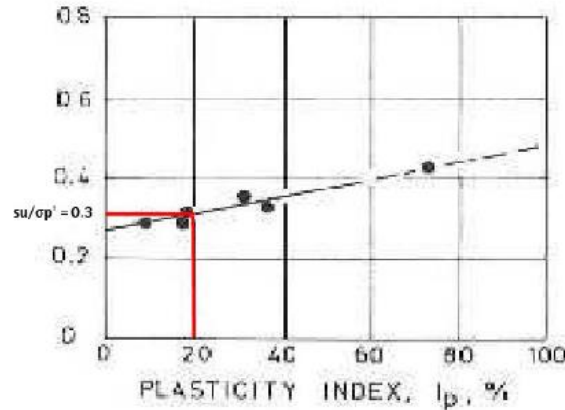
Figure 42. Andersen et al. method applied to Newbury data. Source: Soler Arnal, 2009

$$s_u = 62 \ kPa \qquad \frac{s_u}{\sigma'_p} = 0.3 \qquad \sigma'_p = 206.7 \ kPa$$

The empirical method seems to provide values out of the range defined by the other methods and then, they are not considered to be appropriate to evaluate the preconsolidation stress in this case. For example, the suggestion that the preconsolidation stress as 2.5 times the stress corresponding to the maximum curvature point in Casagrande's construction proposed by Jacobsen is not applicable due to the proximity of this value with point where the preconsolidation stress is defined in the log σ'_p - e plot. Likewise, Solanki and Desai empirical correlation provides a too low value for Newbury data, as well as Chetia and Bora method.

- *Summary of values*

In *Table 7,* the preconsolidation values obtained for the different methods applied are summarized. The preconsolidation stress average is equal to 276.6 kPa.

Method	σ'_p (kPa)
Casagrande	280
Van Zelst	250
Schmertmann	320
Pacheco Silva	275
Sällfors	170
Hardin	318.5
Butterfield	270.5
Oikawa	270
Jose	275
Onitsuka	270
Burland	290
Janbu	320
Jamiolkowski	290
Becker	240
Senol & Saglamer	380
Andersen	206.7
AVERAGE	**276.6**

Table 7. Summary of preconsolidation values obtained from Newbury CRS. Source: Soler Arnal, 2009

Methods based on the traditional log σ - e plot are graphical methods and imply some grade of subjectivity, as in the infamous Casagrande's construction in the determination of the maximum curvature point, or Schmertmann method when choosing the most symmetric Δe curve. However, the proposed method by Pacheco Silva seems to be rather independent of subjectivity, as well as easy to apply.

Bilogarithmic methods are very similar since they are only a modification of the scale representation, moreover, provide similar values than other methods. They are simple to perform and have the advantage of depicting a straighter consolidation curve. Therefore, these methods are appropriate for soils that describe a curved plot for sensitive clays and soft soils.

Some empirical methods were described and these, usually have a correlation with soil characteristics, like the liquid limit or plasticity index. These approaches should be used with some precautions and always compared with other methods, nevertheless the expressions provided are easy to apply.

Methods based in either strain energy or work such as Becker et al., Jamiolkowski, Wang and Frost or Janbu, require a post-processing in the consolidation data. They are mathematically consistent methods and usually provide accurate data. However, these methods are more time consuming and some need to have more measures or additional data than that supplied by usual oedometer tests.

In conclusion, for a good evaluation of preconsolidation stress, it is advisable to perform several of the methods exposed here in in order to set a comparison of the results. Analysis by more than one method allows the user to notice the variations caused by soil and testing disturbances, scale and plotting procedure as well as personal judgement. Depending on the engineering needs, the available resources and time, one or more methods might be used and combined to predict the stress history of the soil in question.

3.3 Indirect estimation: pedotransfer functions

3.3.1 Literature review

Direct measurements are the most exact determination of PCS. However, they are often time-consuming and laborious, require expensive and sophisticated devices and skilled technicians and are impractical for wide-scale applications due to large spatial-temporal variability of soil properties (Elmer Alosnos, 2015). In addition, obtaining equivalent soil mechanical measures in a laboratory setting requires major sampling, resulting in a destructive investigation of the soil (Carter and Gregorich, 2008).

Therefore, besides direct estimation methods from compression curves, researchers seeking practical methods to determine PCS have suggested empirical functions, such as pedotransfer functions (PTFs) (Dias Junior and Pierce, 1995; Horn and Fleige, 2003; Imhoff et al., 2004; Baumgartl and Köck, 2004; Gregory et al., 2006). PTFs give an indirect method to estimate PCS as a more rapid and less expensive valid alternative.

The Encyclopedia of Agrophysics (2011) defined pedotransfer functions as "equations or algorithms expressing relationship between soil properties different in difficulty of their measurement or their availability". The basic premise of pedotransfer functions is that since soil properties and processes are mutually linked, there must be a specific set of soil properties explicitly determining other properties. Although the concept of PTF has long been used in the past to estimate soil properties that are hard to determine, the term was coined for the first time by Bouma (1989) and since then has gained worldwide recognition as a new field of research in soil science, water resources, agronomy, and environmental science (Tranter et al., 2007).

Strong and renewed interest in empirical PTFs is mainly a result of new methods and tools becoming available for PTF development including statistical regression, data mining techniques, and machine learning algorithms. One advantage of using statistical regression is that rigorous estimates of the statistics of the predicted values and the coefficients in the PTF equations can be obtained. However, constructing PTFs using statistical regression requires many iteration steps, such as deciding which properties are to be used as predictors and which regression equation to use (Pachepsky and van Genuchten, 2011).

Pedotransfer functions are commonly used to predict PCS from readily available soil properties (Horn and Fleige, 2009; Van den Akker and Hoogland, 2011). Though most of the PTFs reported in literature pertain to the estimation of soil water retention and saturated hydraulic conductivity, a mathematical function can also be used in predicting soil mechanical properties associated with compaction.

These pedotransfer functions are commonly used to estimate PCS and Cc in function of texture, bulk density, water content, matric potential and OM content (Gupta and Larson, 1982; Lebert and Horn, 1991; Imhoff et al., 2004; Saffih Hdadi et al., 2009; Rücknagel et al., 2012; Schjønning and Lamandé, 2018), except Kirby (1991) who investigated the dependence of PCS and Cc on the state of the soil, of which liquidity index and void ratio emerged as good predictor. A summary of these PTFs are shown in *Table 8* and *Table 9*.

Source	Property	Predictors	Soil Class	N	FTP equations	R^2
Gupta and Larson (1982)	Compression index, Cc	Clay content, % clay (g 100 g^{-1})	Expanding clay	54	$C_c = 2.033 \times 10^{-1} + 1.423 \times 10^{-2} (\%clay) - 1.447 \times 10^{-4} (\%clay)$	0.79
			Non-expanding clay	54	$C_c = 1.845 \times 10^{-1} + 1.205 \times 10^{-2} (\%clay) - 1.108 \times 10^{-4} (\%clay)$	0.89
Lebert and Horn (1991)	Precompression stress, PCS	Internal friction, Ø (°); cohesion, c (kPa); bulk density, ρ_b (Mg m^{-3}); air capacity, Lk (%, v/v); available water capacity, nFk (%, v/v); non-available water capacity, TW (%, v/v); saturated hydraulic conductivity, k_f (x10^3 cm s^{-1}); organic matter, OM (g 100 g^{-1})	Sand	307	$PCS\ (pF=1.8) = 438.10\rho_b - 0.0008(Ø_{1.8})^3 - 3.14TW - 0.11(nFk_{1.8})^2 - 465.60$	0.778
					$PCS\ (pF=2.5) = 410.75\rho_b - 0.0007(Ø_{2.5})^3 - 3.41TW - 0.35(nFk_{2.5})^2 - 384.71$	0.710
			Sandy Loam		$PCS\ (pF = 1.8) = 169.30\rho_b - 29.03(OM)^{0.5} + 6.45k_f + 32.18 \log(C_{1.8}) - 9.44\ Ø_{1.8} + 27.25 \sin(TW) + 119.74 \log(nFk_{1.8}) + 19.51$	0.828
					$PCS\ (pF = 2.5) = 89.50\rho_b - 23.99(OM)^{0.5} + 2.89k_f + 125.76 \log(C_{2.5}) - 1.14\ Ø_{2.5} + 26.90 \sin(TW) + 51.46 \log(nFk_{1.8}) + 77.25$	0.874
			Silt		$PCS\ (pF = 1.8) = 374.15\rho_b - 4.10OM + 3.38Lk_{1.8} - 1.58(k_f)^{-0.5} + 1.79C_{1.8} + 1.09(TW) - 6.37(Ø_{1.8})^{0.67} + 0.088(nFk_{1.8})^2 - 472.77$	0.765
					$PCS\ (pF = 2.5) = 460.71\rho_b - 20.33OM + 9.088Lk_{2.5} - 2.38(k_f)^{-0.5} + 2.86C_{2.5} + 4.50(TW) - 20.96(Ø_{2.5})^{0.67} + 0.304(nFk_{2.5})^2 - 610.62$	0.847
			Clay and Clay Loam (<35%)		$PCS\ (pF = 1.8) = 0.843\rho_b - 0.544(k_f)^{0.33} + 0.022TW + 7.03(C_{1.8})^{-1} + 0.024\ Ø_{1.8} - 0.015nFk_{1.8} + 0.725$	0.808
					$PCS\ (pF = 2.5) = 0.844\rho_b - 0.456(k_f)^{0.33} + 0.026TW + 12.88(C_{2.5})^{-1} + 0.003\ Ø_{2.5} - 0.016nFk_{2.5} + 1.419$	0.804
			Clay and Clay Loam (>35%)		$PCS\ (pF = 1.8) = 4.59\rho_b - 1.02OM - 16.43(k_f)^{0.33} + 0.31TW - 1.57nFk_{1.8} + 3.55C_{1.8} + 1.18\ Ø_{1.8} - 18.03$	0.774
					$PCS\ (pF = 2.5) = 70.65\rho_b - 0.55OM - 7.01(k_f)^{0.33} + 1.32TW +- 1.08nFk_{2.5} + 1.72C_{2.5} + 1.05\ Ø_{2.5} - 100.94$	0.763

Table 8. Existing pedotransfer functions used to predict PCS and other soil mechanical properties (I). Source: Elmer Alosnos, 2015

Source	Property	Predictors	Soil Class	N	FTP equations	R^2
Kirby (1991)	Precompression Stress, PCS	Liquid index I_L; void ratio at p_c, e_{pc}; saturation at e_{pc}, S_{epc}	All soils	170	$PCS = exp(5.856 - 4.352\,I_L - 1.074\,e_{pc})$	0.682
	Compression index, C_c	Void ratio at p_c, e_{pc}; saturation at e_{pc}, S_{epc}	All soils		$C_c = 0.229 + 0.1736e_{pc} - 0.400S_{epc}$	0.514
Imhoff *et al.* (2004)	Precompression Stress, PCS	Clay content, CC (g 100 g^{-1}); initial bulk density, ρ_b (Mg m^{-3}); water content, w (g g^{-1})	All soils	50	$PCS = -566.764 + 442.891\,\rho_b + 4.338CC - 773.057w$	0.70
	Compression index, C_c		CC < 29.42 CC > 29.42		$C_c = 0.248 + 0.006CC - 0.121\rho_b$ $C_c = 0.416 - 0.121\rho_b$	0.77 0.77
Saffih Hdadi *et al.* (2009)	Precompression Stress, PCS Compression Index, C_c	Initial water content, w (% g g^{-1}); initial bulk density, ρ_b (Mg m^{-3})	Very fine		$PCS = 7.71 + 112.21\rho_b - 2.82w$ $C_c = 2.37 - 1.18\rho_b - 0.017w$	0.88 0.95
			Fine		$PCS = 4.19 + 202.54\rho_b - 10.92w$ $C_c = 1.85 - 0.91\rho_b - 0.012w$	0.95 0.98
			Medium fine		$PCS = -223.71 + 347.47\rho_b - 7.93w$ $C_c = 1.36 - 0.59\rho_b - 0.010w$	0.76 0.78
			Medium		$PCS = -136.87 + 155.19\rho_b$ $C_c = 1.27 - 0.628\rho_b - 0.006w$	0.5 0.74
			Coarse		$PCS = -220.68 + 191.45\rho_b - 2.77w$ $C_c = 1.36 - 0.77\rho_b - 0.005w$	0.57 0.87

Table 9. Existing pedotransfer functions used to predict PCS and other soil mechanical properties (II). Source: Elmer Alosnos, 2015

Gupta and Larson (1982) predicted Cc based on clay content. Lebert and Horn (1991) developed regression equations with high degree of significance ($R^2 > 0.7$) to predict soil strength for two water tensions (pF 1.8 and pF 2.5) as a function of bulk density, shear strength parameters (cohesion c and angle of internal friction ϕ), air capacity, water capacity, saturated hydraulic conductivity and OM content. Apparently based on these equations, the effect of water content on soil strength is clearly defined. The drier the soil is, the stronger it gets, its stability decreases when soil gets wetter.

Imhoff et al. (2004) investigated the compressive behaviour and found a significant multiple correlation ($R^2 = 0.70$) between PCS and initial bulk density, water content, and clay content. A similar observation was also reported by Saffih-Hdadi et al. (2009). The findings of Imhoff et al. (2004) and Saffih-Hdadi et al. (2009) highlighted the clear effect of initial soil water content, initial dry bulk density, and soil texture on PCS. They showed that PCS was positively correlated with soil bulk density and negatively correlated with initial soil water content. A positive correlation between PCS and soil bulk density was also reported earlier by Lebert and Horn (1991); Salire et al. (1994); McBride and Joosse (1996); Alexandrou and Earl (1998), Canarache et al. (2000), Silva et al. (2000, 2002) and Rücknagel et al. (2012). Whereas a significant negative correlation between PCS and water content was also observed by Alexandrou and Early (1998), Defossez et al. (2003), Imhoff et al. (2004) and Mosaddeghi et al. (2006).

Nevertheless, Keller et al. (2007) noted that the predictive performances of some of these existing PTFs are not well evaluated and their reliabilities are not well known. Therefore, those PTFs which are based on native data should be preferred over generic PTFs since they provide the flexibility of appending reference databases and acceptable predictive performance (Patil et al., 2012).

According to *Elmer Alosnos's thesis dissertation (2015)*, in which he carried out investigations on precompression stress, the following results present the relationship by PTFs development between PCS and soil properties associated with soil compaction.

The PTFs linear functions to predict PCS were developed using a stepwise multiple linear regression (SMLR) by using R software. The selection of the predictors to develop the PTFs was done on a semi-hierarchical basis and the stepwise regression procedure helped select the significant ones out of the available predictors.

At the outset, initial PTFs were derived using the complete dataset (N=126) of which Sn, Si, Cl, OC, pF, BD, and texture were used as the only predictors. Imhof et al. (2004) also used BD and clay content to predict compression index and PCS. For practical reasons, the wet bulk density (WBD) and saturated hydraulic conductivity (K_{sat}) were not included in the analysis since in practice, measurements of these variables are not easy and time-consuming.

To evaluate the predictive ability of the developed PTFs, three statistical measures were used - the mean absolute error (*MAE*), the root mean square error (*RMSE*) and coefficient of determination (*R²*). Results of the initial runs showed that developed PTFs had very low predictive performances.

The next approach then was to include other variables such as CSR, SQI, and PD as predictors and the dataset was split into two groups based on land use (cropland, grassland). The grassland PTFs have a higher coefficient of determination ($R^2 > 0.40$) compared to cropland PTFs. This may indicate that the underlying causal factors of the PCS variability in cropland is somehow more complex than grassland which cannot be deduced from soil properties alone. This might be due to that cropland was a mix of headland and centre field, which could explain part of the variability.

The newly developed PTFs specific for each land use type and the addition of soil quality indices such as PD and SQI substantially improved the predictive performance (see *Table 10* and *Figures 43-44*). However, further research is needed to improve these PTFs to a reasonable degree of predictive capability.

Method	LU	PTF Equations	MAE	RMSE	R²	R²(adj)
C_DK	CL	log(PCS) = -90.27 + 0.89*Cl + 0.92*Sn + 0.92*Si + 0.24*OC + 0.19*PF - 5.24*StI + 0.54*PD	0.15	0.21	0.35	0.29
	GL	log(PCS) = -142.7 - 0.10*Tx + 1.48*Cl + 1.44*Sn + 1.43*Si + 1.01*PD	0.15	0.23	0.40	0.32
AK_2	CL	log(PCS) = 0.48 + 0.01*Sn + 0.01*Si + 0.17*PF - 2.27*StI	0.14	0.18	0.18	0.14
	GL	log(PCS) = -191.02 -0.13*Tx +1.96*Cl +1.91*Sn +1.90*Si -0.03*Ca +0.14*PF +6.05*StI +1.19*PD	0.10	0.15	0.67	0.59
AK_3	CL	log(PCS) = -0.47 + 0.03*Sn + 0.03*Si + 0.13*CSR	0.17	0.22	0.16	0.13
	GL	log(PCS) = -0.51 - 0.06*Tx + 0.01*Sn + 1.40*BD + 0.4*CSR - 3.16*StI	0.14	0.20	0.34	0.25
AK_4	CL	log(PCS) = 1.14 + 0.15*OC + 2.33*BD + 0.17*PF - 4.86*StI - 1.69*PD	0.13	0.18	0.38	0.34
	GL	log(PCS) = -153.02 - 0.1*Tx 1.57*Cl + 1.54*Sn + 1.53*Si + 4.65*SQI + 1.04*PD	0.12	0.17	0.44	0.34
AK_5	CC	log(PCS) = 1.15 + 0.002*Sn + 0.21*OC + 3.75*BD + 0.16*PF + 0.14*CSR - 7.35*StI - 3.06*PD	0.13	0.44	0.44	0.38
	GL	log(PCS) = -145.27 - 0.09*Tx + 1.49*Cl + 1.46*Sn + 1.46*Si + 3.12*StI + 0.96*PD	0.10	0.15	0.48	0.39
Gea_3	CC	log(PCS) = 2.85 - 0.14*Cl - 0.08*OC - 0.01*Ca - 16.67*BD + 0.07*PF + 16.25*PD	0.10	0.13	0.30	0.25
	GL	log(PCS) = -80.86 -0.05*Tx +0.86*Cl +0.82*Sn +0.82*Si -0.03*Ca +0.15*PF +4.89*StI +0.4*PD	0.08	0.11	0.58	0.48
Gea_4	CC	log(PCS) = 2.03 - 0.16*Cl - 0.003*Sn - 16.77*BD + 0.13 *PF + 16.96*PD	0.18	0.23	0.13	0.08
	GL	log(PCS) = -259.02 -0.15*Tx +2.67*Cl +2.58*Sn + 2.58*Si +0.21*PF -0.34*CSR +10.38*StI +1.59*PD	0.14	0.20	0.64	0.55

LU: land use (CL - cropland, GL - grassland), log(PCS): logarithm of precompression stress (log-kPa), Sn: sand (%), Si: silt (%), Cl: clay (%), BD: dry bulk density (Mg/m³), CSR: clay/sand ratio, OC: organic carbon content (%), Ca: CaCO3, Tx: texture (coded var.), PF: log of water potential, StI: soil structural quality index (%), PD: packing density (g/cm³)

Table 10. List of PTFs to predict precompression stress of arable soils with different land use. The equations represent the best subset regression results and their mean absolute error (MAE), root mean square error (RMSE), and adjusted R2 values. Source: Elmer Alosnos, 2015
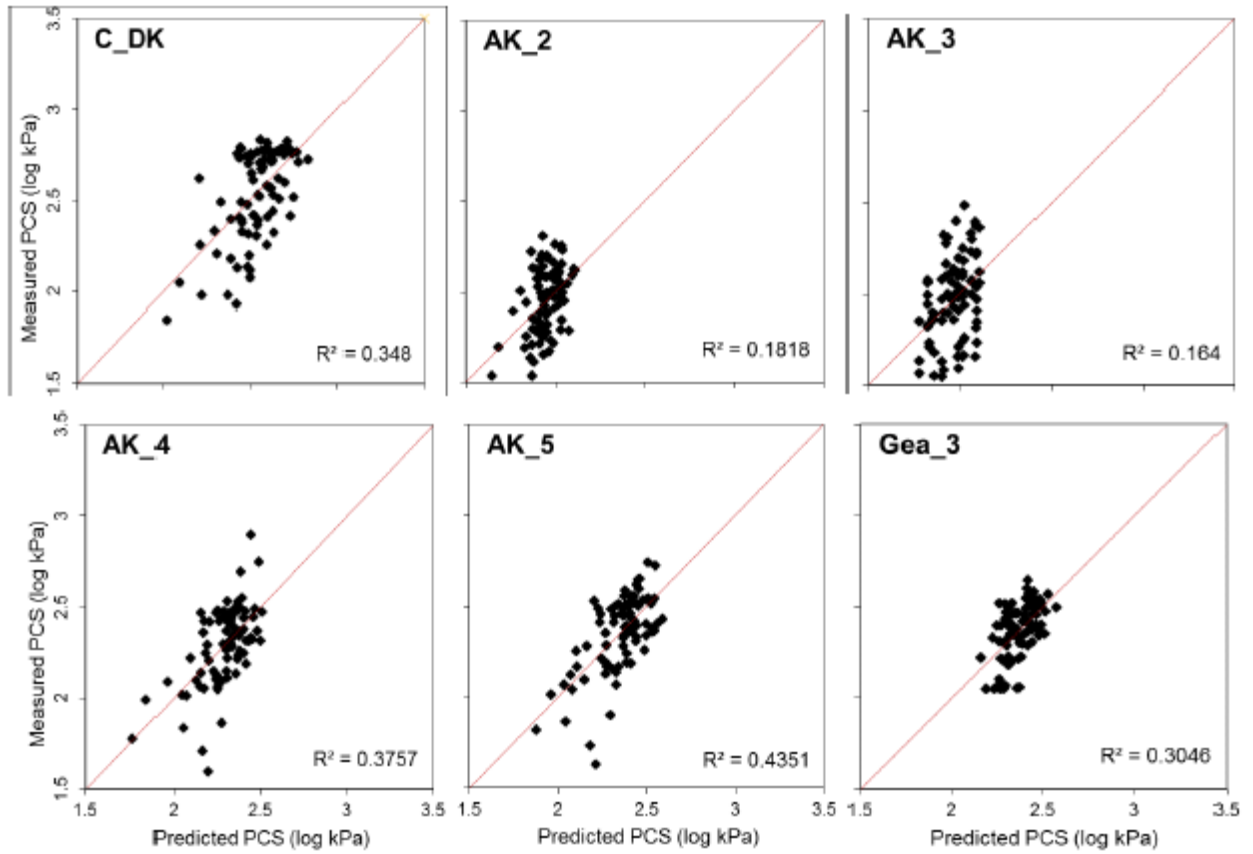
Figure 43. Measured versus PTF-predicted PCS (log kPa) for soil samples collected from cropland. Source: Elmer Alosnos, 2015
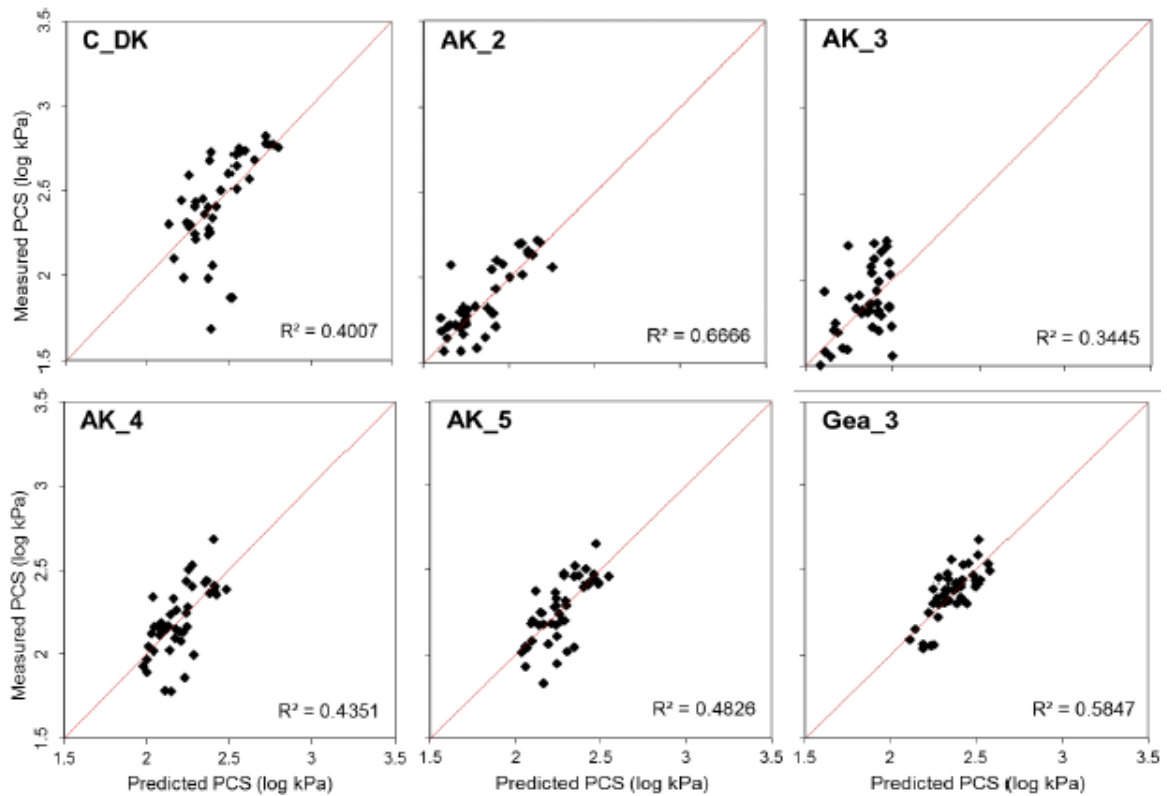
Figure 44. Measured versus PTF-predicted PCS for soil samples collected from grassland. Source: Elmer Alosnos, 2015

58

Schjønning and Lamandé (2018) developed a novel strategy for quantifying σ'$_p$ from stress-strain curves with no need to assume any specific mathematical relationship between stress and strain (Lamandé et al., 2017). They revisited previously published data on σ'$_p$ for a silty clay loam soil at a range of soil matric potentials (Lamandé and Schjønning, 2011c). The data include soil samples with a relatively high variation in clay content, density, as well as soil water content/matric potential. The data set thus seems suitable for estimating the relative influence of these soil properties on σ'$_p$. The aim of this study was to identify the most important drivers of soil precompression stress, σ'$_p$, and to develop pedotransfer functions for prediction of σ'$_p$. They showed that this strategy estimates better reflecting soil's loading history than the typically applied Gompertz approach suggested by Gregory et al. (2006).

Results indicated bulk density and matric potential as primary drivers for σ'p. In the topsoil or plough layer (0 – 20 cm), σ'$_p$ increased with BD for a 77% of the variation. A model combining BD and pF explained > 90% of the variation in the measured σ'$_p$ from the subsoil layer just below ploughing depth. A model combining BD, pF and soil clay content explained 38% for all soil layers considered. A summary of all PTFs developed for each layer is shown in *Table 11*.

Eq. no.	Intcp.	BD	Θ	WR	pF	R^2	RMSE	$P > F$[1]
Plough layer, 0.08–0.12 m, n = 15								
(1)	−36.05	32.85				0.77	1.67	< 0.0001
(2)	32.00			−37.42		0.46	2.56	0.0055
(3)	3.34				3.81	0.23	3.06	0.07
Subsoil layer 0.25–0.29 m, n = 16								
(4)	−59.06	46.38				0.66	2.83	0.0001
(5)	48.72		−115.1			0.40	3.79	0.0087
(6)	46.87			−64.89		0.67	2.79	< 0.0001
(7)	−9.18				10.22	0.68	2.74	< 0.0001
(8)	−49.49	30.46			6.92	0.90	1.60	< 0.0001
Subsoil layers 0.35–0.39, 0.60–0.64 and 0.90–0.94 m, n = 46								
(9)	−17.76	20.93				0.08	4.70	0.052
(10)	29.74		−44.73			0.18	4.45	0.0036
(11)	26.78			−20.78		0.18	4.45	0.0034
(12)	8.58				2.77	0.09	4.68	0.0409
(13)	−22.00	19.56			2.60	0.16	4.54	0.0213

Table 11. Coefficients in models for σpc. Source: Schjønning and Lamandé (2018)

An interaction between clay and pF in this model implied that predicted σ'$_p$ at pF ~ 2 for a given BD was constant across soil clay contents. For pF < 2, predicted σ'$_p$ was lower for clayey soils than for sandy soils. For pF > 2, the model predicted the opposite. The predicted increase in σ'$_p$ when drying out was higher for clay than for sand soils. In *Figure* 46 can be observed how predicted σ'$_p$ varies in terms of BD, pF and clay content.
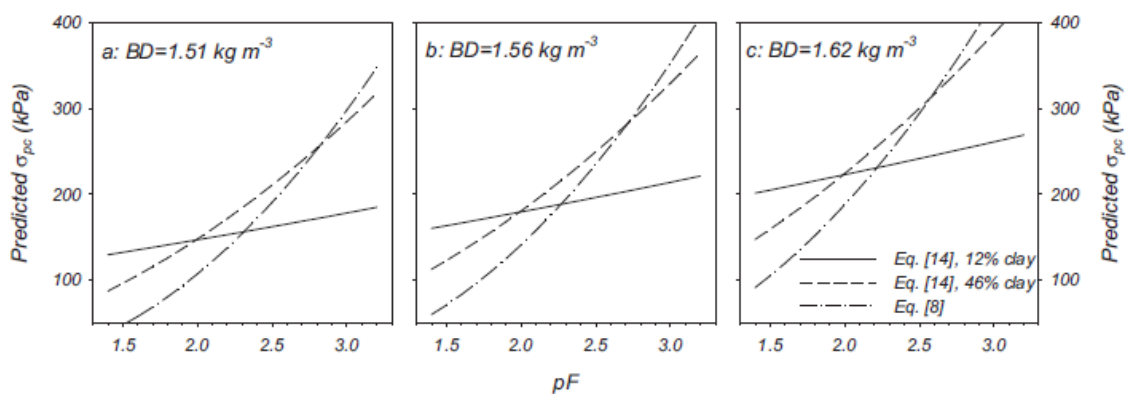
Figure 45. Development in predicted σpc (with soil matric potential (pF) at two levels of soil clay content and at three levels of bulk density. Source: Schjønning and Lamandé (2018)

To their knowledge, no previous studies had identified prediction equations for σ'_p with the precision observed in this investigation. This may partly relate to the novel, numerical procedure in estimating σ'_p from the stress-strain curve. No assumptions of mathematical relations between stress and strain are involved, and no subjective interpretations of best fit are in play. Soil BD and clay content are often readily available from databases, while the moisture regime expressed by pF may be guesstimated by extension officers or even by farmers. It should be noted that in this study, clay content is to some extent confounded with soil depth.

Soil cores being sampled vertically, σ'_p should ideally be related to the normal stress component. However, considerable shear stresses may occur during wheeling (e.g., Horn et al., 1992; Kirby, 1991b). Significant levels of shear stress have been observed to considerable depths below implement as well as traction tyres (Berisso et al., 2013; Lamande et al., 2015; Way et al., 1997). Kirby (1991b) suggested that a stress threshold estimated as σ'_p multiplied by a scaling factor of 0.8 might take into account the effect of shear. Thus, there is an urgent need to increase the knowledge of the shear strength, and the inclusion of shear stresses in prediction of the sustainability of intended field traffic.

Finally, precompression stress is also calculated in Terranimo® by a PTF (see next chapter, Chapter 4). This information would be very useful and interesting for this thesis dissertation, but, unfortunately, this manuscript is currently unpublished. However, thanks to communications with Schjønning and Lamandé, what we could know is that the variation in PCS can be described by a combination of the soil organic matter content, the soil bulk density, and soil suction stress.

3.3.2 Own practical PTFs development

An indirect estimation and analysis of the precompression stress values by a new development of the pedotransfer functions was performed.

The used dataset was provided by the Soil Physics Research Group from UGent. It consists of a total of 126 soil core samples that were taken in 2012-2013 for the *Snowman Project* in seven sampling sites in Flanders and is exactly the same as the one used by Elmer Alosnos in his thesis dissertation (as well as PCS determination). These soil samples were characterized with varying important soil properties, e.g. texture or particle size distribution (expressed as % of sand (Sn), silt (Si) and clay (Cl)), bulk density (BD), organic carbon content (OC), land use (cropland or grassland), initial matric potential (pF) and % of water content.

The statistical procedure that we have followed is very similar than the one from Alosnos, 2015. We estimated the PTFs by stepwise multiple linear regression. This allowed us to predict each dependent PCS value (seven determination methods) by a selection of independent variables (soil properties) that contributed significantly to the model, called predictors. The initial dataset was divided into two groups of datasets, depending on the land use. The PCS determination methods that were used from the compression curves are as follows:

- *PCS_Cas*: Casagrande's procedure.

- *PCS_L1*: stress at the intersection of VCL with the x-axis at strain = 0.

- *PCS_L2*: stress at a predefined strain of 2.5%.

- *PCS_L3*: stress at the intercept of the VCL and a regression line with the first two points of the curve.

- *PCS_L4*: stress at the intercept of the VCL and regression line with the first three points of the curve.

- *PCS_G3*: fitting of three-parameter Gompertz type equation to stress-strain curve.

- *PCS_Gomp*: fitting of four-parameter Gompertz type equation.

The PCS_Cas method was used by Davidowski and Koolen (1974) based on Casagandre (1930) graphical procedure. PCS_L1, PCS_L2, PCS_L3, PCS_L4 correspond to the four methods used by Arvidsson and Keller (2004). These first five methods curves were fitted by the fourth-order polynomial function. PCS_G3 and PCS_Gomp are the modified (three parameters) and the original (four parameters) Gompertz function used by Gregory et al. (2006), respectively.

The initial soil properties that were entered and would play a significant role in the PCS model were: Sn (%), Si (%), Cl (%), OM (%), pF (log of initial matric potential in hPa), BD (mg/m^3), CSR (Clay/Sand ratio), StI (structural stability index, function of OC, Cl and Si, see Moncada et al., 2014). However, as suggested by Schjønning and Cornelis, one new variable was also introduced: preload suction stress, PSS (hPa). The PSS is an expression of the effective stress prior to loading the samples. It is calculated as the product of soil pore saturation and the numerical value of the matric potential (Schjønning and Lamandé, 2018).

The statistical software used for the regression process was SPSS. There are several methods to run the multiple regression in SPSS:

- *Enter*: all the predictor variables are entered the model at one time regardless if those independent variables make a significant contribution to the model.

- *Forward*: it enters the predictor variables that make a signification contribution to the model, one at a time (significant level probability = 0.05).

- *Backward*: all the predictor variables are entered at one time and then, removed one at a time, until there are no more variables to remove (significant level probability = 0.1).

- *Stepwise*: predictor variable is entered if it meets the criteria of making a significant contribution to the model. If it does not meet the criteria to stay in the model, that variable is removed. This method continues until there is no longer any predictor variable that meets the criteria to be entered or removed to the model (significant level probability = 0.05).

We first ran the multiple regression with the stepwise method. However, the results were not very reliable (only pF and BD as significant predictors) and the R^2 coefficients were very low. Afterwards, we tried running the same data with the backward method with a slightly higher significant probability and the results improved significantly.

To measure the accuracy of the newly developed PTFs, two of the most common statistical metrics were computed: mean absolute error (MAE) and root mean square error (RMSE):

$$MAE = \frac{1}{N_t} \sum_{i=1}^{N_t} (PCS_{p_i} - PCS_{m_i})$$

$$RMSE = \sqrt{\frac{1}{N_t} \sum_{i=1}^{N_t} (PCS_{p_i} - PCS_{m_i})^2}$$

PCS_{pi} is the predicted PCS for soil sample i (kPa), PCS_{mi} is the measured PCS for soil sample i (kPa) and N_t the number of samples in each dataset.

Moreover, for a better prediction assessment, the coefficient of determination (R^2 and adjusted R^2) were calculated. These values examine how strong the linear relationship is between the measure PCS from oedometer testing and the predicted PCS from the pedotransfer functions. The adjusted coefficient takes into consideration the number of predictor variables.

Let us take a detailed insight to these results (*Table 12* and *Figures 46-47)* regarding the land use, since as we can observe, results are different from each other:

Cropland

It is shown (*Table 12)* that the soil properties that significantly contributed to the PCS estimation and appeared in most of these PTFs equations were: Structural quality Index (StI) and Clay content (Cl) - negatively correlated- and Bulk Density (BD), Organic matter Content (OC) and Clay/Sand ratio (CSR) - positively correlated-.

The strongest PTF correlation amongst selected predictors was calculated with PCS_L4 (R^2 = 0.417). However, in terms of accuracy, the lowest error deviation was given by PCS_L1 (MAE = 5.1; RMSE = 31.6), in addition, observing *Figure 46,* these PCS values are very well fitted to the predicted values (PCS_L2 as well). However, it is shown that both methods estimated a range of PCS extremely low compared to other methods results (< 150 kPa).

Grassland

In this case, the predictors that significantly contributed most of the PTFs equations were: Silt content (Si) and Preload Suction Stress (PSS) -negatively correlated- and Organic Matter (OM) and Matric potential (pF) -positively correlated- (*Table 12).*

Based on the coefficient of determination, the biggest correlation was obtained by method PCS_G3 (R^2 = 0.455). Based on the estimation error, the best prediction was done again with PCS_L1 outcomes (MAE = - 4.2; RMSE = 31.8), but, same reason as before, PCS values are quite underestimated. However, *Figure 47* shows that PCS_G3 method gave a very well regression performance by fitting to the predicted values line.

Method	LU	PTF Equations - *SPSS*	MAE	RMSE	R^2	R^2 (adj)
PCS_Cas	CL	$1.463 - 0.017\,Cl + 0.148\,OC + 0.187\,pF + 0.584\,BD - 0.027\,StI$	-4.5	161.5	0.313	0.267
	GL	$2.252 - 0.004\,Si + 0.032\,Cl$	-34.1	147.4	0.200	0.159
PCS_L1	CL	$2.133 - 0.019\,Cl + 0.001\,PSS + 0.065\,CSR - 0.029\,StI$	5.1	39.6	0.193	0.151
	GL	$0.918 - 0.005\,Si + 0.023 + Cl + 0.430\,pF - 0.001\,PSS + 0.205\,CSR$	-4.2	31.8	0.318	0.224
PCS_L2	CL	$1.732 - 0.029\,Cl + 0.337\,BD + 0.195\,CSR - 0.019\,StI$	-11.8	55.1	0.193	0.151
	GL	$-0.487 - 0.003\,Si + 0.515\,pF + 0.964\,BD - 0.002\,PSS + 0.304\,CSR - 0.036\,StI$	-9.0	37.7	0.279	0.152
PCS_L3	CL	$1.125 - 0.014\,Cl + 0.141\,OC + 0.169\,pF + 0.644\,BD - 0.047\,StI$	-14.9	94.8	0.364	0.322
	GL	$2.352 - 0.005\,Si + 0.427 + OC - 0.047\,StI$	-17.8	79.4	0.141	0.073
PCS_L4	CL	$1.372 - 0.002\,Si - 0.028 + Cl + 0.184\,OC + 0.163\,pF + 0.656\,BD + 0.130\,CSR - 0.068\,StI$	-23.2	87.9	0.417	0.362
	GL	$2.429 - 0.005\,Si + 0.380\,OC - 0.049\,StI$	-13.5	-73.2	0.185	0.120
PCS_G3	CL	$3.219 - 0.101\,OC - 0.0533\,BD$	-28.2	76.8	0.183	0.152
	GL	$1.192 + 0.017\,Cl + 0.533\,pF - 0.002\,PSS + 0.091\,CSR$	-23.6	63.0	0.455	0.396
PCS_Gomp	CL	$2.608 - 0.003\,Si - 0.080\,CSR$	-75.8	184.2	0.105	0.071
	GL	$-0.440 + 0.052\,Cl + 0.248\,OC + 0.770\,pF + 0.519\,BD - 0.003\,PSS$	-48.8	150.2	0.401	0.318

Table 12. PTF Equations and predictability coefficients by SPSS for each PCS calculation method and land use. Source: own elaboration.
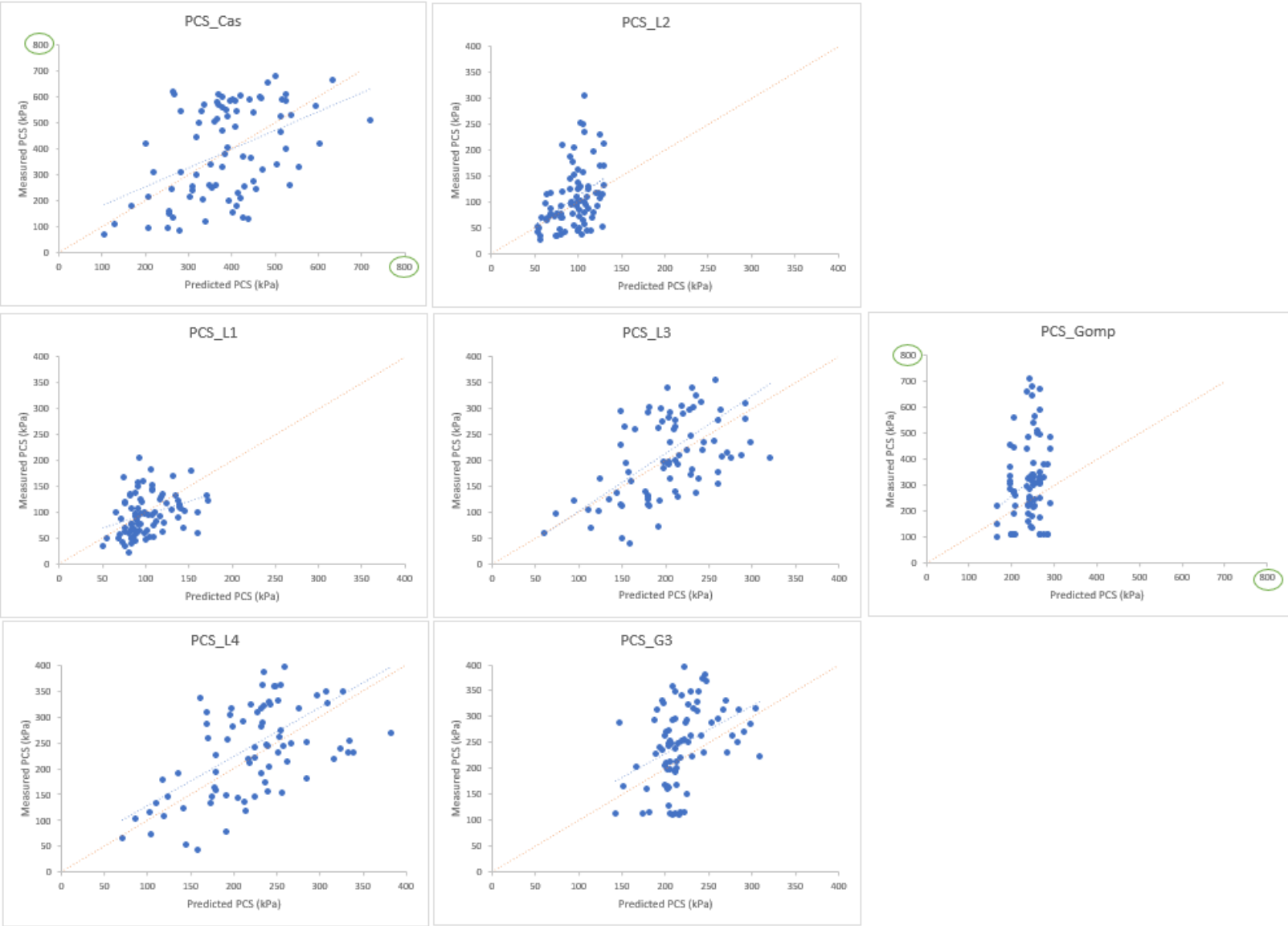
Figure 46. PCS predicted (x-axis) vs. PCS measured (y-axis) in Cropland. Source: own elaboration.
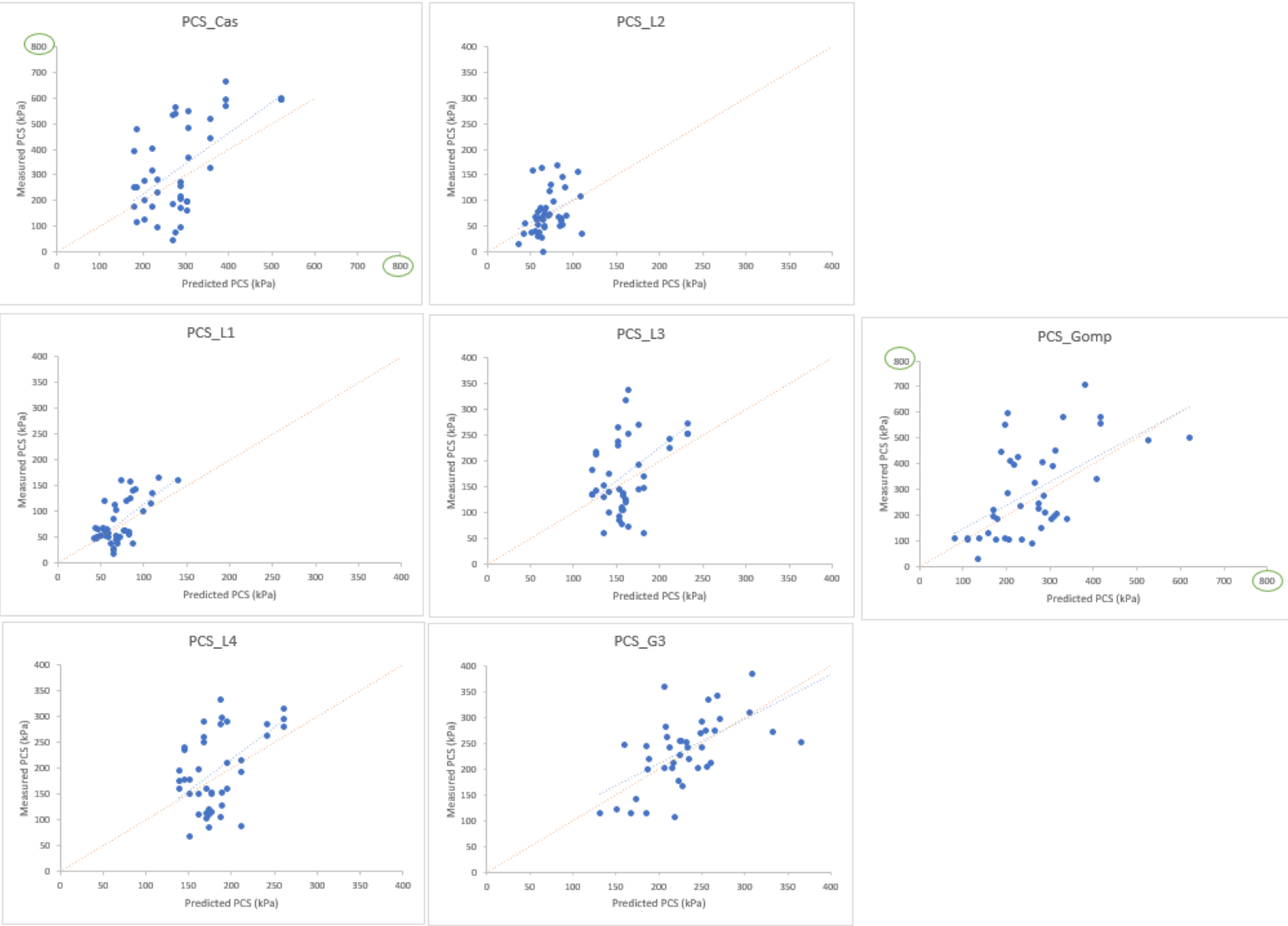
Figure 47. PCS predicted (x-axis) vs. PCS measured (y-axis) in Grassland. Source: own elaboration.

3.4 Discussion

In this chapter, we have detailed covered and analysed a wide range of different relevant matters and ideas that have to do with the important soil compaction concept called precompression stress. There are different ways of obtaining this parameter such as in-situ measurement, laboratory compaction tests by procuring the stress-strain relationship and indirect estimation by development of pedotransfer functions.

Keller et al. 2004 performed several studies in which different compaction tests were compared to observe the influence on PCS. The in-situ plate sinkage test and the oedometer test gave similar PCS values, with no significant difference (PCSs from plate sinkage test were a bit lower than expected). Dawidowski et al. (2001) did not find any significant difference between results from confined uniaxial compression tests and in situ plate sinkage tests and suggested that, in spite of different mechanisms involved in the two compression tests, both methods can be applied interchangeably.

Loading duration can clearly affect PCS determination in compaction tests. Mattos (1981) found that compaction increases with increasing loading time for soils drier than the plastic limit but not for those that are wetter (Keller, 2004). This is in accordance with Elmer's results where higher deformations were recorded for soils subjected to longer loading durations.

The precompression stress is also further dependent on sample dimensions, especially on sample height (at constant sample diameter) as shown for an Ultuna clay in Keller & Arvidsson (2003). De Lima and Keller (2019) showed that the relative impact of soil-wall friction on sample average behaviour decreased with increasing d/h. These results suggest that the effect of soil-wall friction on sample-average bulk density cannot be neglected unless d/h > 8.

Method of PCS determination is another important factor. Most calculation methods assume a distinct inflection point in the log σ-e measurements. This can be a subjective choice, in particular for undisturbed, unsaturated soils where this point becomes less pronounced (Brumund et al., 1976; Dias Junior, 1994). The most popular and widely used method is Casagrande's graphical procedure. However, its quality performance is quite questionable since this form of visual determination is very subjective and scale-dependent (Keller, 2004). In addition, the highest values were found by De Pue, 2019 and by Alosnos, 2015 as well. It seems to be very sensitive to small variations in the strain data. The low robustness of this method results in a large variation in PCS, suppressing its statistical relevance (Jan de Pue, 2019).

Most methods also require a linear VCL, but it can be subjective to select which points belong to this VCL. The sigmoid shape of the log σ-e relation can complicate the selection of VCL points. Conversely, this shape is a requirement for the robust fit of a sigmoid model (Gregory et al., 2006). The fit of a polynomial model does not require a specific shape, only the presence of an inflection point in the data. Methods proposed by Junior and Pierce (1995) (PCS_{L3}, PCS_{L4}) are robust and the obtained PCS is well correlated to the soil properties and load history (Jan de Pue, 2019). These results are in agreement with our findings. A disadvantage is that the selection of points used in the linear regression of the VCL can be arbitrary. Consequently, these methods would be problematic to use as a standard practice.

The inflection point of a fourth-degree polynomial does not depend on the choice of pre-set stresses, nor does it assume a sigmoid shape or a linear VCL, therefore, subjectivity is eliminated. It was demonstrated that this method is robust, and the resulting PCS showed a significant relation with the soil properties and stress history of the soil.

The proliferation of calculation methods illustrates the lack of consensus concerning the value and interpretation of PCS The lack of standardization undermines the usability of PCS (Keller et al., 2011). Jan de Pue, 2019, in agreement with previous studies, found that the methods are not interchangeable (Arvidsson and Keller, 2004; Cavalieri et al., 2008).

In general, PCS shows a high variability in most studies. In our results we could observe how PCS in *Figures 46-47* varies from other methods and studies. This is often attributed to the heterogeneity between samples (Baumgartl and Köck, 2004; Cavalieri et al., 2008), but the robustness of the calculation methods is also open to questioning. The significant differences in PCS values is just an indication that the method to determine PCS must be carefully chosen (Cavalieri et al., 2008).

For a right PCS evaluation, we recommend performing several of the methods exposed herein in order to set a comparison of the results, since analyses and results depend on several factors and contexts that the researcher should consider.

Most methods showed a significant influence of land use, sampling depth and texture class on PCS. Several methods found PCS significantly higher in the headland and at 40 cm than at 70 cm depth (De Pue, 2019; Alosnos, 2015). It is hypothesized that undisturbed soil samples from different land use (pasture, headland and centre position of arable land) or sampling depth (compacted layer and subsoil layer) have a significant influence on PCS (De Pue, 2019). This has also been proven by our PTFs development, where cropland and grassland have quite different equations and notably differ from one another.

Regarding soil properties, the precompression stress mainly depends on soil texture, bulk density, organic content and soil wetness (Hamza and Anderson, 2005). Among these, wetness is regarded as the most important and most dynamic factor influencing soil compaction processes (Soane and Van Ouwerkerk, 1994). In agricultural soils, loads are applied to unsaturated soils and σ'_p has been shown to increase with decreasing soil water content (Lebert et al., 1989; Lebert and Horn, 1991).

Soil suction is another very important soil characteristic. Some researchers have shown that PCS increases with increasing soil suction (Alexandrou and Earl, 1998; Defossez et al., 2003; Imhoff et al., 2004; Mosaddeghi et al., 2006). Water influences the structural stability and strength of soil since it acts both as a lubricant and as a binding agent of soil particulates (Carter and Gregorich, 2007). In the development of pedotransfer functions to predict PCS from readily available soil properties, pF is usually considered as a relevant factor (Lebert and Horn, 1991; Schjønning and Lamandé, 2018). This is in accordance with Elmer's results, in which he showed that PCS increases with decreasing water potential (more negative in kPa, more positive in pF) as observed too in our PTFs development (*Table 12*).

In the last figures, *Figures 46-47,* by comparing cropland and grassland plots, it should be noted that PCS values for cropland results are more dispersed and its variability is higher (in agreement with Elmer Alosnos, 2015). This can be attributed to frequent passes of tractor wheels along this section of the cropland. Headlands serves as field entrances and turning points for field machinery. In cropland centre and grassland, the upper part of the subsoil has higher PCS than the lower part. In addition, cropland was a mix of headland and centre field, which might explain its variability Apart from differences on exposure of soil to field traffic, differences in pedological processes, soil moisture conditions, and swelling-shrinking intensity should be considered as well (Keller et al., 2004).

PCS indirect estimation by pedotransfer functions are typically a function of texture, bulk density, water content, matric potential and OM content (Gupta and Larson, 1982; Lebert and Horn, 1991; Imhoff et al., 2004; Saffih Hdadi et al., 2009; Rücknagel et al., 2012; Schjønning and Lamandé, 2018), as most of our PTFs equations show.

Imhoff et al. (2004) investigated the compressive behaviour and found a significant multiple correlation between PCS and initial bulk density, water content, and clay content. A similar observation was also reported by Saffih-Hdadi et al. (2009). The findings of Imhoff et al. (2004) and Saffih- dadi et al. (2009) highlighted the clear effect of initial soil water content, initial dry bulk density, and soil texture on PCS. They showed that PCS was positively correlated with soil bulk density and negatively correlated with initial soil water content. A positive correlation between PCS and soil bulk density was also reported earlier by Lebert and Horn (1991); Salire et al. (1994); McBride and Joosse (1996); Alexandrou and Earl (1998),

Canarache et al. (2000), Silva et al. (2000, 2002) and Rücknagel et al. (2012), whereas a significant negative correlation between PCS and water content was also observed by Alexandrou and Early (1998), Defossez et al. (2003), Imhoff et al. (2004) and Mosaddeghi et al. (2006). This agrees with our PTFs development, since positive correlation was found with BD and negative correlation was found with PSS (which directly depends on water content).

PTFs used in Terranimo® depends on soil organic matter content, bulk density and soil suction stress. The trend in soil strength predicted by the pedotransfer function used includes a decrease with increasing clay content. This agrees with general experience and with our findings. Clay-holding soils being mechanically very weak when wet but strong when dry. Further, the increase in strength with decrease in matric potential (increase in pF) is much more prominent for clay-holding than for sandy soils. Finally, precompression stress increases with increase in soil organic matter content.

Finally, Keller et al., 2004 performed a series of compaction tests and wheeling events in which they discovered that measured stresses residually deformed the soil layer down to 0.5 – 0.7 m depth. Residual strain was observed in the field when σ exceeded approximately 40 kPa, and when the ratio of σ/σ'_p exceeded roughly 0.1, although ε_{res} was very small at $\sigma/\sigma'_p < 0.5$. These values were similar to those obtained on confined uniaxial compression curves. Based on these results, it could be proposed that the stress in the subsoil should not exceed 40 kPa to avoid compaction, when the soil is at around field capacity. This residual displacement indicated that the PCS thus did not work as a distinct threshold value between reversible and irreversible deformation.

It could be argued that the measured displacements and deformations were rather small, however, little compaction might be enough to negatively affect the function of a soil. In addition, with regard to multiple passes of a vehicle, the total deformation will increase with increasing number of passes (Arvidsson et al., 2001; Horn et al., 2003; Trautner, 2003). According to Kirby (1991), compaction damage is to be expected when the normal stress exerted by the tyre or track exceeds a value somewhat less than the precompression stress, since shear stresses will cause more compression than the normal stress alone. The approximation that there is no soil compaction if the applied stress is smaller than σ'_p is probably acceptable for civil engineering purposes. The question is whether this approximation is good enough for the protection of soil physical quality for agricultural purposes. Therefore, we encourage further development and investigation.

4. Terranimo®

4.1 Introduction

Terranimo® is a web-based computer model for evaluating the risk of soil compaction under agricultural vehicles. It is primarily designed for farmers, agricultural contractors, consultants, and enforcement authorities, but has scientific applications as well. Terranimo® can help in optimizing the use of agricultural machinery in the field and in preventing damage to the soil structure by indicating the conditions under which there is a high risk of harmful soil compaction occurring.

The origin of Terranimo® was not instantaneous but has been a constant development thanks to the cooperation of agricultural researchers from different European organizations. Outcomes from projects funded by the Danish Ministry of Food, Fisheries and Agriculture included a relatively simple simulation model, "Jordværn online" (English: "SoilGuard online"), for soil stress distribution in the tyre-soil contact area (Schjønning et al., 2006; Green et al., 2011). This tool took use of the mathematical model complex for describing the stress distribution along and across the driving direction suggested by Keller (2005). A modified version of the Keller model labelled 'FRIDA' – as later described by Schjønning et al. (2008) – was implemented in "Jordværn online". The model was parameterized by the FRIDA parameter prediction equations provided by Schjønning et al (2006).

Later, Thomas Keller from the ART Agricultural Research Station in Reckenholz and Matthias Stettler from the School of Agricultural, Forest and Food Sciences HAFL joined forces with Per Schjønning, Mathieu Lamandé, Poul Lassen and Margit S. Jørgensen from the Department of Agroecology at Aarhus University, Research Centre Foulum to create a decision support tool also including the mechanical strength of the soil. This model was called Terranimo®.

4.2 Characteristics

The basic idea behind Terranimo® is simple and not new: the stress (pressure) exerted on the soil by agricultural equipment is compared with the capacity of the soil to resist compaction (soil strength). If the soil strength is greater than the soil stress, then no permanent deformation will occur and hence soil damage is not to be expected. If this is not the case, then soil compaction is unavoidable, and one should refrain from driving on the soil. This can be done for all the soil profile (to 150 cm depth).

The model estimates the risk of compaction for realistic operating conditions. Its relative simplicity makes it easy to adjust the model according to the latest knowledge. These stress and strength aspects are interacting in a complicated way. The results may thus be valuable for understanding the dynamics when arable soil is loaded with machinery. The knowledge gained may help identify the most beneficial traffic systems for sustainable farming. Terranimo® is continuously updated with the most recent results in soil compaction research.

This decision support tool is thus considered of interest for researchers and extension officers interacting with farmers. However, the simple design with default or easily modified machinery and soil conditions makes the tool also useful for farmers interested in reducing compaction of their soils. Terranimo® may help identify the 'weakest points' in some specific management system. The potential benefit of taking into use wider, low pressure tyres or machinery with more axles etc can be quantified. Also, the effect of soil moisture conditions on soil vulnerability to compaction can easily be displayed and may be an eye-opener to a better management of the fields.

Correct assessment of soil stress and soil strength is required for correct predictions. Greater demands for precision in simulation require greater effort for the exact description of the field situation. Thus, in order to satisfy a wide variety of user demands, two versions of the model were developed:

1. *Terranimo® light* for a simple and quick rough assessment.
2. *Terranimo® expert* for a detailed analysis of the soil compaction risk under specific conditions

Terranimo® International is the common label for a range of national versions, including Terranimo® Global. For the time being (January 2020), six national versions are available: Denmark, Norway, Finland, Belgium-Flanders, United Kingdom and France. Model calculations are identical for all versions. They primarily deviate with respect to the default soil types, soil moisture conditions, and list of machinery that are displayed for the user when opening the specific version. In addition, Terranimo® Global offers a number of typical FAO soil types.

In the Danish, Norwegian and British versions, soil texture of user-selected locations may be imported from a national soil data base. The Danish and Norwegian versions also include the option of estimating the soil matric potential for a given location at a given date as based on weather data input to a soil-plant-atmosphere-continuum model.

The Swiss part of the Terranimo® founding group (Matthias Stettler and Thomas Keller) also has created a specific Terranimo® version for official regulation of field traffic by the Swiss authorities. This version deviates from Terranimo® International in miscellaneous ways.

Terranimo® International can be accessed through the web portal "www.terranimo.dk". Technical aspects of the Terranimo® International model are described by Lassen et al. (2013).

The 2020 version of Terranimo® allows an estimate of the effect of repeated wheeling. This new facility is still subject to evaluation and further change. The model does not estimate compaction effects on soil functions (including crop yields). The strength of the tool is thus primarily the possibility to assess, whether stresses exceeds the soil mechanical strength – hence likely inducing plastic/permanent deformation of the soil – for a specific traffic event. In other words, Terranimo® is primarily a risk assessment tool.

Terranimo® is designed with three separate components (*Figure 48*): Database, Model and User interface. Each component can be implemented on different servers. Terranimo® also makes use of an external model for calculation of soil water content (DAISY model) and country-specific soil and weather databases.
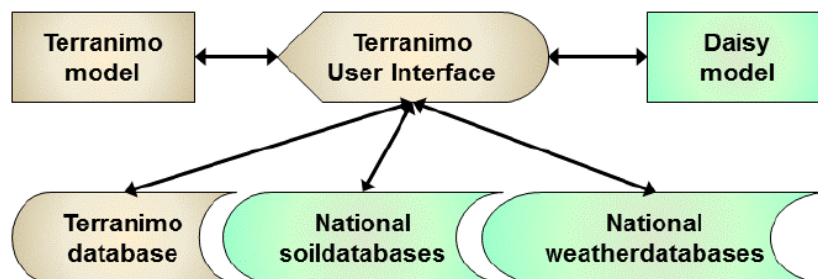
Figure 48. Terranimo system components (model, user interface and database), the external model and national databases and the interactions between them. Source: Lassen et al. 2013.

4.3 User interface

Terranimo® includes four tabs, two for inputs (machinery and soil) and two for outputs (stresses in the tyre-soil interface and stresses transmitted to the soil profile)(*Figure 49*).

4.3.1. Input data

The model by default is set up with a version-specific soil type and a default machinery when opening the tool.
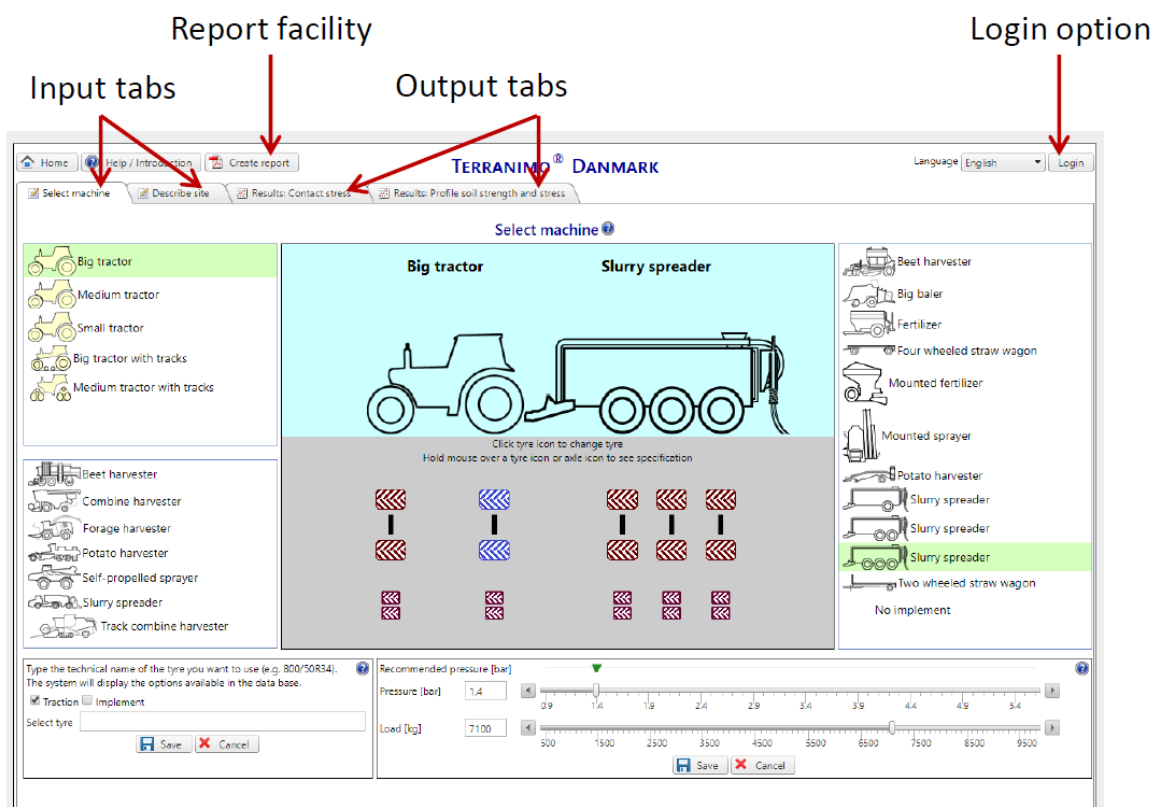
Figure 49. Terranimo user interface overview. The 'select machine' tab. Source: An introduction to Terranimo (2020)

The user may first select in the '*Select machine*' tab other machines or change tyres on the machine axles (*see Figure 49)*. The wheel loads and tyre inflation pressures may be changed as well.

Wheel load and tyre inflation pressure are decisive for soil stress, since they can describe it with sufficient precision for a given soil depth regardless of the brand and type of tyre. This relationship is illustrated for the reference depth of 35 cm in *Figure 50*. It was demonstrated that the influence of tyre inflation pressure predominates in shallow soil layers, whereas wheel load becomes the determining factor in deeper layers (Schjønning et al., 2012; Keller et al., 2004). Thus, tyre inflation pressure determines the stress in the topsoil, whereas wheel load determines the stress in the subsoil. However, it should be noted that stress throughout the soil profile also depends strongly on the stress distribution at the surface, especially the maximum stress. The correct tyre inflation pressure will spread out the exerted stress and decrease the maximum stress.
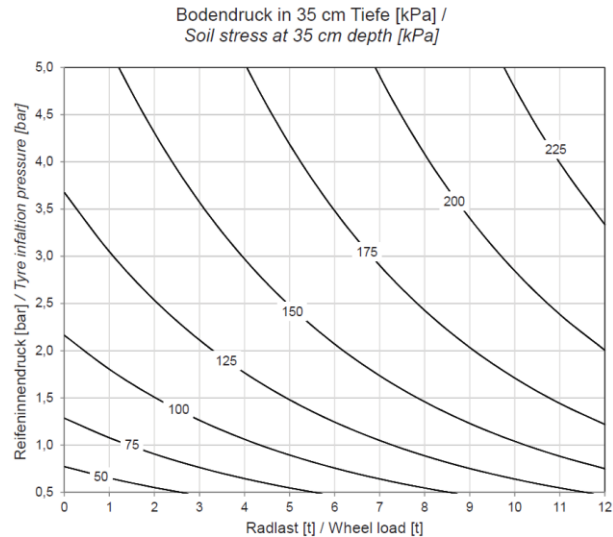
Figure 50. Soil stress nomogram. The contour lines show the stress at 35 cm soil depth as a function of wheel load and tyre inflation pressure. Source: Stettler et al., 2014

Afterwards, in the '*Describe site'* tab, *Figure 51*, alternative soil types and moisture conditions can be chosen. In the left part, you can either select the default soil type for the given country version in '*Soil texture'*-the textural composition is listed for 15 layers of 10 cm increment- or manually give in the textural composition your own data in '*Manual texture'*. The '*Texture from soil database'* is an option only active until now for Denmark, Norway, and United Kingdom.

In the right part of the '*Describe site'* tab (*Figure 51*), the user can select the soil water conditions at which the simulation should be carried out. out. Soil strength and stress transmission are dependent on the soil moisture conditions. The user may choose among pre-defined moisture conditions: '*Automatic by wetness'*. '*Moist'* corresponds to field capacity as found for example in the spring. In contrast, '*Wet'* and '*Dry'* should be selected in case traffic on winter-wet or medium dry summer situation should be simulated, respectively. Based on user's choice, the matric potentials of the fifteen 10 cm increment layers of the soil profile are displayed. As for soil texture, users may manually input matric potentials in case these are known, e.g. from tensiometer readings, '*Manual matric potential'*.

Figure 51. The user interface for input of soil texture and moisture conditions (tab 'Describe site'). Source: An introduction to Terranimo (2020).

The 'DAISY matric potential' option is only active for Denmark and Norway. Weather data are automatically read at weather stations close to the location selected. The soil matric potential is then calculated by the DAISY Soil-Plant-Atmosphere-Continuum model (Abrahamsen and Hansen, 2000).

4.3.2 Output results

Results of the model can be divided in two phases or sections. First, the contact stress, vertical stresses at the tyre-soil contact area. Second, profile soil strength and stress, in which vertical stresses are transmitted through the soil profile and compared to the subsoil strength.

The '*Results: Contact stress*' tab provides a graph of the stresses in the contact area for all tyres on the selected machinery. *Figure 52* shows the situation for a tractor-trailer combination for slurry application for a sandy soil in Scotland trafficked at field capacity water conditions. All trailer tyres are Nokian ELS tyres loaded with each ~ 60 kN (6 tonnes). To illustrate the effect of the tyre inflation pressure, the tyres on the front trailer axle have been inflated to 3 bars rather than the rated 1.2 bar. Below the graph, key figures for stresses in the contact area are given for each tyre.
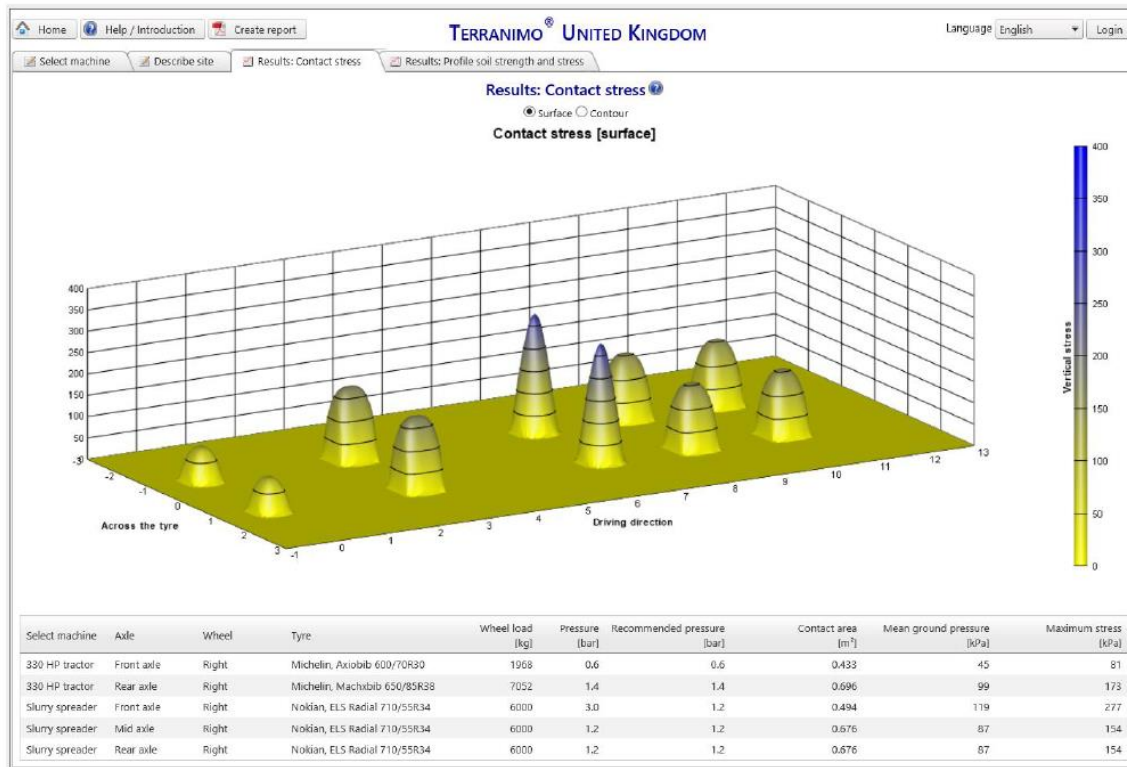
Figure 52. The contact area stress. Here for a tractor-trailer combination with trailer tyres loaded with each ~60 kN (6 tonnes) and equipped with Nokian ELS 710/55R34 at 3 bar (first axle) or the recommended 1.2 bar (middle and rear axles. Source: An introduction to Terranimo (2020).

The '*Results: Profile soil strength and stress*' tab provides graphics comparing stress from the wheels with strength of the soil. *Figure 52* illustrates the possibility of evaluating how stress and strength relate at two different moisture conditions for a self-propelled sprayer.

The case relates to a loamy soil in Belgium trafficked at either field capacity (-100 hPa matric potential) or wet water conditions (-50 hPa). The curved line depicts the stress from the wheel, while soil strength can be read as the risk of compaction of three hazard levels (colours) under the current conditions:

- Green: Ideal situation. Stress < 75% of soil strength for all soil depths (at least for the non-tilled part of the soil profile. Ideal situation. The chosen vehicle can be driven on the soil in its present moisture state with no hazard of compaction.

- Yellow: critical transition zone with a considerable risk of compaction. 75% < Stress < 125% of soil strength. All possible means of stress reduction should be implemented.

- Red: serious compaction damage is expected. Stress > 125% of soil strength. One must refrain from driving on the soil unless suitable immediate measures can be taken to reduce the compaction hazard to at least the yellow level (e.g. reducing the wheel load or tyre pressure).

The case shown in *Figure 53* indicates the importance of only driving on soils at moisture conditions that provide the necessary strength to carry the machines. Identical tyres and wheel loads for all four wheels on the sprayer were selected.

Please note that soil strength (coloured areas) as well as stress from the tyres (the blue lines) are both different for the front and the rear tyres. This is due to the effect of the repeated wheeling. The

pass of the first tyre affects soil conditions hence creating other conditions for the pass of the second tyre.

Wet soil
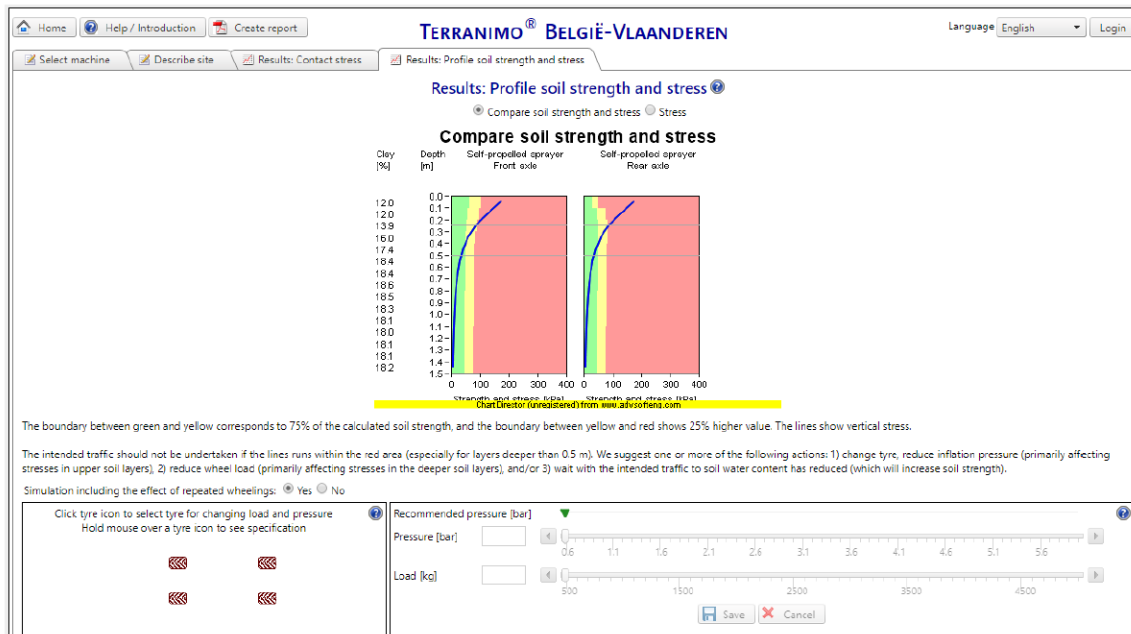
Field capacity moisture conditions
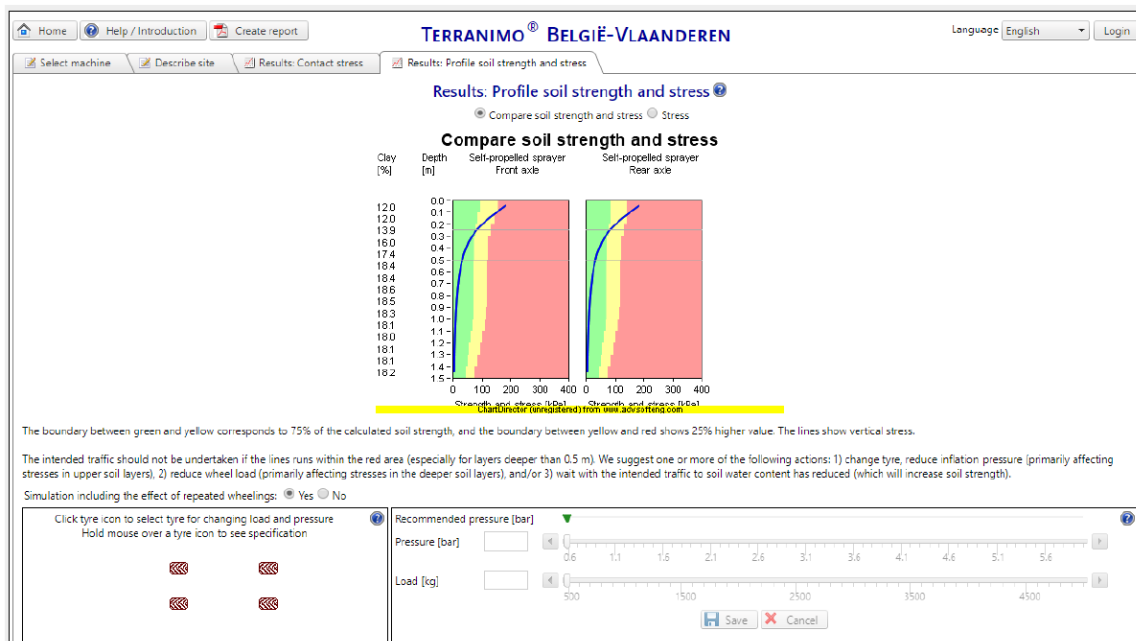
Figure 53. Comparison of stress and strength for the front and rear tyres of a self-propelled sprayer driving on a loamy soil in Belgium at field capacity moisture conditions (top) or when the soil is moderately dry (bottom). Also note the effect of repeated wheeling (front and rear tyre type, load and inflation pressure identical). Source: An introduction to Terranimo (2020).

The boxes below the graphs provide the opportunity to play interactively with the effect of modifying wheel loads as well as tyre inflation pressures. Please note that the modifications introduced in such an exercise is only 'local' and will be lost when leaving the '*Results'* tab. Neither will they appear in the report in case that is generated.

4.4 Model approach calculations

In this section, principles, models, and calculations behind Terranimo are discussed. We have divided the section into three main parts: boundary conditions at the tyre-soil interface, vertical stress propagation through the soil profile and determination of the soil strength together with the effect of repeated wheeling.

4.4.1 Soil strength

Terranimo® estimation of soil strength is based on the principle behind the **precompression stress** concept. Soil is assumed to behave elastically with increase in stress up to the PCS level. At higher stresses, soil deformation is plastic / permanent (Horn, 1993; *Figure 54*). Although this concept has proven problematic (e.g., Cavallieri et al., 2008; Keller et al., 2011), it seems to be the best option for quantification of soil strength in a soil compaction context (Schjønning et al., 2015a).

In *Figure 54*, the PCS (soil strength) is given by the breakpoint of the stress-strain plot with stress given in a logarithmic scale. The colours of the log (stress) – strain lines correspond to the colours in *Figure 53*. In real laboratory tests of soil, the transition between the elastic and plastic stress ranges is not as distinct as in the *Figure 54*. This is the reason for giving a yellow alert when approaching soil strength and a red alert only when stress exceeds soil strength by 125%.
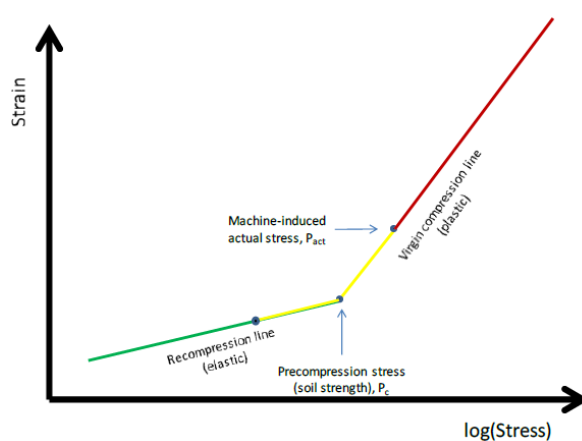
Figure 54. Sketch of the principles in determination of the precompression stress (soil strength) from laboratory tests, and the use of the stress-strength relation in Terranimo®. Source: An introduction to Terranimo (2020).

In Terranimo®, soil precompression stress is calculated by a *pedotransfer function* developed on a data set of results from uniaxial, confined compression tests (Schjønning and Lamandé, manuscript in preparation). This dataset includes a total of 584 field-sampled, undisturbed soil cores from nine locations (clay content range 4-17%) and four soil depths (0.3, 0.5, 0.8, 1.1 m), which were tested at three matric potentials (-50, -100 and -300 hPa; pF 1.7, 2.0, 2.5). The variation in precompression stress could be described by a combination of the soil *organic matter content*, the soil *bulk density*, and soil *suction stress* (calculated as the matric potential times soil saturation).

The trend in soil strength predicted by the pedotransfer function shows a decrease with increasing clay content. This is in agreement with general experience, clay-holding soils being mechanically very weak when wet but strong when dry. Furthermore, the increase in strength with decrease in matric potential (increase in pF) is much more prominent for clay-holding than for sandy soils. Finally, precompression stress increases with an increase in soil organic matter content and soil bulk density.

As concerns soil strength, the relationships are somewhat more complex than for soil stress. The parameters interact with one another. Matric potential has variable impacts on soil strength, depending upon clay content. Light soils with low clay content are in principle more stable than heavy soils under moist conditions, but as they dry out, they experience significantly lesser increases in soil strength than is the case with clay-rich soils. The effect of clay content is relatively minor around field capacity.

Soil deform plastically when stress exceeds soil strength. The deformation can be estimated from the slope (C_c) of the virgin compression line. A pedotransfer function for estimating this slope was developed from the same data set as described above for soil precompression stress. Multiple regression showed that C_c could be estimated from soils' content of clay, soil bulk density and suction stress (as defined above).

In Terranimo®, plastic soil deformation is calculated for all soil layers for each pass of a wheel. The effects on soil strength and contact area stress distribution are estimated by the FRIDA model. The stresses exerted on the soil are then also affected due to a change in the contact area stress distribution. The net effect on the relation between soil strength and stress is shown as an output. It is possible for the user to choose simulation without the effect of repeated wheeling as well.

PCS measured values were obtained by Gompertz equation (Gregory et al., 2006). This document fitted the measured test data to the compression curves by three different functions (4th polynomial, symmetrical logistic sigmoidal and asymmetrical Gompertz sigmoidal). This study also showed and compared three different methods of PCS calculation (Casagrande, Intercept of the VCL and the initial (no stress) horizontal line and Point of maximum curvature derived from the curvature function). It was found that sigmoidal curves yielded with lower absolute deviations from known values than polynomial-based estimates. The point of maximum curvature based on the Gompertz sigmoidal function gave the most accurate estimate of PCS.

4.4.2 Tyre-soil interface

The vertical stresses distribution exerted from the wheels at the tyre-soil contact area is estimated by the **FRIDA model** (Schjønning et al., 2008). This model describes the shape of the tyre-soil contact area with a super ellipse, which includes three parameters, a, b, and n, where a and b are the half-length of the minor and major axes, respectively, and n is the squareness of the super ellipse. FRIDA is able to describe the actual conditions very well, in particular the predominant influence of tyre inflation pressure (*Figure 55*).
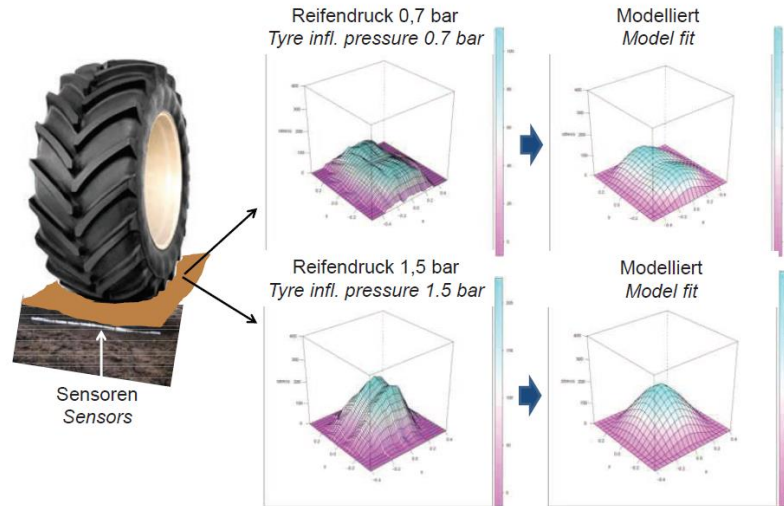
Figure 55. Measured (left diagrams) and FRIDA modelled stress states between tyre and soil at different tyre inflation pressures. The example here shows a Michelin 650/65R38 Multibib with 3.5 t wheel load. Source: Stettler et al., 2014

Schjønning et al. 2008 found that the contact area doubled when the inflation pressure was reduced from 240 to 50 kPa (*Figure 56*). The measured peak stress increased significantly with tyre inflation pressure. At the recommended inflation pressure, both tyres displayed a stress distribution across the width of the wheel that could be evaluated as optimal regarding a minimised topsoil compaction.
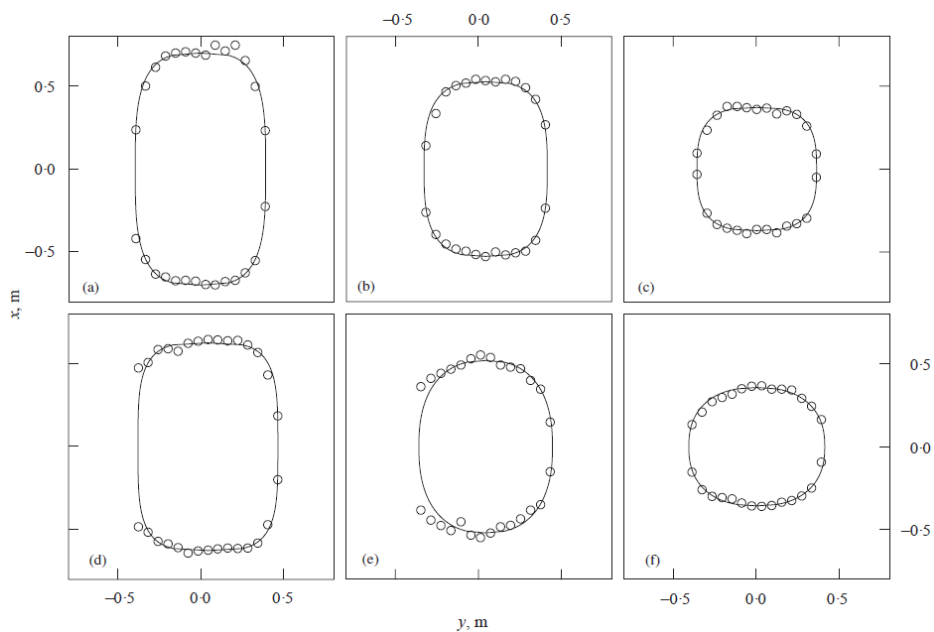
Figure 56. Examples of measured (circle points) and super ellipse fitted (line) periphery of the contact area for the 650/65R30.5 (a–c) and the 800/50R34 tyre (d–f) at three inflation pressures (50 kPa: a, d; 100 kPa: b, e; 240 kPa: c, f). Driving direction is along the x-axis. Source: Schjønning et al. 2008

The FRIDA parameters α and β reflect the tyre's ability to distribute the stress in the driving direction and in the transversal direction, respectively. Both parameters increased with increases in the relevant contact area dimension (length or width). A power-law function and a decay function are described by these parameters α and β, respectively (Keller, 2005).

The parameters of the FRIDA model are estimated by multiple regression from tyre and loading characteristics as described by Schjønning et al. 2015 (tyre carcass volume, V_{tc}, wheel load, F_w, tyre deflection, L and an expression of tyre inflation pressure, K_r) . It was found that the tyre volume

(V_{tc}) and a ratio of actual to recommended inflation pressure (F_w) accounts for nearly all the variation in measured contact areas. The α parameter was further affected by F_w, while K_r and L were added to model performance for the β parameter (Schjønning et al., 2015).

In addition, a difference between traction and implement tyres was found. At recommended inflation pressures, the traction tyres on average have about 14% of the tyre periphery in contact with the soil, while implement tyres have about 18% contact, e.g., the tyre–soil contact length is slightly larger for implement tyres. The model system for prediction developed in this study is valid for not recently tilled soil at a water content close to field capacity (Schjønning et al., 2015).

The contact area of a tyre and hence the stress distribution is influenced by the strength of the topsoil. Terranimo® accounts for this as follows. First, the contact area is calculated from the loading characteristics of the selected tyre as mentioned above, using the pedotransfer functions provided by Schjønning et al. (2015b). Next, this estimate is modified based on the strength of the topsoil. They made a comparison between the large number of contact areas measured by Schjønning et al. (2006) for a not-recently-tilled field capacity soil and the estimates of tyre contact areas for either a 'soft' or a 'rigid' surface suggested by O'Sullivan et al. (1999).

The calculated values from the O'Sullivan et al. (1999) equations appeared to fit reasonably to 1.3 or 0.8 times the Schjønning et al. (2006) measured values for 'soft' and 'rigid' surfaces, respectively. The precompression stress for soils at field capacity and with a typical bulk density corresponding to a relative contact area of 1 was about 100 kPa. Based on these 'fix-points', we established a relation between the precompression stress and the relative contact area ('full line' in *Figure 57*.
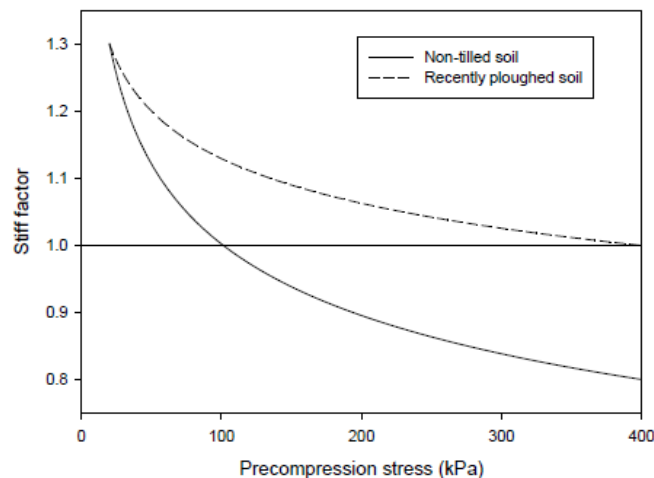
Figure 57. Terranimo® prediction of topsoil strength effects on the tyre-soil contact area. Source: Schjønning et al. 2015. Source: An introduction to Terranimo (2020).

The topsoil strength influence on the contact area for a recently ploughed soil was estimated by field tests of stress distribution in the contact area that were carried out for a range of soil surface conditions (Schjønning et al., 2006; Lamandé and Schjønning, 2011ab; unpublished data). This gave rise to the suggested relation between precompression stress and relative contact area displayed by the 'broken line' in *Figure 57*. We note that this relation is less well supported by data than that for not-recently-tilled soil and should only be used for soil that has been ploughed recently.

In the Terranimo® code, the relative contact area is restricted to a maximum of 1.3 for very weak (wet) soil. Similarly, constant relative contact areas of 0.8 and 1.0 for non-tilled and tilled soil, respectively, are used for topsoil strengths higher than 400 kPa.

4.4.3 Stress propagation in the soil profile

The vertical stresses in the soil profile below the wheels are calculated semi-analytically by the well-known Söhne (1953) approach with the FRIDA-estimated contact area point stresses as input (section 4.4.2). The stress propagation is also based on the formulas of Boussinesq (1885) and Fröhlich (1934), precursors of Söhne's model.

In accordance with Söhne, the concentration of stresses is modified according to soil strength. He developed the division of the contact area into smaller areas, making it possible to model non-uniform stress distributions. In Terranimo®, the suggested values of concentration factor (ν) are assumed as:

- Dry soil (pF 2.7): $\nu = 4$ ('hard')
- Moist soil (pF 2.0): $\nu = 5$ ('firm')
- Wet soil (pF 1.7): $\nu = 6$ ('soft')

The concentration factor ν, originally developed by Frölich is a key element, it determines the pattern of the stress propagation in the soil. Taking further a pF value of 4.2 (the 'wilting point', e.g. a very dry soil) to correspond to total elasticity, it is assumed $\nu = 3$ at those conditions. From non-linear regression, it was obtained an exponential pedotransfer function to predict ν from the matric potential (pF). This means that the concentration factor used in Terranimo® varies continuously with the user-defined or DAISY-modelled matric potential of the soil.
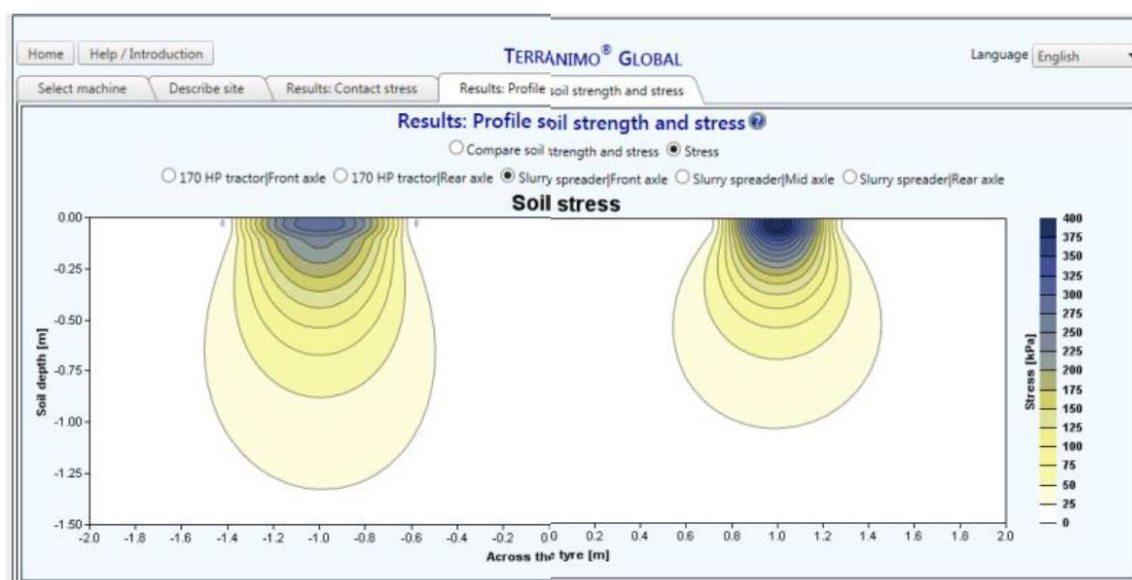
Figure 58. Terranimo-predicted stress distribution in the soil profile below a similarly loaded and inflated implement tyre at field capacity water content (left) and at the wilting point (right). Source: An introduction to Terranimo (2020).

Figure 58 shows stress isobars below a Nokian ELS 710/55R34 mounted on a slurry trailer, loaded with ~ 60 kN (6 tonnes) and inflated to 2.2 bar. The tyre to the left illustrate stress transmission in a 20% clay soil at field capacity (pF = 2.0, ν ~ 5), while that to the right reflects the situation for the same soil drained to the wilting point (pF = 4.2, ν ~ 3). Please note that in addition to the difference in concentration factor between the two simulations (the depth of stress penetration), also the contact area and the stress distribution in the contact area are affected by the change in moisture conditions. The net result is much higher topsoil stresses but lower subsoil stresses in the dry than the moist soil.

4.5 Practical case in Valdepeñas, Spain

In this section, we wanted to carry out a self-practical analysis in *Terranimo® expert* to experiment and become more familiar with this tool.

My father is a vine farmer who have been working on the countryside for almost 50 years. The idea is to study a work case in Spain and use all the information that he provides me as the input data in Terranimo®, e.g. machinery, soil characteristics, tyre inflation, etc. Thus, I will determine the output stresses transmitted to the soil and evaluate if there is any risk of compaction.

Figure 59. My father's tractor and plough. Source: own elaboration

4.5.1 Input

For vineyards, the *machinery* required are tractors that can pass through crop lines without any problem. Since lines are around 2 m distant from each other, a small machine is used: 90 HP tractor of 5800 kg weight. Depending on the task, these tractors typically use two different implements: one is trailer, which is used during the harvest to collect all the grapes, however, this machinery never goes into the field, so this case is not considered. The other one is the plough. This equipment does go into the field, so this plough has a weight of 2000 kg. (*Figure 60*).

Regarding tyre characteristics:

- *Front tyres*: Mitas traction AC 70 T tyres. Dimension: 320/70R20. Wheel load: 600 kg. Inflation pressure: 0.60 bar (recommended).
- *Back tyres:* Mitas traction HC 70 tyres. Dimension: 420/70R28. Wheel load: 2300 kg. Inflation pressure: 1.50 bar (recommended).
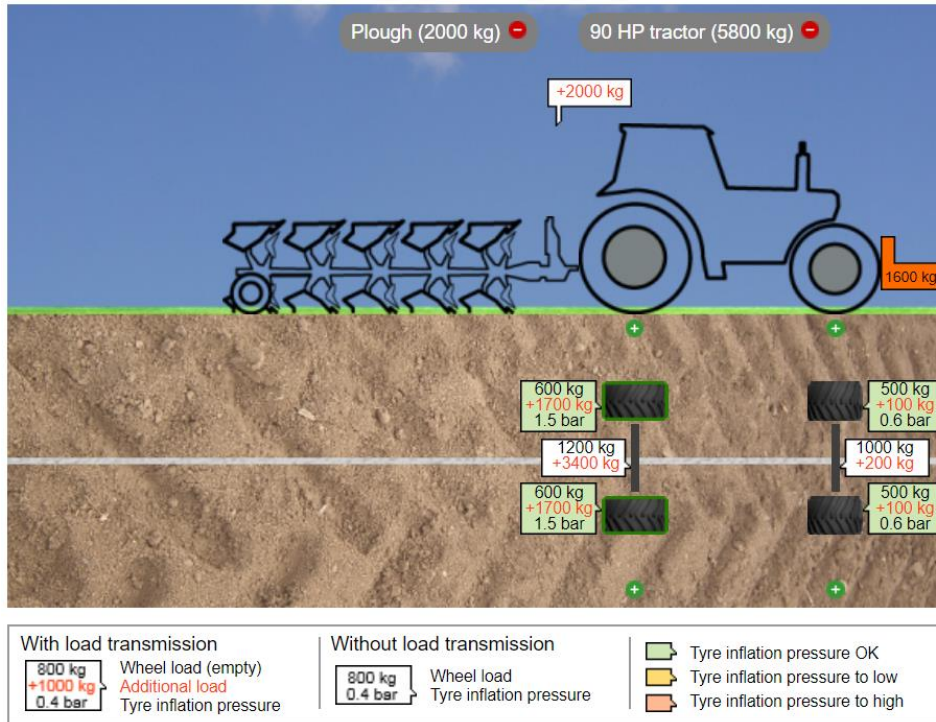
Figure 60. Machine and tyre characteristics. Source: own elaboration in Terranimo®

The crop field is located in the outskirts of my town, called Valdepeñas. It belongs to the province of Ciudad Real, region of Castilla La Mancha, south-centre of Spain. This land is typically known because of the great culture of wine and vineyards cultivation, since the climate (dry with barely rain and great differences between summer-winter) and the soil characteristics (clay loam texture) make it ideal for this type of crop. Soil texture and soil matric potential are shown in *Figure 61* and *Figure 62*, respectively.

No.	Bottom [cm]	Clay [%]	Silt [%]	Sand [%]	Organic matter [%]	Bulk density [g/cm³]
1	10	25	28	47	0.8	2.5
2	20	28	29	43	0.8	2.6
3	30	31	32	37	0.7	2.6
4	40	35	32	33	0.7	2.7
5	50	39	33	28	0.5	2.7
6	60	47	31	22	0.5	2.8
7	70	45	35	20	0.3	2.8
8	80	47	36	17	0.3	2.8
9	90	50	35	15	0.2	2.8
10	100	55	30	15	0.2	2.9

Figure 61. Soil texture characteristics. Source: self-created in Terranimo®

No.	Bottom [cm]	Matric potential [hPa]
1	10	400
2	20	400
3	30	350
4	40	330
5	50	300
6	60	300
7	70	250
8	80	200
9	90	150
10	100	130

Figure 62. Soil matric potential. Source: own elaboration in Terranimo®

4.5.2 Output

The first obtained result shows the decision chart topsoil for expected stress from wheel loads vs. soil strength (*Figure 63*). 23 kPa stresses are expected for the front wheels while 77 kPa stresses for the rear wheels. We see that both of them are clearly within the range of no risk of compaction, since they are quite lower than the soil strength (assumed as the precompression stress) = 250 kPa.

90 HP tractor	Soil stress	Soil strength
Left inner front wheel	23 kPa (0.23 bar)	250 kPa (2.5 bar)
Right inner front wheel	23 kPa (0.23 bar)	250 kPa (2.5 bar)
Left inner rear wheel	77 kPa (0.77 bar)	250 kPa (2.5 bar)
Right inner rear wheel	77 kPa (0.77 bar)	250 kPa (2.5 bar)

Legend	
No soil compaction risk	
Considerable risk of soil compaction - reduce wheel load or tyre inflation pressure	
CAUTION: High risk of subsoil compaction - avoid driving on the field	

100kPa = 1bar

Figure 63. Decision chart. Source: own elaboration in Terranimo®

In the next figure, *Figure 64*, soil stress vs. soil strength is plotted as well, this case for the 1.0 m depth, together with the clay content and matric potential in the soil. Black (front wheels) and brown (rear wheels) curves show vertical soil stress. The limit between green and yellow corresponds to 75% of estimated soil strength. Below this limit, there is no risk of compaction. The limit between yellow and red corresponds to 125% of estimated soil strength. Above this limit, severe soil compaction is to be expected. For the first 20 cm, rear wheels are inside the transition (yellow) zone. Therefore, considerable risk of compaction could be expected and special caution should be considered.
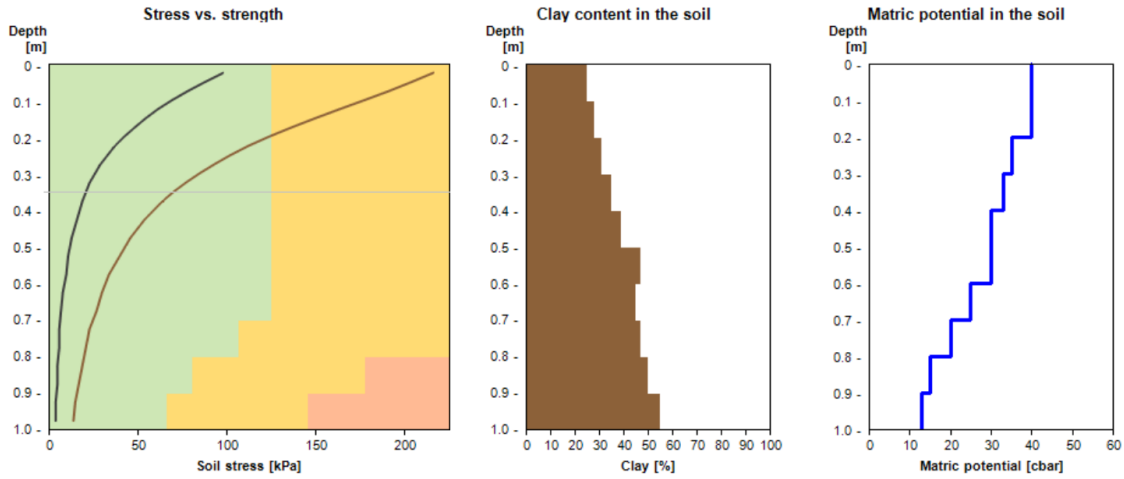
Figure 64. Stress vs. strength – Clay content – Matric potential. Source: own elaboration in Terranimo®

Next, the following 3D diagram shows the vertical stresses and contact characteristics and pressures at the soil/tyre interface. We notably observe maximum stresses of 240 kPa and mean ground pressures of 104 kPa for the rear wheels (*Figure 65*).

90 HP tractor	Contact area	Contact area width	Contact area length	Maximum stress	Mean ground pressure
Left inner front wheel	0.12 m²	0.37 m	0.37 m	117 kPa	49 kPa
Right inner front wheel	0.12 m²	0.37 m	0.37 m	117 kPa	49 kPa
Left inner rear wheel	0.22 m²	0.48 m	0.51 m	240 kPa	104 kPa
Right inner rear wheel	0.22 m²	0.48 m	0.51 m	240 kPa	104 kPa
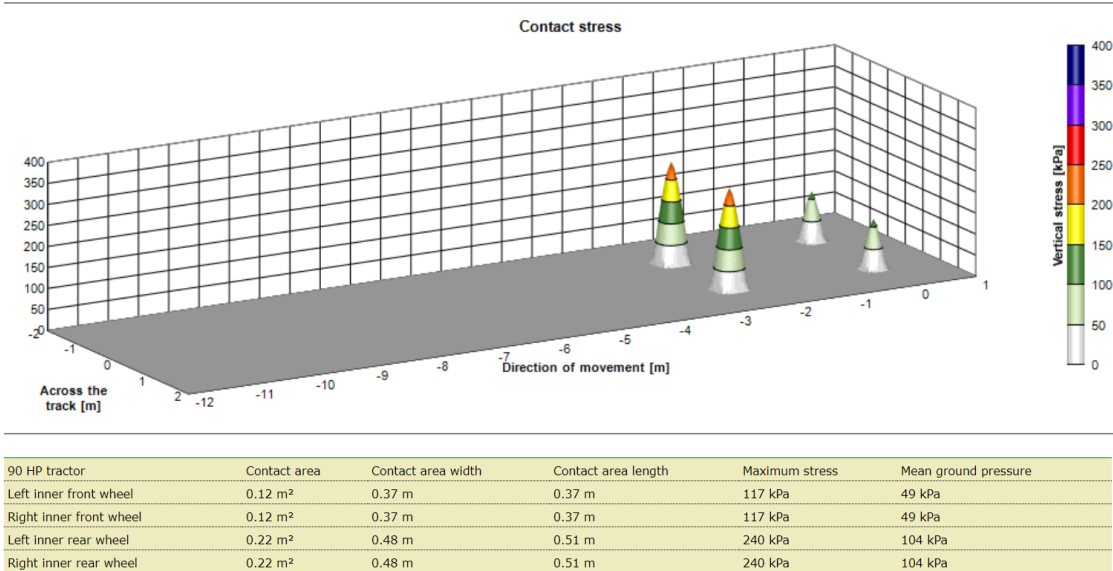
Figure 65. 3D diagram of the contact pressure. Source: own elaboration in Terranimo®

Finally, soil stress distribution based on the Söhne model are shown at the front axle (*Figure 66*) and rear axle (*Figure 67*). Again, highest stresses are expected for the rear wheels, which are around 250 kPa at a surface level (0.10 m depth). This behaviour is normal since rear axle has to carry most of the tractor weight plus the extra 2 tones due to the plough. Therefore, based on this analysis performed in Terranimo®, we can conclude that no severe risk of compaction will be expected, except in the top 10 cm at the rear wheels, at which special caution should be put.

Wheels	Manufacturer	Tyre name	Tyre dimension	Wheel load [kg]	Pressure [bar]
Left inner front wheel	Mitas	AC 70 T	320/70R20	600 kg	0.6 bar
Right inner front wheel	Mitas	AC 70 T	320/70R20	600 kg	0.6 bar
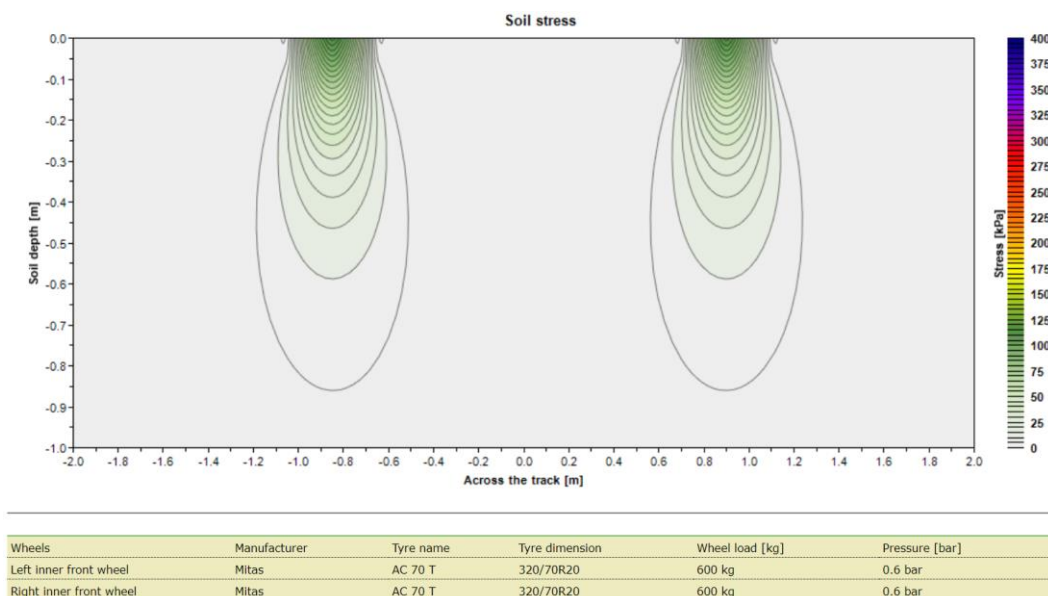
Figure 66. Soil stress at the front axle. Source: own elaboration in Terranimo®

Wheels	Manufacturer	Tyre name	Tyre dimension	Wheel load [kg]	Pressure [bar]
Left inner rear wheel	Mitas	HC 70	420/70R28	2300 kg	1.5 bar
Right inner rear wheel	Mitas	HC 70	420/70R28	2300 kg	1.5 bar
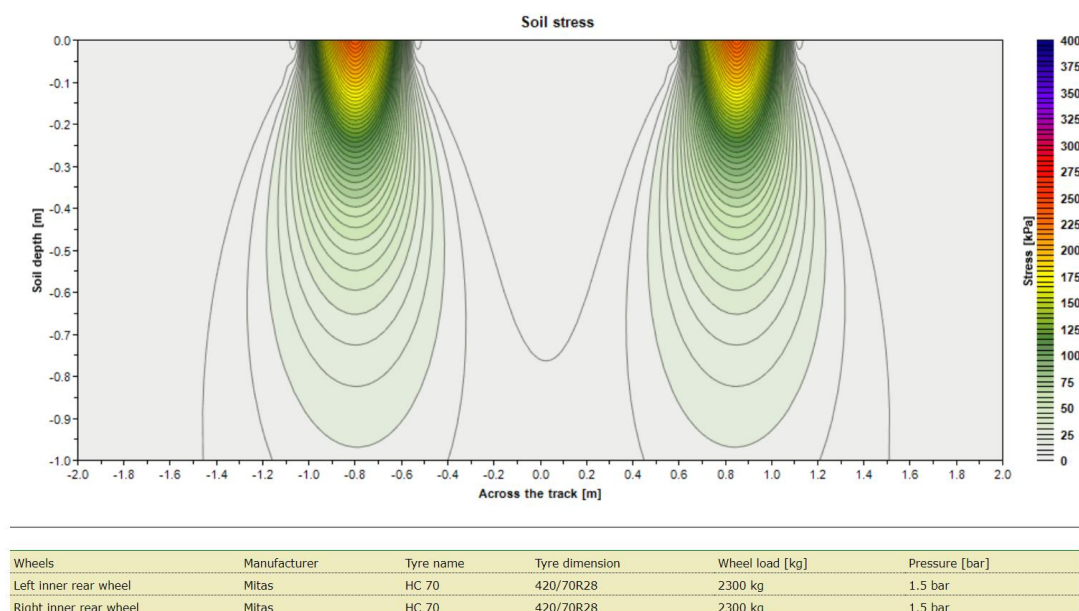
Figure 67. Soil stress at the rear axle. Source: own elaboration in Terranimo®

4.6 Discussion

Terranimo® is such a powerful tool to evaluate the risk to soil compaction from agricultural traffic, not only for farmers, consultants, and enforcement authorities, but also for scientific applications. By linking established findings on stress propagation and soil strength as well as new models for simulating stress distribution between tyres and the soil surface with modern internet technology, it was possible to develop an interesting and user-friendly tool for assessing the risk of soil compaction under agricultural machinery.

It was demonstrated that the influence of tyre inflation pressure predominates in shallow soil layers, whereas wheel load becomes the determining factor in deeper layers (Schjønning et al., 2012; Keller et al., 2004). In *Figure 53* we clearly observe the effect of the tyre inflation pressure and the

importance of not exceed the recommended range by the manufacturer, since the tyres on the front trailer axle were inflated to 3 bar rather than the rated 1.2 bar, resulting in extremely higher stresses (almost the double) at the contact area. In our practical case we could see the importance of the recommended inflation pressure as well. *Figure 67* shows that stresses for the rear axle at the tyre/soil interface are already high (~ 250 kPa) for the recommended pressure (1.5 bar), therefore, the stresses would be critically severe if we would had considered different values. At the recommended inflation pressure, tyres displayed a stress distribution across the width of the wheel that could be evaluated as optimal regarding a minimised topsoil compaction.

By comparing the results obtained in Terranimo® for the different cases (example by "Introduction to Terranimo® 2020" vs. our practical case in Valdepeñas, Spain), we claim that the second case has lower risk of soil compaction than the first one, even if soil texture is of worse quality and lower permeability (clay loam vs. sandy loam). This might be due to the reason that agricultural machinery required to treat vineyards in Spain is quite lighter and impose lower stress to the ground than Belgium machinery that is typically used to treat their crop fields, e.g. cereal. In addition, water content and matric potential play a very important role since Belgium fields are normally in wetter conditions than fields from south-centre of Spain.

There are plans to improve Terranimo® on an ongoing basis. Along with updating the data banks (e. g., entry of data on new tyre models) and improving the user interface, there are plans for gradually overcoming the critical points mentioned. A long-term goal is the linkage of Terranimo® with sensor data and with the terminal on the machine. Such an instrument would provide the operator with invaluable information automatically and in real time for optimizing field use.

Based on all of this information, we highly recommend the use of this great and interesting Terranimo® tool to every person or institution that concerns soil compaction and we encourage further researching on the purpose of improving its functionality.

5. Conclusions

Soil compaction assessment and prediction is extremely important for reaching a well and controlled soil behaviour. From a soil physics/agricultural perspective, compaction is a risk and the goal is to minimize its effect on field crops. From a geotechnics/engineering point of view, soil compaction and consolidation should be managed on purpose for a better foundation resistance.

Advantages and drawbacks for laboratory and in-situ tests have been discussed for both approaches. Which ideal tests should be performed will depend on the situation and, mainly, on the engineer/researcher knowledge and experience. We encourage further development on new compaction tests, especially for the agricultural approach, in which most of the actual tests were specifically developed for engineering purposes.

It has been shown that the precompression stress is such a great tool to use it as a threshold value to obtain when the soil will suffer severe risk of compaction and unrecoverable deformation. However, this analysis is questionable since it was proved that little residual strain appeared before reaching the PCS value. Therefore, further investigation should be done.

Different factors affecting PCS estimation of strain-stress relationships from compression tests were studied, such as type of method, loading duration, type of method, soil properties, moisture content, etc. Regarding which direct estimation method is the optimal, despite there are some methods more robust than others, it can be concluded that for an adequate evaluation, a set of several performances should be carried out to compare and analyse different results, considering that they are not interchangeable.

Pedotransfer functions are a very interesting and strong tool in predicting the precompression stress parameter. There are plenty of different PTFs equations in literature that estimate PCS from a wide variety of soil properties as predictors variables. Some of the most and stronger ones are soil particle size distribution, bulk density, matric potential and OM content, in agreement with our own PTF development. Nevertheless, we highly recommend a more extended research since obtained equations have, to some extent, low coefficients of determination.

Last but not least, this study showed that Terranimo® is a formidable user-friendly tool to determine stresses transmitted through the soil profile by agricultural machinery, which are mainly affected by machinery weight, tyre inflation pressure and soil water conditions. It should be noted that is important to mind the recommended inflation pressure by the tyre manufacturer, since little deviation could cause high detrimental effects on our soil. In addition, one should avoid driving when water content and moisture conditions are significant. Thus, Terranimo® is such a powerful to evaluate the risk of soil compaction in cultivated field and should be much more recognised.

References

Alakukku, L. (1996). Persistence of soil compaction due to high axle load traffic. Soil and Tillage Research. Volume 37. Pages 211-222.

Alexandrou, A. & Earl, R. (1995). In situ determination of the pre-compaction stress of a soil. Journal of Agricultural Engineering Research 61, 67-72.

Alexandrou, A. & Earl, R. (1998). The relationship among the pre-compaction stress, volumetric water content and initial dry bulk density of soil. Journal of Agricultural Engineering Research, 71, 75–80

Alosnos, Elmer (2015). Determination and Prediction of Risk to Soil Compaction from Agricultural Operations. Master dissertation. UGent.

Amr M. Sallam, Newel K. White, and Alaa K. Ashmawy. (2004). Evaluation of the Purdue TDR Method for Soil Water Content and Density Measurement. Final Report, University of South Florida, Tampa, Florida, 127.

Andersen A., Berre T., Kleven A., Lunne T.(1979). Procedures used to obtain soil parameters for foundation engineering in the North Sea. Marine Geotechnology, Vol.3, p.201-266.

Arvidsson J., Sjöberg, E. and van den Akker J. J. (2003). Subsoil compaction by heavy sugar beet harvesters in southern Sweden: Iii. risk assessment using a soil water model. Soil and Tillage Research, 73(1-2):77–87.

Arvidsson, J. (1997). Soil Compaction in Agriculture – From Soil Stress to Plant Stress. Doctoral Thesis. Agraria 41, Swedish University of Agricultural Sciences, Uppsala, Sweden.

Arvidsson, J. (1998). Effects of cultivation depth in reduced tillage on soil physical properties, crop yield and plant pathogens. European Journal of Agronomy. Volume 9. Pages 79-85

Arvidsson, J., Keller, T. and Gustafsson, K. (2004). Specific draught for mouldboard plough, chisel plough and disc harrow at different water contents. Soil and Tillage Research, 79(2):221–231.

Arvidsson, J., A Trautner, J. J. H van den Akker, Per Schjønning (2001). Subsoil compaction caused by heavy sugar beet harvesters in southern Sweden: II. Soil displacement during wheeling and model computations of compaction. Soil and Tillage Research. Volume 60. Pages 79-89.

Arvidsson, J., Håkansson, I. (2014). Response of different crops to soil compaction. Short-term effects in Swedish field experiments. Soil and Tillage Research. Volume 138. Pages 56-63.

Baumgartl, T. and Köck, B (2004). Modeling volume change and mechanical properties with hydraulic models. Soil Science Society of America Journal, 68(1):57–65.

Becker D.E., Crooks J.H.A., Been K., Jefferies M.G. (1987). Work as a criterion for determining in situ and yield stresses in clays. Canadian Geotechnical Journal, Vol.24, p.549-564.

Berli, M. (2001). Compaction of agricultural subsoils by tracked heavy construction machinery. PhD thesis, ETH Zurich.

Bouma, J. & Batjes, N.H. (2000). Trends of world-wide soil degradation, 33-43.

Briaud, Jean-Louis (2013). Introduction to geotechnical engineering: unsaturated and saturated soils. 172-190.

BIBLIOGRAPHY

Brumund W.F., Jonas, E., and Ladd C.C. (1976). Estimating in situ maximum past (preconsolidation) pressure of saturated clays from results of laboratory consolidometer tests. Transportation Research Board Special Report, (163).

Burland J.B. (1990). On the compressibility and shear strength of natural clays. Geotechnique, Vol.40, p.329-378.

Butterfield R. (1979). A natural compression law for soils. Geotechnique, Vol.29, p.468-480.

Casagrande, A. (1936). The determination of pre-consolidation load and its practical significance. In: Proceedings of the First International Conference on Soil Mechanics and Foundation Engineering, Vol. 3, 22-26 June 1936. Harvard University, Cambridge, MA, USA, pp. 60-64.

Cavalieri, K. M. V., Arvidsson, J., da Silva, A. P. and Keller, T. (2008). Determination of precompression stress from uniaxial compression tests. Soil and Tillage Research, 98(1):17–26.

Chamen, T., L. Alakukku, S. Pires, C. Sommer, G. Spoor, F. Tijink, and P. Weisskopf (2003). Prevention strategies for field traffic-induced subsoil compaction: a review: Part 2. equipment and field practices. Soil and tillage research, 73(1-2):161–174.

Christopher L. Meehan, and Jason S. Hertz. (2011). Using Electrical Density Gauges for Field Compaction Control. Delaware Centre for Transportation. University of Delaware, Newark, Delaware, 149.

Clayton, C.R.I (1995). The Standard Penetration Test (SPT): Methods and Use.

Craig, R.F (2004). Craig's Soil Mechanics. 7th edition. 21-27, 71-75, 227-240.

Dawidowski, J. and Koolen, A. (1994). Computerized determination of the preconsolidation stress in compaction testing of field core samples. Soil and Tillage research, 31(2-3):277–282.

Dawidowski, J.B., Morrison, J.E. & Snieg, M. (2001). Measurement of soil layer strength with plate sinkage and uniaxial confined methods. Transactions of the American Society of Agricultural Engineers 44, 1059-1064.

De Lima, R.P, Keller, T. (2019). Impact of sample dimensions, soil-cylinder wall friction and elastic properties of soil on stress field and bulk density in uniaxial compression tests. P 15-24.

De Neve, S. and Hofman, G. (2000). Influence of soil compaction on carbon and nitrogen mineralization of soil organic matter and crop residues. Biology and fertility of soils. p544-549.

De Pue, Jan (2019). Advances in modelling vehicle-induced stress transmission in relation to soil compaction. Ghent University – Faculty of bioscience engineering. 63-81.

Defossez P, Richard, G. (2002). Models of soil compaction due to traffic and their evaluation. Soil and Tillage Research. Volume 67. Pages 41-64.

Défossez, P., G. Richard, H. Boizard, M. F. O'Sullivan. (2003). Modeling change in soil compaction due to agricultural traffic as function of soil water content. GeodermaVolume 116. Pages 89-105.

Dexter, A. (1975). Uniaxial compression of ideal brittle tilths. Journal of Terramechanics, 12(1):3–14.

Dexter, A.R. (2002). Soil mechanical notes. Course in agricultural soil mechanics, Swedish University of Soil Sciences, Uppsala, Sweden.

BIBLIOGRAPHY

Dias Junior M. S. (1994). Compression of three soils under long-term tillage and wheel traffic. PhD thesis, Michigan State University.

Earl, R. (1997). Assessment of the behaviour of field soils during compaction. Journal of Agricultural Engineering 68, 147-157.

Ellen M. Rathje, Stephen G. Wright, Kenneth H. Stokoe II, Ashley Adams, Ruth Tobin, and Manal Salem. (2006). Evaluation of Non-Nuclear Methods for Compaction Control. Technical Report, Centre for Transportation Research. The University of Texas, Austin, Texas, 144.

Ernest S. Berney IV, and James D. Kyzar. (2012). "Evaluation of Nonnuclear Soil Moisture and Density Devices for Field Quality Control." Transportation Research Record, (No. 2310), 18–26.

Ernest S. Berney, Mariely Mejías-Santiago, and James D. Kyzar. (2013). Non-Nuclear Alternatives to Monitoring Moisture-Density Response in Soils. Final report, The US Army Engineer Research and Development Centre, Washington, DC, 117.

European Environment Agency (2019). Soil, land and climate change

Gregory, A. S. et al. (2006): Calculation of the compression index and precompression stress from soil compression test data. Soil & Tillage Research 89, pp. 45–57.

Gupta, S., Hadas, A. and Schafer, R. (1989). Modelling soil mechanical behaviour during compaction. In Mechanics and related processes in structured agricultural soils, pages 137–152.

Guzmán Abril, A.A. (2013). "Manual Operativo del Aparato de Globo de Hule ASTM D 2167, Análisis Comparativo y Descriptivo con el Método del Cono de Arena ASTM D 1556 Para la Determinación de la Densidad de Campo." Trabajo de Graduación, Universidad de San Carlos de Guatemala, Guatemala.

Hakansson, I., Ward B. Voorhees, Paavo Elonen, G. S. V. Raghavan, Hugh Riley (1987). Effect of high axle-load traffic on subsoil compaction and crop yield in humid regions with annual freezing. Soil and Tillage Research. Volume 10, Pages 259-268.

Hamza, M.A., Anderson, W.K., (2005). Soil compaction in cropping systems. A review of the nature, causes and possible solutions. Soil Tillage Res. 82, 121-145.

Hardin. B.O. (1989). 1-D Strain in normally consolidated cohesive soils. Journal of Geotechnical Engineering, Vol.115, No.5, p.689-710.

Hartge and Horn, 1984. K.H. Hartge, R. HornUntersuchungen zur Gültigkeit des Hooke'schen Gesetzes bei der Setzung von Böden bei wiederholter Belastung.

Holtz, D.R. and Kovacs, D.W. (1981) An Introduction to Geotechnical Engineering. Prentice-Hall, Inc.

Horn, R. and M. Lebert, (1994). Soil compactability and compressibility. In B. D. Soane and C. van Ouwerkerk, editors, Soil compaction in crop production, volume 11, chapter 3, pages 45–69. Elsevier

Horn, R., Domzal, H., Slowinska-Jurkiewicz, A. & van Ouwerkerk, C. (1995). Soil compaction process and their effects on the structure of arable soils and the environment. Soil and Tillage Research 35, 23-36.

Imhoff, S., Da Silva, A. P. and Fallow, D. (2004). Susceptibility to compaction, load support capacity, and soil compressibility of hapludox. Soil Science Society of America Journal, 68(1):17–24.

BIBLIOGRAPHY

J. H. Taylor, W. R. Gill (1984). Soil compaction: State-of-the-art report Journal of Terramechanics. Volume 21, Pages 195-213

Jamiolkowski M. & Marchetti S. (1969). Determination of preconsolidation load from a controlled gradient consolidometer. Proc. 7th International Conference SMFE, Mexico City, p.523-524.

Janbu N. (1969). The resistance concept applied to deformation of soils. Proc. 7th International Conference SMFE, Mexico City, 1969, p.191- 196.

Jeff Brown. (2007). Non-Nuclear Compaction Gauge Comparison Study. Final Report, Vermont Agency of Transportation Materials and Research Section National Life Building, Montpelier, VT, 16.

Jones, R.J.A, G Spoor, A. J Thomasson (2003). Vulnerability of subsoils in Europe to compaction: a preliminary analysis. Soil and Tillage Research. Volume 73. Pages 131-143

Jose B.T., Srudharan A., Abraham B.M (1989). Log-Log method for determination of preconsolidation pressure. Geotechnical Testing Journal. Vol.12, p.230-237.

Joshua Eli Robert Wells. (2014). "Calibration of Non-Nuclear devices for construction quality control of compacted soils." Thesis, University of Kentucky, Lexington, Kentucky.

Junior M. D. and Pierce F (1995). A simple procedure for estimating preconsolidation pressure from soil compression curves. Soil Technology, 8(2):139–151.

Kanali, C.L., P. G. Kaumbutho, C. M. Maende, J. Kamau. (1996). Establishment of safe axle loads for sugarcane soils under varying moisture content Journal of Terramechanics. Volume 33,Pages 81-90.

Keller, T. and Arvidsson, J. (2004). Technical solutions to reduce the risk of subsoil compaction: effects of dual wheels, tandem wheels and tyre inflation pressure on stress propagation in soil. Soil and Tillage Research, 79(2):191–205.

Keller, T., (2005). A Model for the prediction of the contact area and the distribution of vertical stress below agricultural tyres from readily available tyre parameters. Biosyst. Eng. 92, 85–96.

Keller, T., J. Arvidsson, J.B. Dawidowski, A.J. Koolen (2014). Soil precompression stress II. A comparison of different compaction tests and stress–displacement behaviour of the soil during wheeling. Soil & Tillage Research.

Keller, T., Johan Arvidsson, Per Schjønning, Mathieu Lamandé, Matthias Stettler and Peter Weisskopf (2012). In Situ Subsoil Stress-Strain Behavior in Relation to Soil Precompression Stress.

Keller, T., M. Lamandé, P. Schjønning, and A. R. Dexter (2011). Analysis of soil compression curves from uniaxial confined compression tests. Geoderma, 163(1-2):13–23.

Keller, T., Pauline Défossez, Peter Weisskopf, Johan Arvidsson, Guy Richard (2007). SoilFlex: A model for prediction of soil stresses and soil compaction due to agricultural field traffic including a synthesis of analytical approaches. Soil and Tillage ResearchVolume 93, 391-411.

Keller, Thomas (2004). Soil Compaction and Soil Tillage – Studies in Agricultural Soil Mechanics Department of Soil Sciences. Doctoral thesis. Swedish University of Agricultural Sciences, Uppsala.

Keller, Thomas, Lamandé, Mathieu (2010). Challenges in the development of analytical soil compaction models. Soil and Tillage Research 111(1):54-64.

BIBLIOGRAPHY

Kirby, J.M (1991). Strength and deformation of agricultural soil: measurement and practical significance. Soil Use and Management 7, 223-229.

Kirkegaard, J.A., So, H.B., Troedson, R.J., Wallis, E.S., (1992). The effect of compaction on the growth of pigeonpea on clay soils. I. Mechanisms of crop response and seasonal effects on a Vertisol in a sub-humid environment. Soil Tillage Res. 24, 107-127.

Koolen, A. J., Kuipers, H. (1983). Agricultural Soil Mechanics.

Kulli, B., Gysi, M., Flühler, H. (2003). Visualizing soil compaction based on flow pattern analysis. Soil and Tillage Research. Volume 70, Issue 1. Pages 29-40.

Lamandé, M. and Schjønning, P. (2011a). Transmission of vertical stress in a real soil profile. part i: Site description, evaluation of the Söhne model, and the effect of topsoil tillage. Soil and Tillage Research, 114(2):57–70.

Lamandé, M. and Schjønning, P. (2011b). Transmission of vertical stress in a real soil profile. part ii: Effect of tyre size, inflation pressure and wheel load. Soil and Tillage Research, 114(2):71–77.

Lamandé, M., Schjønning, P., and Labouriau, R. (2017). A novel method for estimating soil precompression stress from uniaxial confined compression tests. Soil Science Society of America Journal, 81 (5):1005–1013.

Lang, H.-J., Huder, J. & Amann, P (1996). Bodenmechanik und Grundbau. Das Verhalten von Böden und Fels und die wichtigsten grundbaulichen Konzepte. Springer-Verlag Berlin, Germany, 320 pp.

Lassen, P., M. Lamandé, M. Stettler, T. Keller, M.S. Jørgensen, H. Lilja, L. Alakukku J. Pedersen and P. Schjønning (2013). Terranimo®-A Soil Compaction Model with internationally compatible input options. Turin Conference-Sustainable Agriculture through ICT innovation.

Lebert, M., Burger, N. & Horn, R (1989). Effects of dynamic and static loading on compaction of structured soils. Mechanics and Related Processes in Structured Agricultural Soils. NATO ASI Series E, Applied Science 172. Kluwer Academic Publishers, Dordrecht, pp. 73-80.

Lebert, M. and Horn, R. (1991). A method to predict the mechanical strength of agricultural soils. Soil and Tillage Research, 19(2-3):275–286.

Lekea, A. (2015). "Evaluation of the Electrical Density Gauge for In-Situ Moisture and Density Determination." Thesis, University of Cape Town, Cape Town.

Leonards, G.A (1962). Foundation Engineering.

Leussink, H. (1954). Das seitliche Nichtanliegen der Bodenprobe im Kompressions-Apparat als Fehlerquelle beim Druck-Setzungs-Versuch. In: Fortschritte und Forschungen im Bauwesen. Grundbau – Vorschriften und Versuche, Heft 17, Franckh'sche Verlagshandlung, Stuttgart, Germany, pp. 153-160.

Lunne, T., Robertson, P.K., John Powell, P (1997). Cone Penetration Testing in Geotechnical Practice Soil Mechanics and Foundation Engineering 46.

M Pagliai, A Marsili, P Servadio, N Vignozzi, S Pellegrini (2003). Changes in some physical properties of a clay soil in Central Italy following the passage of rubber tracked and wheeled tractors of medium power. Soil and Tillage Research. Volume 73, Issues 1–2. Pages 119-129.

BIBLIOGRAPHY

McBride, R. and Joosse, H (1996). Overconsolidation in agricultural soils: Ii. pedotransfer functions for estimating preconsolidation stress. Soil Science Society of America Journal, 60(2):373–380.

Mosaddeghi, M. R., A. J. Koolen, M. A. Hajabbasi, A. Hemmat, T. Keller (2007). Suitability of pre-compression stress as the real critical stress of unsaturated agricultural soils. Biosystems Engineering Volume 98, Issue 1. Pages 90-101.

Mosaddeghi, M.R., A. Hemmat, M. A. Hajabbasi, M. Vafaeian, A. Alexandrou (2006). Plate Sinkage versus Confined Compression Tests for In Situ Soil Compressibility Studies. Biosystems EngineeringVolume 93, Issue 3.Pages 325-334.

Mosaddeghi, M.R., Hemmat, A., Hajabbasi, M.A. & Alexandrou, A. (2003). Pre-compression stress and its relationship with the physical and mechanical properties of a structurally unstable soil in central Iran. Soil and Tillage Research 70, 53-64.

Muhs, H. & Kany, M. (1954). Einfluss von Fehlerquellen bei Kompressionsversuchen. In: Fortschritte und Forschungen im Bauwesen. Grundbau – Vorschriften und Versuche, Heft 17, Franckh'sche Verlagshandlung, Stuttgart, Germany, pp 125-152.

Munir Nazzal. (2014). Non-Nuclear Methods for Compaction Control of Unbound Materials. Research Report, National Cooperative Highway Research Program, Washington, D.C., 167.

Nieves, A. (2013). Intelligent Compaction. TECHBRIEF, Executive Summary, FHWA, Washington, DC, 6.

Nieves, A. (2014). Intelligent Compaction. TECHBRIEF, Executive Summary, FHWA, Washington, DC, 9.

Oikawa H. (1987). Compression curve of soft soils. Soils and Foundations Vol.27, p.99-104.

Onitsuka K., Hong Z., Hara Y., Yoshitake S. (1995). Interpretation of oedometer test data for natural clays. Soils and Foundations, Vol.35, p.61-70.

Onshore Structural Design Calculations. (2017). Power Plant and Energy Processing Facilities. Chapter 8 – Soil Investigation and Pile Design. 352-356.

Pacheco Silva F. (1970). A new graphical construction for determination of the pre-consolidation stress of a soil sample. Proceedings of the 4th Brazilian Conference of Soil Mechanics and Foundation Engineering. Rio de Janeiro, Brazil, Vol.2, No.1, p.225-232.

Pachepsky, Y., Martinus Th. Van Genuchten M.Th. J (2011). Pedotransfer Functions.

Parada, Gabriel (2018). Comparison study between field compaction control devices of unbound materials. 9-19.

Passioura, J.B., (2002). Soil conditions and plant growth. Plant Cell Environ. 25, 311-318.

Radford, B.J., Bridge, B.J., Davis, R.J., McGarry, D., Pillai, U.P., Rickman, J.F., Walsh, P.A., Yule, D.F., (2000). Changes in the properties of a Vertisol and responses of wheat after compaction with harvester traffic. Soil Tillage Res. 54, 155-170.

Renault, P., Stengel, P., (1994). Modelling oxygen diffusion in aggregated soils. I. Anaerobiosis inside the aggregates. Soil Sci. Soc. Am. J., 58, 1017-1023.

BIBLIOGRAPHY

Rücknagel, O. Christen, B. Hofmann, and S. Ulrich (2012). A simple model to estimate change in precompression stress as a function of water content on the basis of precompression stress at field capacity. Geoderma, 17

Rücknagel, R. Brandhuber, B. Hofmann, M. Lebert, K. Marschall, R. Paul, O. Stock, and O. Christen (2010). Variance of mechanical precompression stress in graphic estimations using the Casagrande method and derived mathematical models. Soil and Tillage Research, 106(2):165– 170.

Sällfors G. (1975). Preconsolidation pressure of soft high plastic clays. PhD Thesis, Department of Geotechnical Engineering, Gothenburg.

Schjonning & Lamande (2018). Models for prediction PCS from readily available soil properties

Schjønning, P, Lamandé, M., Keller, T., Pedersen J., Stettler, M. (2012). Rules of thumb for minimizing subsoil compaction.

Schjønning, P., J. J. van den Akker, T. Keller, M. H. Greve, M. Lamandé, A. Simojoki, M. Stettler, J. Arvidsson, and H. Breuning-Madsen (2015b). Driver-pressure-state-impact-response analysis and risk assessment for soil compaction, an European perspective. In Advances in agronomy, volume 133, pages 183–237..

Schjønning, P., Lamandé, M. (2020). An introduction to Terranimo. Aarhus University, Dept. Agroecology.

Schjønning, P., Lamandé, M., Tøgersen, F.A., Arvidsson, J., Keller, T., (2008). Modelling effects of tyre inflation pressure on the stress distribution near the soil-tyre interface. Biosyst. Eng. 99, 119–133.

Schjønning, P., Mathieu Lamandé, Thomas Keller, Rodrigo Labouriau (2020). Subsoil shear strength – Measurements and prediction models based on readily available soil properties.

Schjønning, P., Matthias Stettler, Thomas Keller, Poul Lassen, Mathieu Lamandé (2015). Predicted tyre–soil interface area and vertical stress distribution based on loading characteristics.

Schmertmann, J (1955). The undistrubed consolidation behaviour of clay. Trans. ASCE, 120:1201– 1233.

Schmidbauer, J. (1954). Fehlerquellen und deren Ausschaltung beim Druck-Setzungsversuch (Kompressionsversuch). Franckh'sche Verlagshandlung, Stuttgart, Germany, pp. 162-174.

Senol A., Saglamer A. (2002). A new method for determination of the pre-consolidation pressure in a low-plasticity clay. The Electronic Journal of Geotechnical Engineering.

Smith, Ian (2014). Smith's Elements of Soil Mechanics. 9th Edition. 173-174

Soane, B.D. and Van Ouwerkerk, C. (2013). Soil compaction in Crop Production.

Soane, B.D., van Ouwerkerk, C., (1994). Soil compaction problems in world agriculture. In: Soane, B.D., van Ouwerkerk, C. (Eds.), Soil Compaction in Crop Production. Elsevier Science, pp. 1-21.

Soil compaction handbook. (2011). MULTIQUIP INC., Carson, California.

Soils and Aggregate Compaction. (2016). The Virginia Department of Transportation,

Soler Arnal, Pilar (2009). Review and analysis of preconsolidation stress determination methods for laboratory consolidation tests. Georgia Institute of Technology. 41-62.

BIBLIOGRAPHY

Stettler, Matthias; Keller, Thomas; Weisskopf, Peter; Lamandé, Mathieu; Lassen, Poul and Schjønning, Per (2014). Terranimo® – a web-based tool for evaluating soil compaction. Landtechnik 69(3), 2014, pp. 132–138

Tranter, G., Minasny, B., McBratney, A.B., Murphy, B., McKenzie, N.J., Grundy, M. & Brough, D. (2007). Building and testing conceptual and empirical models for predicting soil bulk density. Soil Use and Management, 23, 437–443.

Trautner, A (2003.) On Soil Behaviour During Field Traffic. Doctoral Thesis. Agraria 372, Swedish University of Agricultural Sciences, Uppsala, Sweden.

Van Den Akker, J. J. H. (2004). SOCOMO: A soil compaction model to calculate soil stresses and the subsoil carrying capacity. *Soil and Tillage Research*, *79*, 113–127.

Van den Akker, J.J (2008). Soil compaction. Environmental assessment of soil for monitoring: volume I, indicators & criteria, pages 107–124. Office for the Official Publications of the European Communities, Luxembourg.

Van den Akker, J.J.H, Schjønning, P., Unger, P.W., and Kaspar, T.C. (1994). Soil compaction and root growth. A review. Agron. J. 86, 759-766.

Van den Akker, J.J.H., Hoogland, T. (2011). Comparison of risk assessment methods to determine the subsoil compaction risk of agricultural soils in The Netherlands. Soil and Tillage Research. Volume 114. Pages 146-154

Van Zelst, T.W. (1948). An investigation of factors affecting laboratory consolidation of clay. Proc. Second International Conf. Soil Mech. Foundation Engrg., Rotterdam, Vol.VII, p.52-61.

Xuewen Chen, Richard M. Cruse, Shuang Niu, Xingyi Zhang (2019). Effect of loading time on soil structural failure.

Yong Cho, Koudous Kabassi, Ziqing Zhuang, Heejung Im, Chao Wang, Thaddaeus Bode, and Yong-Rak Kim. (2011). Non-Nuclear Method for Density Measurements. Final Report, The Charles W. Durham School of The Charles W. Durham School Architectural Engineering & Construction, Omaha, Nebraska, 75.

Zupan, M., (2006). Common Criteria for Risk area Identification According to Soil Threats. Italy: JRC Ispra. ESBN Research Report No. 20, EUR 22185 EN.

Prevention of soil compaction by agricultural operations: a geotechnical perspective

Ramón López Rodero
Student number: 01901870

Supervisors: Prof. dr. ir. Gemmina Di Emidio, Prof. dr. ir. Wim Cornelis
Counsellors: Dr. ir. Juan Carlos Rojas Vidovic (USFX), Adriaan Vanderhasselt,
Prof. dr. ir. Adam Bezuijen

Master's dissertation submitted in order to obtain the academic degree of
Master of Science in Civil Engineering

Academic year 2019-2020